



*A National Center of Excellence in Advanced Technology Applications*

ISSN 1520-295X

# Bare-Earth Algorithms for Use with SAR and LIDAR Digital Elevation Models

by

Charles K. Huyck, Ronald T. Eguchi,  
and Bijan Houshmand

ImageCat Inc.

Union Bank of California Building

400 Oceangate, Suite 1050

Long Beach, California 90802

Technical Report MCEER-02-0004

October 16, 2002

This research was conducted at ImageCat Inc. and was supported primarily  
by the Earthquake Engineering Research Centers Program of the National Science Foundation  
under award number EEC-9701471.

## NOTICE

This report was prepared by ImageCat Inc. as a result of research sponsored by the Multidisciplinary Center for Earthquake Engineering Research (MCEER) through a grant from the Earthquake Engineering Research Centers Program of the National Science Foundation under NSF award number EEC-9701471 and other sponsors. Neither MCEER, associates of MCEER, its sponsors, ImageCat Inc., nor any person acting on their behalf:

- a. makes any warranty, express or implied, with respect to the use of any information, apparatus, method, or process disclosed in this report or that such use may not infringe upon privately owned rights; or
- b. assumes any liabilities of whatsoever kind with respect to the use of, or the damage resulting from the use of, any information, apparatus, method, or process disclosed in this report.

Any opinions, findings, and conclusions or recommendations expressed in this publication are those of the author(s) and do not necessarily reflect the views of MCEER, the National Science Foundation, or other sponsors.

## **Bare-Earth Algorithms for Use with SAR and LIDAR Digital Elevation Models**

by

Charles K. Huyck<sup>1</sup>, Ronald T. Eguchi<sup>2</sup> and Bijan Houshmand<sup>3</sup>

Publication Date: October 16, 2002

Submittal Date: October 1, 2001

Technical Report MCEER-02-0004

Task Numbers 01-3031 and 01-3034

NSF Master Contract Number EEC 9701471

1 Vice President, ImageCat, Inc., Long Beach, California

2 President, ImageCat, Inc., Long Beach, California

3 MCEER Consultant, Pasadena, California

MULTIDISCIPLINARY CENTER FOR EARTHQUAKE ENGINEERING RESEARCH  
University at Buffalo, State University of New York  
Red Jacket Quadrangle, Buffalo, NY 14261

---



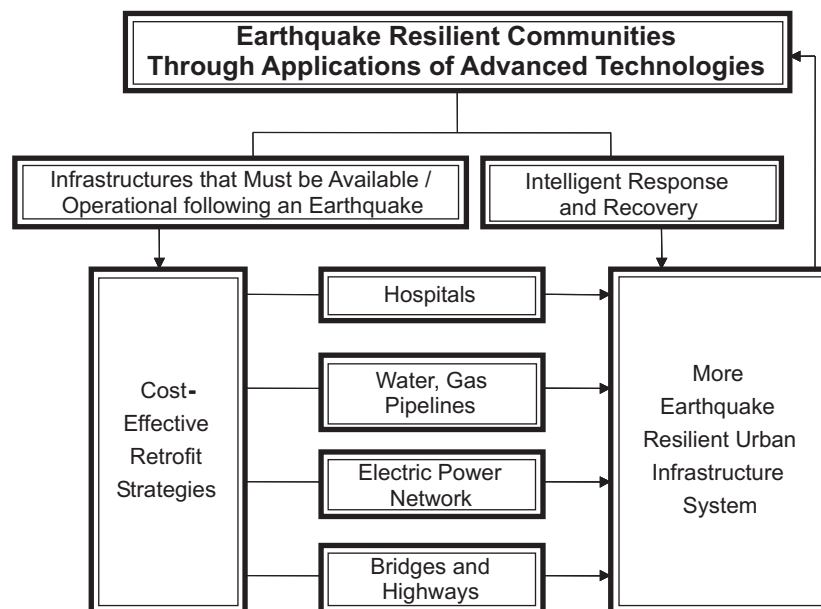
## Preface

The Multidisciplinary Center for Earthquake Engineering Research (MCEER) is a national center of excellence in advanced technology applications that is dedicated to the reduction of earthquake losses nationwide. Headquartered at the University at Buffalo, State University of New York, the Center was originally established by the National Science Foundation in 1986, as the National Center for Earthquake Engineering Research (NCEER).

Comprising a consortium of researchers from numerous disciplines and institutions throughout the United States, the Center's mission is to reduce earthquake losses through research and the application of advanced technologies that improve engineering, pre-earthquake planning and post-earthquake recovery strategies. Toward this end, the Center coordinates a nationwide program of multidisciplinary team research, education and outreach activities.

MCEER's research is conducted under the sponsorship of two major federal agencies: the National Science Foundation (NSF) and the Federal Highway Administration (FHWA), and the State of New York. Significant support is derived from the Federal Emergency Management Agency (FEMA), other state governments, academic institutions, foreign governments and private industry.

MCEER's NSF-sponsored research objectives are twofold: to increase resilience by developing seismic evaluation and rehabilitation strategies for the post-disaster facilities and systems (hospitals, electrical and water lifelines, and bridges and highways) that society expects to be operational following an earthquake; and to further enhance resilience by developing improved emergency management capabilities to ensure an effective response and recovery following the earthquake (see the figure below).



A cross-program activity focuses on the establishment of an effective experimental and analytical network to facilitate the exchange of information between researchers located in various institutions across the country. These are complemented by, and integrated with, other MCEER activities in education, outreach, technology transfer, and industry partnerships.

*The study described in this report examines the use of remote sensing technologies in creating building inventories for earthquake loss estimation. A key step in constructing these building inventories using remotely sensed data is to separate the built environment from the ground, i.e., the bare earth. The report describes an approach using SAR to detect the bare earth by employing a series of filters that depend on knowing the general heights of buildings, trees and other physical features on the surface of the earth. The bare-earth algorithm is validated and applied to three study regions in the Los Angeles area. The authors also investigate the efficacy of using LIDAR (light detection and ranging) data in constructing building inventories. LIDAR data is more detailed and accurate than SAR data, and the results from the two technologies were compared. The next report in this series will focus on using the results of the bare-earth algorithm to estimate the building stock.*

## ABSTRACT

In many applications, an important element of using highly detailed elevation data is the ability to separate the elevation of the ground from the elevation of vegetation and the built environment. Often, algorithms that accomplish this task are proprietary or are not easily adaptable to Geographic Information Systems (GIS) programs. This report presents a "Bare-earth" algorithm that uses a mild, multifaceted approach of running several spatially-based filters to determine which areas are most likely to be associated with the ground elevation.

This report represents the first of a two-volume series that examines the use of remote sensing technologies in creating building inventories for earthquake loss estimation. As previous studies have shown, one of the most problematic areas of loss estimation is quantifying assets at risk. In many cases, databases constructed for other uses (tax assessor data, census data) are modified to estimate building exposure. At best, these databases are marginally complete and only represent values associated with taxable properties. Thus, many structures that are important from the standpoint of regional earthquake loss are not included (e.g., government buildings, educational facilities).

A key step in constructing these building inventories using remotely sensed data is to separate the built environment from the ground, i.e., the bare earth. We show in this report that detecting the bare earth must be based on a series of filters. The most essential of these are: 1) a majority filter that helps to screen out anomalous or spurious data; 2) a local minimum filter that is effective at screening out tall and moderate-sized buildings; 3) a median filter that is particularly effective at screening out short to medium height buildings; 4) a slope filter that is designed to eliminate topographic changes associated with objects such as buildings; and 5) a variance filter that focuses on eliminating large clusters of buildings.

The report contains numerous examples that help to validate the approach under a variety of conditions. The algorithms that are contained in this report are expected to have other applications beyond building inventory development. We expect that these same models will also have applications in flood modeling, dispersion studies of gaseous materials, and possibly in

transportation studies (i.e., determine highway gradients). This study is part of MCEER's Thrust Area 3 that deals with response and recovery after major disasters.



## ACKNOWLEDGMENTS

This research was conducted at ImageCat, Inc. and was supported in whole or in part by the Earthquake Engineering Research Centers Program of the National Science Foundation under Award Number EEC-9701471 to the Multidisciplinary Center for Earthquake Engineering Research.

We would also like to thank Professors Masanobu Shinozuka and Kathleen Tierney for their guidance and enthusiastic support in helping this research team adapt these new and emerging technologies for earthquake loss estimation. Additionally, we want to acknowledge the following individuals for their important contributions to this effort.

Dale Benson, USGS, Denver, CO

Becky Bottlemy, USGS, Denver, CO

Mike Hearne, NOAA, Charleston, SC

Babak Mansouri, ImageCat, Inc., Long Beach, CA

Bryan Mercer, Intermap, Calgary, Canada

Gary Meredith, NOAA, Charleston, SC

Gary Merrill, USGS, Denver, CO

David Tralli, Jet Propulsion Laboratory, Pasadena, CA

Marc Wride, Intermap, Denver, CO



## TABLE OF CONTENTS

SECTION	TITLE	PAGE
<b>1.0</b>	<b>INTRODUCTION</b>	<b>1</b>
1.1	The Current State of Geospatial Data	3
1.2	Geographic Information Systems	5
1.3	Digital Elevation Data and Remote Sensing	7
<b>2.0</b>	<b>DETECTION OF THE BARE EARTH FROM A DEM</b>	<b>11</b>
2.1	Envisioning the Problem	13
2.2	Overview of Approach	13
2.3	Cleaning and Identifying Reliable Elevation Values	14
2.3.1	Extracting Cells with Low Correlation	14
2.3.2	Applying the Majority Filter	16
2.3.3	Negative Values	18
2.4	Topographical Filters	18
2.4.1	Local Minimum	20
2.4.2	Local Median	24
2.4.3	Slope Between Neighboring cells	27
2.4.4	Variance in Slope	29
2.5	Combining the Filters	33
2.6	Allocation and Smoothing	33
<b>3.0</b>	<b>VALIDATION OF THE BARE-EARTH ALGORITHM</b>	<b>37</b>
3.1	Spot Checking Elevation with GPS Data	37
3.2	Comparing Elevations with National Geodetic Survey Data	38
3.3	Comparisons with USGS 30-Meter DEM data	44
3.3.1	Visual Inspection of Selected Sites or Areas	46
3.3.2	Visual Inspections of Transects	50
3.3.3	Comparison of Elevations at Street Intersections	53
<b>4.0</b>	<b>GENERATING THE BARE EARTH TERRAIN USING SAR TECHNOLOGY</b>	<b>57</b>
4.1	San Fernando Valley	58
4.2	Downtown Los Angeles	61
4.3	Wilshire Blvd./Santa Monica Area	66
4.4	Assessment of Bare-Earth Algorithm	69
<b>5.0</b>	<b>TESTING THE BARE-EARTH ALGORITHM WITH LIDAR DATA</b>	<b>71</b>
5.1	Manhattan Beach and Redondo Beach	72
5.2	Long Beach	74

## **TABLE OF CONTENTS (CONTINUED)**

<b>SECTION</b>	<b>TITLE</b>	<b>PAGE</b>
<b>6.0</b>	<b>CONCLUSIONS AND RECOMMENDATIONS</b>	<b>77</b>
<b>7.0</b>	<b>REFERENCES</b>	<b>81</b>
<b>APPENDIX A</b>		<b>A-1</b>

## LIST OF ILLUSTRATIONS

FIGURE	TITLE	PAGE
1-1	Raster and Vector Data Models	6
1-2	SAR Interaction with the Built Environment	9
2-1	Absolute Elevation, the Bare Earth and the Height of Objects on the Earth	11
2-2	The Process used to detect the Height of the Bare Earth and the Built Environment	15
2-3	Correlation of Intensity for Industrial Study Area	16
2-4	Results of the Majority Filter	17
2-5	Applying the Majority Filter to Clean and Identify Reliable Data	19
2-6	Results of the Minimum Filter	21
2-7	Minimum Filter Flowchart	23
2-8	Removing Cells More Than Six Meters Above the Local Minimum Elevation	24
2-9	Median Filter Flowchart	26
2-10	Removing Cells More Than One Meter Above the Median Elevation	27
2-11	Results of the Median Filter	27
2-12	Results of the Maximum Slope Filter	28
2-13	Maximum Slope Filter	30
2-14	Results using the Variance in Slope Filter	31
2-15	Removing Cells where the Standard Deviation is greater than what would be expected from the Natural Terrain	32
2-16	Multiple Criteria Algorithm for Screening Out Cells likely to be associated with Trees and the Built Environment	33
2-17	Results of the Euclidean Allocation Filter	34
2-18	Methodology for using Bare-Earth Algorithm to Estimate the Heights of Buildings	36
3-1	Histogram Showing the Difference between SAR and NGS Elevations at Survey Data Points	40
3-2	NGS Survey Points where SAR Bare-Earth Elevations were 7 Meters Below the Surveyed Elevation	41
3-3	NGS and Bare-Earth SAR Elevations at Survey Data Points in the Los Angeles Basin	43
3-4	NGS and Raw SAR Elevations at Survey Data Points in the Los Angeles Basin	43
3-5	NGS, Raw SAR and Bare-Earth SAR Elevations at Survey Data Points in the Los Angeles Basin	43
3-6	NGS, Raw SAR and Bare-Earth SAR Elevations at Survey Data Points in the San Fernando Valley	44

## LIST OF ILLUSTRATIONS (CONTINUED)

FIGURE	TITLE	PAGE
3-7	Graph of Elevation Values Along a Transect	53
3-8	USGS DEM and Bare-Earth SAR Elevations at Street Intersections	55
3-9	Comparison of SAR-derived Bare-Earth Elevations with the Heights of Houses, as determined through use of Raw SAR Data	56
4-1	Study Areas	57
4-2	Ground Elevations and Building Footprints for San Fernando Valley	59
4-3	Ground Elevations and Building Footprints for San Fernando Valley (with Annotation)	60
4-4	Ground Elevations and Building Footprints for Downtown Los Angeles	62
4-5	Ground Elevations and Building Footprints for Downtown Los Angeles (with Annotation)	63
4-6	Comparison of SAR-derived Bare-Earth Elevations and with Aerial Photograph (Industrial Area of Los Angeles)	64
4-7	Aerial Photo of Downtown Los Angeles	65
4-8	Three-Dimensional View of Downtown Los Angeles constructed using Bare-Earth Algorithm and SAR Data	65
4-9	Ground Elevations and Building Footprints for the Wilshire Blvd. and Santa Monica Area	67
4-10	Ground Elevations and Building Footprints for the Wilshire Blvd. and Santa Monica Area (with Annotation)	68
4-11	Slope of the Wilshire Blvd./Santa Monica Region as Computed from USGS 30-meter DEMs	69
5-1	Bare Earth Results using LIDAR Data in Manhattan Beach	73
5-2	Three-Dimensional View of Cliff leading up from the Beach. Image created from USGS Aerial Data Draped Over LIDAR Data	74
5-3	Large Buildings on a Cliff in Long Beach	75

## LIST OF TABLES

<b>TABLE</b>	<b>TITLE</b>	<b>PAGE</b>
1-1	Number of Buildings by Height and Material Type	2
3-1	The Difference between SAR and NGS Elevations (in meters) of Digital Survey Data Points	41
3-2	Study Areas Chosen for Evaluating the Bare-Earth Algorithm	47
3-3	Sample of Image Catalog and Statistical Profile Generated for the USC Study Region	49
3-4	Elevation Data from a Linear Sample	51





## **SECTION 1**

### **INTRODUCTION**

This report represents the first of a two-volume series that examines the use of remote sensing technologies in building inventory development. As previous studies have shown, one of the most problematic areas of earthquake loss estimation is quantifying assets at risk. In many cases, databases constructed for other uses (tax assessor data, census data) are modified to estimate building exposure. At best, these databases are marginally complete and, in some cases, only represent replacement values associated with taxable properties. Thus, many structures that are important from the standpoint of regional loss are not included (e.g., government buildings, educational facilities).

In a recent Multidisciplinary Center for Earthquake Engineering Research (MCEER) report (1999), the authors propose a methodology where remote sensing technologies can be used to construct building inventories for loss estimation software. The authors point out that with the recent introduction of high-resolution sensors, it is now possible to image and characterize the properties of structures (i.e., buildings, roads, bridges, etc.) whose dimensions are on the order of several meters or less in size. One of the more promising technologies identified was synthetic aperture radar or SAR.

There are two important considerations in translating SAR data into building inventory information: 1) being able to outline the footprints of buildings, and 2) characterizing building heights. With these two parameters, it is possible to construct enough information to quantify total square footage and possibly building construction type. With total square footage, one can estimate the replacement cost of a building, thus providing a key piece of information in characterizing exposure. By knowing the height of a building, one might infer a particular building material type (e.g., steel, concrete, wood, etc.) or construction system for some specific geographic region or area of the country.

Table 1-1 shows the distribution of buildings in Los Angeles County by story height and material type. The data source for this information was the Los Angeles County Tax Assessor's Office; therefore, non-taxable properties such as government buildings are not included in this

summary. The table shows that the most predominant construction type is wood-frame construction, accounting for all but 0.03 percent of the total. However, for story heights greater than four stories, the inventory is comprised of either steel, concrete or brick/concrete block/other concrete buildings. For buildings in the 4 to 7 story height category, it is more likely that the building type is brick/concrete. For buildings greater than 7 stories, it is likely that the material type would be some kind of steel construction or concrete. A more careful analysis by use (residential, commercial, and industrial) may help to refine these distributions further.

**Table 1-1 Number of Buildings by Height and Material Type**

<b>No. of Stories</b>	<b>Wood-Frame</b>	<b>Steel-Frame</b>	<b>Concrete</b>	<b>Brick, Concrete Block</b>	<b>Total</b>	<b>% Total</b>
<b>0-3</b>	1,677,951	746	896	52,397	1,731,990	99.95
<b>4-7</b>	0	136	127	175	438	0.027
<b>8+</b>	0	190	121	56	367	0.023
<b>Subtotals</b>	1,677,951	1,072	1,144	52,628	1,732,795	100
<b>% Total</b>	96.83	0.06	0.07	3.04	100	100

**Source: Los Angeles County Tax Assessor's Office (1994)**

Table 1-1 points out that an important parameter in estimating the size and construction type of a building is building height. As this report will indicate, there are a number of advanced technologies that will provide building elevation information (i.e., absolute height) relative to some datum, e.g., mean sea level. However, in order to estimate building height, it is necessary that we also measure and subtract out the elevation of the ground. This report documents our efforts to develop a “Bare-earth<sup>1</sup>” algorithm using several different remotely sensed databases.

This report has been written for a technical audience that may or may not be familiar with the fields of Geographical Information Systems and Remote Sensing. General discussions of GIS, the distinction between raster and vector data, the analysis of elevation data within a GIS framework, and sources of elevation data are included in Section 1. In Section 2, we introduce our approach for detecting the bare earth using a series of filters that depend on knowing the

general heights of buildings, trees and other physical features on the surface of the earth. As the reader will see, the methodology is based on eliminating those features that are least likely to be associated with the natural terrain of the region. In Section 3, we discuss the validation of our Bare-earth algorithm using a variety of methods and datasets. In all comparisons, data from the Los Angeles area are used. Section 4 contains the results of several applications of the Bare-earth algorithm in the Los Angeles area. To assess its effectiveness for different land-use conditions, we include three examples: residential, commercial and industrial area. In Section 5, we investigate the efficacy of using LIDAR (light detection and ranging) data in constructing building inventories. Using data provided by the National Oceanic and Atmospheric Administration (NOAA) on coastal areas of California, we were able to apply our algorithms using the more detailed and accurate LIDAR data. In the end, we compare these results to those calculated using the SAR data. An appendix to this report discusses some basic concepts related to SAR imaging and data interpretation. These discussions are meant to help those that are unfamiliar with the concept of remote sensing, in particular, SAR imaging.

## **1.1 The Current State of Geospatial Data**

In the eighties, geospatial data was an extravagance of large corporations, the military, and other government agencies. Most of the powerful Geographic Information Systems (GIS) and image processing programs that could use these data ran on the UNIX platform. As desktop, laptop, and hand-held computers became more powerful, these programs were ported to other platforms that allowed efficient sharing of information throughout organizations. It followed naturally that as these programs became more popular, the need for comprehensive training increased. Colleges, universities and training facilities across the world responded by offering a broad range courses, principally in Geography departments. Students were instructed in how to “relate” different databases where the common link between them was a geographic location. Even with the presence of more GIS analysts, however, spatial data has yet to be used to its fullest potential.

---

<sup>1</sup> Bare earth is a term often used to describe the surface of the earth without the built environment or vegetation. Therefore, a bare-earth elevation is one that corresponds to ground elevation.

The process of using spatial data in Geographic Information Systems requires a thorough understanding of the data and the analytical tools that are available to process these data. GIS professionals often find themselves in a facilitator role, explaining to engineers, social scientists, politicians, and others exactly what information is stored and how it can be used to answer important questions. Since the power of geospatial data is largely derived from its ability to relate separate and often complex datasets, communication is extremely important. That is, one needs to understand the capabilities of such systems in order to ask the right questions.

Digital spatial data is an extremely valuable resource. It is commonly asserted by GIS professionals that seventy to eighty percent of all data has a spatial element. Exploiting the value of this information, however, can be a challenge and does require a comprehensive understanding of spatial analysis techniques and methodologies. As more examples of GIS analysis become available, there should be greater understanding of the efficacy of digital maps as statistical tools or devices. Newspapers, for example, routinely publish small illustrative maps with their stories. It is not uncommon to see radar data overlaid onto three-dimensional terrain maps in television weather reports. Internet sites offer maps with driving instructions that are based on sophisticated routing algorithms that calculate the most efficient path between two locations. These are just a few examples of how spatial data have been used in the popular media.

The idea that the reliability of a map depends on the reliability of the underlying data is key to understanding geospatial data. The presidential election in 2000 illustrates how the presence of map data in the media has begun to focus attention on data reliability. As digital maps become more prevalent in business and the general media, the public as a whole will gain a better appreciation of the process used to generate these maps. As we find new ways of using GIS maps to describe our environment, GIS concepts will begin to be understood by more people.

Additionally, technical issues are currently impeding the effective use of spatial data in general and elevation data specifically by most users. The elevation of the Earth's surface is a very important parameter in GIS. For example, it is much easier to interpret quantitative data on a map if presented within a topographic structure. Adding a three-dimensional perspective is even

more effective when viewing phenomenon that are influenced by the contour of the earth, e.g., landslides, weather patterns, or flood zones.

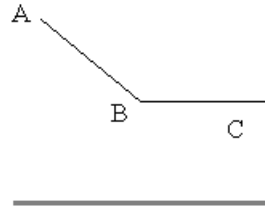
As modeling with GIS becomes more sophisticated, there will be a strong demand for elevation data not only as a visual component, but also as an analytical component. The surface of the earth is used in GIS to conduct “line of sight” studies for locating telecommunication equipment in urban areas, for modeling dispersion of hazardous gases between buildings, or predicting blast zones from high explosives. Algorithms have also been developed to delineate watershed zones and flood inundation areas based on the use of ground elevation data (Garbrecht et al., 1999). Detailed elevation data are required to analyze vulnerability to landslides (Monmonier, 1997). In order for these applications to use elevation data, there must be an integration of raster GIS models and vector GIS models.

## **1.2 Geographic Information Systems**

GIS is a branch of Information Systems (IS). In general, the focus of most GIS programs is to link various forms of vector data (points, lines and polygons) to their database attributes. Elevation data are usually represented using a raster model. A raster data file consists of a two dimensional array of values that represent a given condition or phenomena everywhere within its domain. Figure 1-1 displays how the same phenomena can be displayed in both raster and vector formats. In Figure 1-1a, the raster data represents a linear feature with the value of "5" as a series of grid cells. The cells are typically square with the real world position of the corner cells stored with the file. Operating on a raster model is usually fast, efficient, and optimal for imagery and elevation data. In Figure 1-1b, the same feature is represented as a line. Internally, the GIS software stores information on what nodes form the line (A, B, and C). The software stores the location of these points in real world coordinates (with varying degrees of accuracy). Each line is given a unique number. The unique number is used to link the line segment to the attribute data, in this case the number five. Vector analysis is ideal for spatial queries and integration with traditional information systems.

5	0	0	0	0
0	5	0	0	0
0	0	5	5	5
0	0	0	0	0
0	0	0	0	0

**a. Raster**



**b. Vector**

**FIGURE 1-1 Raster and Vector Data Models:**

The ability to analyze elevation data is greatly facilitated by a raster-based GIS model (Berry, 1995). Most government and commercial GIS applications depend heavily upon vector data, so that the data can easily be integrated into other databases. Depicting raster and vector data in the same GIS is routinely done for display purposes. For example, it is common to see an aerial photograph or a satellite image displayed with vector data such as highways or city boundaries overlaid. However, analytically, each data set is operated on separately and sometimes using different programs or modules.

There has been a lag in the integration of raster-based technologies into standard GIS tool sets. The raster tools that have become available through add-ons such as "Spatial Analyst" for ArcView and "Vertical Mapper" for MapInfo Professional provide functionality primarily for site suitability modeling where interpolation of vector data is required rather than image processing. To a GIS professional, there are key differences between "images" (remotely-sensed data) and "grids" (cell data populated by vector data), even though the format of these data are essentially the same, i.e., two-dimensional arrays of numbers at a given location with a given cell size.

Converting raster data to vector data in a GIS is an error-prone, largely interactive process that often results in splinters (fragmented polygons of data). It is difficult, for example, to classify remotely sensed data into land use categories for a vector based analysis, such as an overlay with hazard (e.g., earthquake ground motions) data. The data usually need to be run through a cleaning or filtering algorithm that "clumps and sieves" the raster data into congruent polygons to reduce splintering.

Currently, classification algorithms that separate images into several categories of land are much more effective if there is user intervention (referred to as supervised classification). The user essentially trains special algorithms (e.g., maximum likelihood or neural network algorithms) to interpret images for future use (Mather, 2000). This process can be error prone and usually requires the specialist to validate the results. There are libraries of spectral responses that classify images without user intervention, but many of these have been tailored towards agriculture and environmental applications.

Typically, satellite data or other raster data are brought under vector data to observe change or provide other visual information. As users become more sophisticated, the demand for integrated databases will increase, and the need for user-friendly applications to merge raster and vector data will become evident. This type of integration is key to using remotely sensed data for decision support systems (DSS).

### **1.3 Digital Elevation Data and Remote Sensing**

Measuring the elevation of the Earth's surface is one area where a number of industries have come to understand the importance of obtaining accurate data. Publicly available databases of ground elevation are often not detailed enough for analytical applications and users have come to question the reliability of that data. The most commonly used source of elevation data is the Digital Elevation Models (DEMs) from the U.S. Geological Survey. There is no statistical analysis of the accuracy of these DEMs with respect to the real world, only with respect to the contour maps from which they were derived (Bottlemy, 2000). The integration of raster and vector data, the demand for three-dimensional modeling and visualization tools, and the desire to have powerful vector databases merged with raster and image processing tools will all contribute to an increase in the demand for more accurate elevation data. The following discussion provides a list of methods used to create DEMs that depend on remote sensing technologies.

***Global Positioning Systems.*** Global Positioning System (GPS) data are collected by receiving radio signals from a constellation of satellites, all broadcasting data. By measuring the time it takes to receive each signal, a GPS unit can calculate the distance to each satellite. After calculating the distance to three or more satellites, the unit can triangulate its position. It is

possible to create a ground surface elevation map using GPS equipment, however, it is not very practical since it would take many, many measurements to populate even a very small area.

***Light Detection and Ranging.*** Light Detection and Ranging, or more commonly referred to as LIDAR, is an airborne remote sensing technology that, like GPS, produces extremely accurate ground elevations for a series of point locations. The technology works by measuring the time it takes for light to be transmitted from the sensor to the ground and back to the sensor. By cross-referencing this distance with detailed GPS information on the location of the aircraft, the elevation of the ground can be calculated (Baltsavias, 1999). These points are then averaged to create a ground elevation surface. Elevation data from LIDAR must be measured from almost directly below the sensor. Because of this, data can only be collected for relatively narrow swaths of land. An airplane or helicopter must transect a city many times in order to obtain a complete data set. This process can be very expensive for large areas.

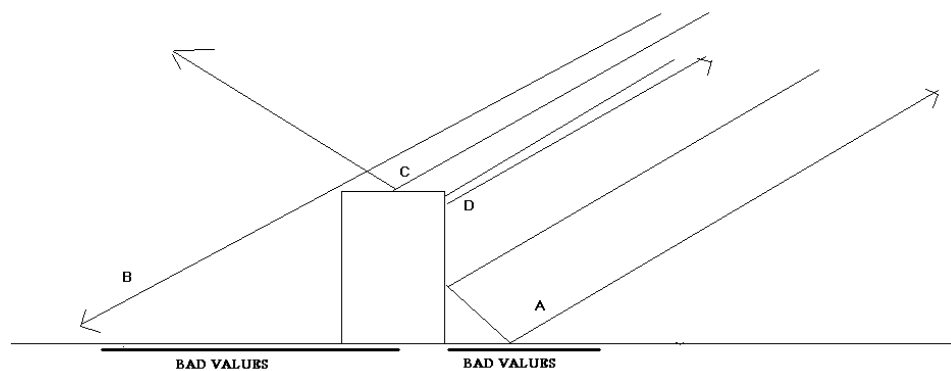
***Interferometric Synthetic Aperture Radar.*** Interferometric Synthetic Aperture Radar (IFSAR) offers a cost-effective alternative to LIDAR. Although the elevations derived using SAR data are not nearly as accurate as the elevations from LIDAR, these data are much less expensive to collect and process. Radar imaging technology is based on sending microwave signals from an airborne or space-borne sensor to earth and measuring the time it takes for the signal to come back to the sensor. In the case of interferometry, signals are produced from two antennae. Each antenna records the amplitude and phase of the radar wave as it travels back to the sensor. The difference in phase and angle between the two antennae can be analyzed to produce an elevation map of the ground and everything on it (Perry et al., 1998). In two-pass interferometry, the same SAR sensor visits the same scene in a different time. The signal phase difference measures the elevation of the region.

A major advantage of IFSAR is that high-resolution data can be collected and processed relatively quickly by airplane, which potentially makes it very useful for both disaster response and building inventory collection. Radar also has the advantage of penetrating cloud cover, making it very useful for immediate disaster response. This is particularly true for large floods. During the Midwest U.S. Floods of 1993, for example, optical imagery (e.g., Landsat and Spot data) was not available for several months because of extensive cloud cover. In contrast, radar



imagery data (i.e., ERS-1 data) was available to help determine the extent of flooding (Brakenridge et al., 1994). Because the data are collected from the side of the plane (referred to as "side-looking"), a much wider swath is possible. When the data are averaged over large regions, extremely precise measurements of change in the horizontal direction are possible (Zebner et al., 1994).

When SAR elevation data are analyzed at individual locations, the results can be problematic, especially in an urban environment. As the radar waves encounter tall buildings, they will often ricochet from several surfaces before they return to the antennae (Figure 1-2, line A). This phenomenon is referred to as "lag". Much of the data will also bounce away from the antennae, as with line C. A large area on the ground will be left with no values, as between the building and the location where ray B contacts the ground. This is referred to as "shadowing". In order to use radar data to find the heights of buildings, the maximum SAR reading for a building should be used. This yields the height of the building in reference to sea level. To find the height of the building in reference to the ground, there must be a separate data layer that measures the elevation of the "Bare Earth", or the height of the ground without vegetation or buildings. If a building is located in the shadows of other buildings, it is possible that the height of that building will not be detected at all. This is common in clusters of tall buildings, where it is very hard to detect a shorter building (Houshmand, 2000).



**FIGURE 1-2 SAR Interaction with the Built Environment**

In residential areas, there are very few problems with shadowing; however, the heights of the buildings are much closer to the inherent error associated with the data. The SAR X-Band data provided by Intermap for this study (10 GHz, wavelength = 3.24 cm) has an absolute value error of one standard deviation that ranges from 1.5 to 5 meters (see [http://www.intermaptechnologies.com/HTML/mapp\\_star3i.htm](http://www.intermaptechnologies.com/HTML/mapp_star3i.htm)). In residential areas, the heights of the buildings are much closer to this noise level. Another source of error in residential areas is “mixed pixel” effects. When the height of an area is measured with SAR, the responses from several radar waves are averaged to give one reading. The data that are averaged are associated with an individual pulse of waves, which covers a 5-meter square area. The effect is somewhat analogous to a huge flashlight, where the center is focused on a specific area, but the area that reflects diffuse light is much larger. In residential areas where buildings are so close to the ground, the height that becomes averaged over this 5-meter area will often mix the height of the ground with the height of the structure, resulting in a diminished residential building height. These mixed pixels make it difficult to determine the height of individual structures.

The potential for extracting and quantifying information about the built environment with remotely sensed data is enormous. LIDAR data combined with high-resolution multi-spectral optical data are the best sources for extracting these data (Brunn et al., 1997). Unfortunately, the cost to collect these data is high, particularly for large areas. Using SAR data to detect and statistically profile the built environment is challenging but the results are promising. It may be that for most disaster response situations, lower resolution SAR data may be more than adequate.

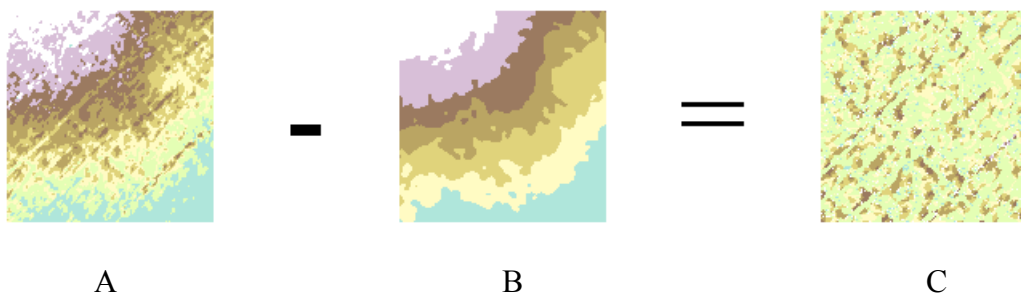
In the next section, we present our approach for detecting the bare earth. As the reader will see, we do this by employing a series of filters that eliminate those datasets that are clearly not associated with the ground surface.

## SECTION 2

### DETECTION OF THE BARE EARTH FROM A DEM

In order to analyze the heights of buildings using SAR data, one must model the height of the ground without vegetation or manmade structures. When digital elevation information is extracted from SAR data, it estimates the height of the earth's surface and everything on it, all in relation to an arbitrary location (e.g., sea level). Only when you subtract out the height of the bare earth do you get the heights of structures, trees and other features.

In Figure 2-1(A), the elevations of houses and trees are obscured by the height of the hill. Subtracting the height of the hill brings the height of the built environment into view and makes the heights of structures available for analysis. Bare-earth algorithms separate the ground elevation from the heights of buildings and trees. This allows the two components of elevation to be analyzed separately. Once the height of the built environment and vegetation has been separated from the natural terrain, elevations associated with trees can be separated from the built environment either through spectral analysis or by setting a threshold for the minimum height of buildings (Weidner, et al., 1995).



**FIGURE 2-1 Absolute Elevation (A), the Bare Earth (B) and the Height of Objects on the Earth (A minus B equals C).**

Under ideal circumstances, SAR data are very accurate. If the terrain is gently sloping, with the right amount of smoothing to eliminate inherent errors, precise measurements of elevation can be made. In an urban environment, however, it is much more difficult to reliably capture accurate elevations. For example, the SAR data that are collected from an aircraft are side-looking.

Thus, all objects behind other objects are not visible. This can be a problem where there are many tall buildings. Additionally, large swaths of land in front of large buildings may be obscured, because the radar waves ricochet from the ground to the building and back to the sensor. These phenomena are known collectively as “lag” and “shadow.” Another problem with SAR data is that the angle of the building with respect to the sensor determines the strength of the response, and thus the reliability of the reading. The exact same process that produces reliable results when imaging a sand dune will produce unusable results when imaging Lower Manhattan, for example. The appendix to this report explores some of these anomalies in detail.

When imaging smaller buildings, the results can also be problematic. Small, single-family dwellings often produce the equivalent of mixed pixel effects in optical data. In these instances, radar waves reflect from many different objects in the area associated with one, 5-meter by 5-meter area. This may include houses, trees, and the ground itself. The result is an average elevation, which diminishes the height of single-story buildings. When the elevation data are plotted, the mixed pixel effects cause right angles to become rounded. The effect is frequently compared to a "canopy", as it appears as if cloth has been draped over the buildings. The images are sometimes likened to melting ice cream. For larger buildings, it is possible to use the maximum response for a building footprint, but for smaller single-family dwellings, even the highest elevation may have mixed pixel effects.

Despite these apparent deficiencies, SAR data offers several important advantages over other imaging technologies, especially when analyzing large urban areas. First, using SAR technology, it is possible to image a relatively large area during a single flight. For the Los Angeles area, Intermap Technologies was able to use a swath of 8 kilometers to image “strips” of the Los Angeles Basin. This swath can be compared to one of several hundred meters that is characteristic of LIDAR applications. Second, because SAR technology is based on radar technology, it is not impeded by poor weather conditions or even nighttime conditions. For this reason, SAR imaging is considered a useful post-disaster remote sensing tool. Finally, when used as part of a dual antennae or repeat-pass system (e.g., interferometric), useful information on elevation changes over time or between before and after scenes of a disaster can be produced. This information can be important in identifying areas that have been affected by large-scale

tectonic movement, landslides or collapsed structures. In the remaining sections of this chapter, we present an approach for creating bare-earth elevations using high-resolution SAR data.

## **2.1 Envisioning the Problem**

Finding which SAR elevations are part of the ground surface is a challenging task. Although one can come up with logical statements that should detect the ground, variances in topography and problems with the SAR data render any one algorithmic solution less than adequate. For example, it is logical that the ground could be associated with the most frequent elevation in a given area; say a city block. However, there are many blocks that are populated with large structures or groups of buildings with the same height. In hilly areas, the height associated with the ground may repeat only for a very short distance. Another way in which the ground height could be estimated would be to try to find the elevations of streets. However, streets are often above or below ground level. Cars and trucks can obscure the true elevation of streets. In addition, noise in the SAR data makes it necessary to verify that individual elevations are in agreement with the surrounding elevations. Logically, the ground should be the lowest elevation within a certain distance. But what distance does one pick? A short distance might interpret the tops of buildings as ground level; a large distance would exclude changes in elevation. We found that a mild, multifaceted approach centered around the spatial characteristics of features on the ground in relation to their surroundings is the most reliable way to determine the location of the ground.

## **2.2 Overview of Approach**

To find the height of the bare earth, we follow a three-step process. First, elevations are extracted from the raw SAR DEM data based on low correlation values of intensity or reflectance. Elevations with high correlation values are run through a filter to eliminate noisy and erroneous data (Figure 2-2, step 1). These filtered SAR data and the original raw data are then passed through a series of spatially based criteria to determine which elevations can safely be assumed to be part of the ground (Figure 2-2, step 2). In attempting to delineate the ground surface, we remove as much of the built environment as possible while still leaving a significant portion of the ground. The height of the ground at selected locations is then used to interpolate

elevation values in areas covered by the built environment. Finally, a median filter is used to smooth the data thus eliminating sharp transitions in elevation. The bare-earth elevation data are then subtracted from the cleaned and filtered elevation data, leaving the estimated height of vegetation and the built environment (Figure 2-2, step 3). Each of these steps is discussed in detail in the following sections.

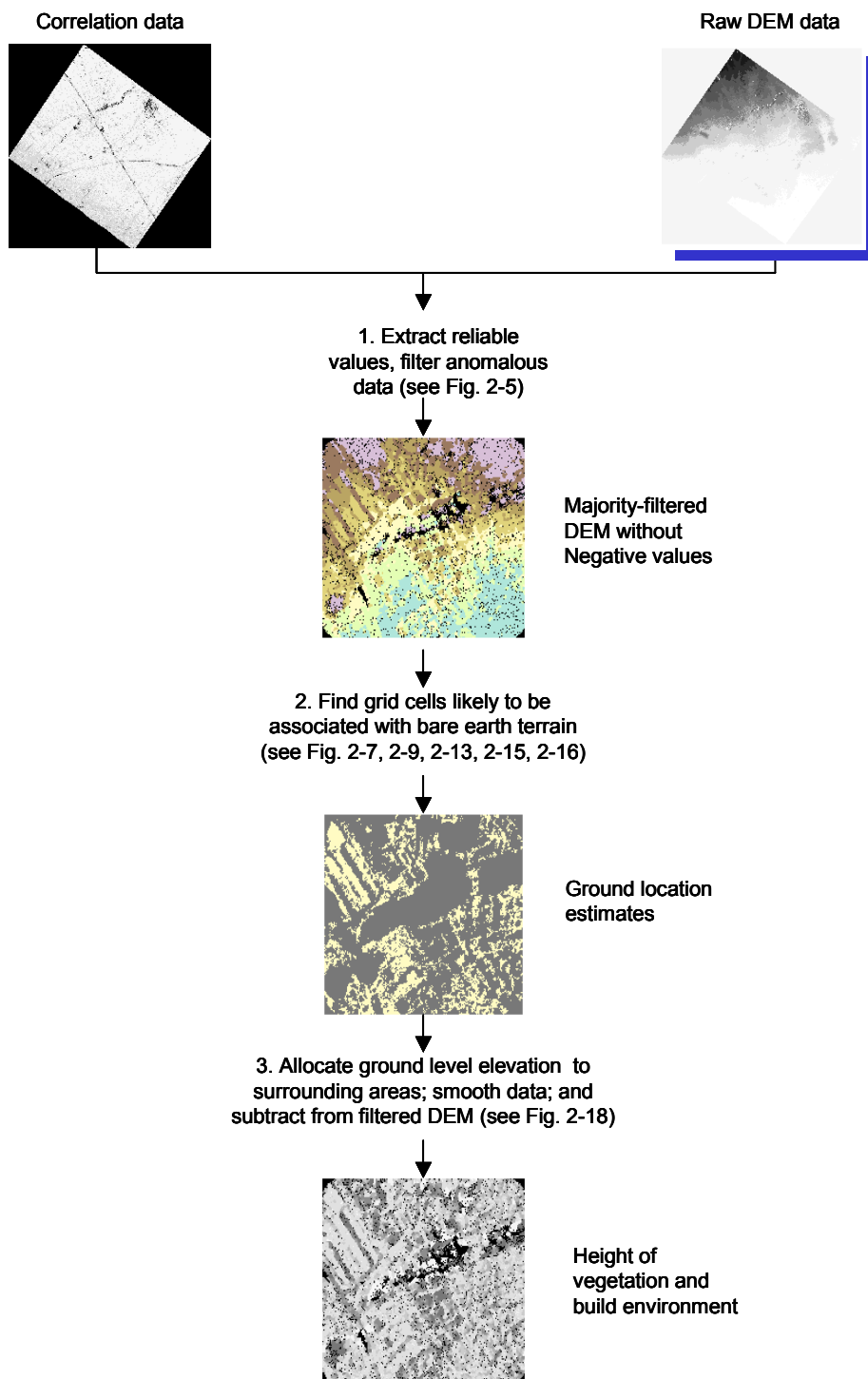
The following steps include procedures to filter and smooth intermediate data sets. It is important to note that these filtering processes are not performed on the final data set. As a result, they should not introduce any additional error in the original elevation data. They simply provide a framework for eliminating data that are not associated with the ground surface.

## **2.3 Cleaning and Identifying Reliable Elevation Values**

As discussed previously, digital elevations derived from SAR sensors are subject to error for numerous reasons. In order to effectively use these data, the data must be cleaned and cross-referenced with surrounding data values. If these values are positive (i.e., elevations above mean sea level), they must be further analyzed to see if they are likely to be part of the ground. At this point of the analysis, negative values are removed from the original data set.

### **2.3.1 Extracting Cells with Low Correlation**

Screening the data for reliable values begins with removing elevations with poor correlation indices. Interferometric SAR, or IFSAR, produces a DEM by measuring the difference in phase recorded by two antennae. This phase difference is then converted to a distance through a process called phase unwrapping. The two antennae can be on the same satellite or airplane, or they can be on separate satellites running in tandem. A correlation analysis is generally performed on the intensities of the signals measured between the two antennae. The intensity is a measure of the strength of the signal received by the antennae. The higher the correlation between two signals, the more dependable the digital elevation values are. Elevation values computed from poor-intensity correlations are likely to be spurious and unreliable.



**FIGURE 2-2 The Process used to detect the Height of the Bare Earth and the Built Environment**

Poor correlation can indicate that a physical object, such as a tall building, has altered the geometry of the return signal in such a way that one antenna receives a weaker signal (see Appendix A). Poor correlation can also be caused by a weak signal return, generally associated with long, flat surfaces such as freeways or bodies of water. In Figure 2-3, the darker areas in the left frame indicate areas of low correlation and generally outline streets. This is evident by comparing the left image with the middle image, which is an aerial photograph of the same area. The frame on the right depicts in black, areas where the correlation value is below 0.85. In general, these darker areas are not considered good candidates for extracting ground elevations because numerous factors contribute to their variation or uncertainty.



**FIGURE 2-3 Correlation of Intensity for Industrial Study Area**

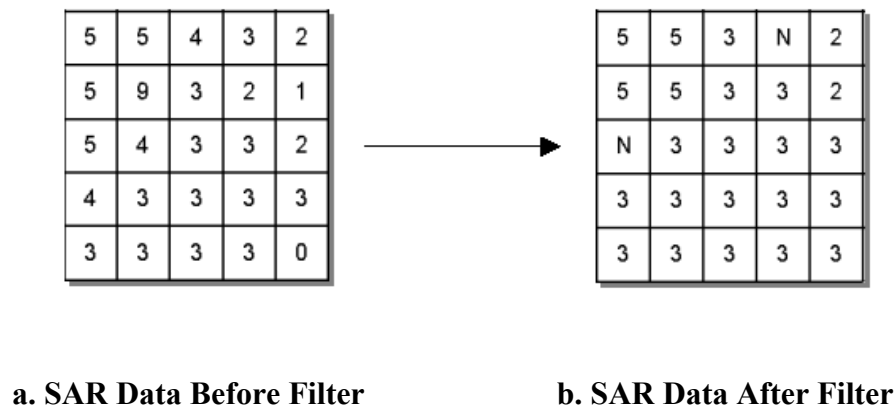
### **2.3.2 Applying the Majority Filter**

After the poor correlation data are extracted, the elevations are rounded to the nearest meter and smoothed with a majority filter, which is described below. Rounding the data to the nearest meter allows us to pass the data through the majority filter, a critical step in eliminating spurious data points.

Anomalous data points can be real elevations, or they can be associated with noise and error. A majority filter works by scanning through each individual elevation and comparing it with the elevations of surrounding cells. Each cell is replaced by the elevation that occurs most frequently amongst the surrounding cells and the cell being analyzed. The number of cells included in this evaluation depends on the window specified for the filter. In our majority filter,



we used a 3 by 3 window size that compares a middle cell with the eight adjacent cells. If a majority value cannot be established because two or more cell values occur with the same frequency (a tie) or because each cell contains a different value, the elevation value is replaced by a null value. In Figure 2-4a, there are two instances where a majority value cannot be established and thus, these cells are replaced by null values. Figure 2-4b displays the null values. Cells with a null value are not considered in the bare-earth calculations.



**FIGURE 2-4 Results of the Majority Filter (N=Null)**

The majority filter cleans the data in several ways. It removes some of the elevations that are associated with cars, bushes, lampposts and other small objects within the terrain. It also helps to reduce the effects of speckle noise and other SAR data errors. Data elevations that cannot be verified by the neighboring cells are less likely to be associated with the bare earth. Although it is easy to imagine cases in which the majority filter would throw out useful data (extracting some of the ground surface), SAR data in its raw state is generally unusable. Much of the literature on SAR data discusses different algorithms for filtering the data. Visually interpreting raw SAR data is very difficult, which is why the data are frequently averaged, a process known in image processing as "multi-looking". Loss of some data is unavoidable when working with SAR data. Without filtering the data, noise and small changes in elevation would be considered as ground elevations, leading to an over estimation in ground height and an underestimation of the heights of buildings.

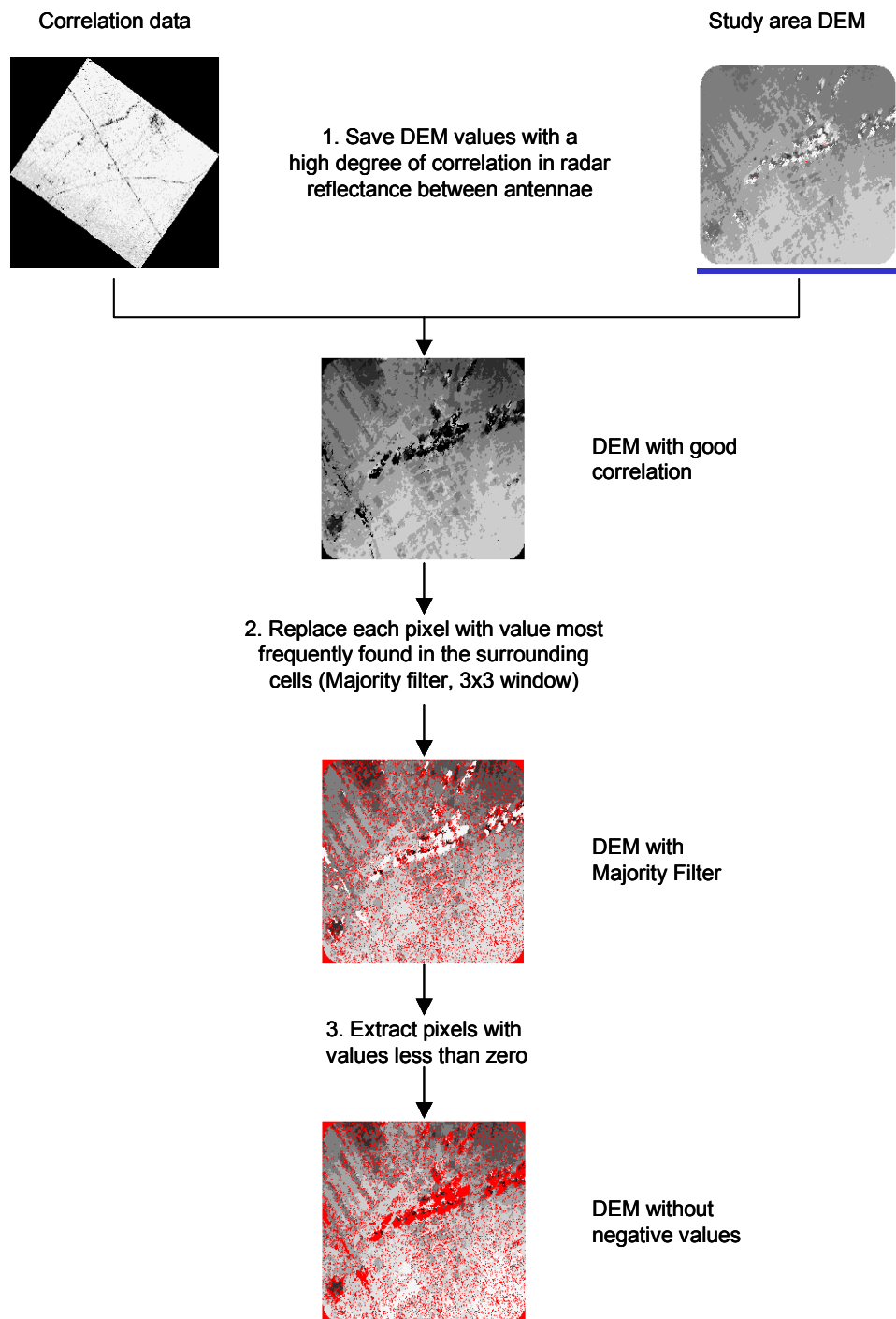
Running various filters on the data can also introduce errors. The error associated with running a majority filter on the data can be twofold. A valid elevation can be replaced by the elevation of neighboring cells. If a valid fluctuation in the elevation occurs so as to affect a 2.5 by 2.5 meter grid cell, but not its neighbors, it is unlikely that a change in this cell will significantly influence the computed height of a structure. Therefore, the general smoothing of the data set should not greatly change the elevation. The second way in which a majority filter can introduce error is if a valid bare-earth elevation is removed from the data and is no longer considered as a bare earth candidate. The more cells that remain after the cleaning and filtering process, the more data that will be used to create the ground surface elevation, and the more accurate the final surface will be. However, it is much more disruptive to the final surface elevation to have spurious elevations considered than to have good elevations thrown out. Even though a certain percentage of cells with anomalous heights may be valid bare-earth elevations, an elevation that cannot be validated by its neighboring cells is inherently unreliable as a bare earth candidate, and thus, is removed. This process of applying the majority filter is presented in Figure 2-5.

### **2.3.3 Negative Values**

In the vast majority of cases, elevation values at or below sea level are incorrect. Negative or zero values occur in SAR data because of lag and shadowing effects (see Appendix A). These values can be safely removed from the data set.

## **2.4 Topographical Filters**

Identifying the ground elevation presents a compromise between interpreting large flat buildings as ground and undercutting hilly terrain. We found that a multi-criterion approach involving the spatial characteristics of features on the ground in relation to their surroundings was the best way to determine the location of ground elevations. These spatial characteristics include the minimum height of the surrounding area, the median elevation of the surrounding area, the immediate slope of the cell with respect to the surrounding elevations and the change in slope over a wider region. Although the algorithm does not work in mountainous regions and interprets the middle of very large structures as ground (such as the Convention Center in downtown Los Angeles), it does a very good job of minimizing any potential miscalculations by addressing the problem from several different perspectives.



**FIGURE 2-5 Applying the Majority Filter to Clean and Identify Reliable Data**

Through a series of filters that analyze the elevation of a cell with respect to neighboring elevations, assumptions are made as to what topographical qualities of an area are likely to represent the ground surface. The following sections present the assumptions used in this study to determine the ground surface. These assumptions are:

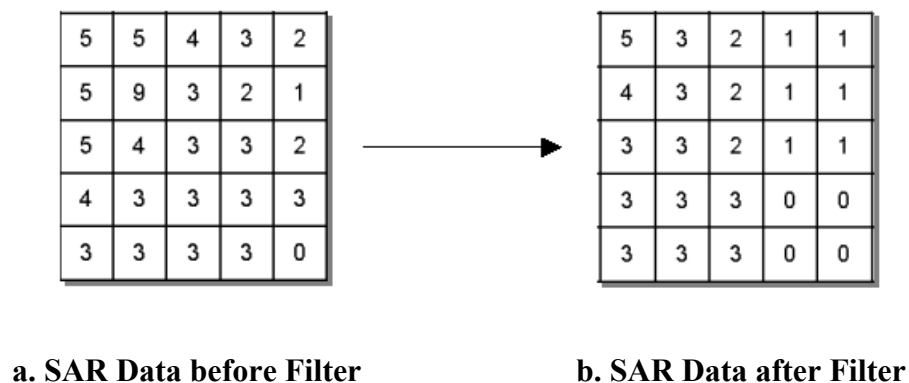
1. The ground represents the lowest elevation within a certain distance.
2. The ground is at or below the median elevation within a certain distance.
3. The ground has a slope or gradient that is less than the changes in elevation associated with objects on the ground, such as trees and buildings.
4. The slope of the ground varies less than the slope of the built environment.

#### **2.4.1 Local Minimum**

The most obvious way to find the ground is to locate the lowest point within a certain distance. Occasionally, this will return the elevation of a ditch or a construction site, or bad data resulting from lag or shadows, but usually this value will correspond to the height of the ground. The difficulty in executing this approach is finding the appropriate search radius. To read the correct elevation beyond the footprint of a large building, such as a mall or a school, the search radius would have to be very large, the size of an average city block or more. When you have a slight incline in another area, this same approach selects the minimum height at the bottom of the hill, which leads to an overestimation of building stock. As the search radius decreases, the tops of the largest buildings will be interpreted as ground height, and an over estimation of the ground height will occur, which leads to an underestimation of building stock. For the purpose of finding the height of the ground, it is important to have a search radius that is large enough that it would look beyond most buildings. If a building is larger than twice the radius chosen, then the center of the building area will be mistaken for a possible ground elevation. If these heights are not removed by another methodology, the height of the structure could be underestimated. In practice, however, much of the building remains and the maximum heights in these areas will be combined with the building footprint to produce an accurate building height.

In this study, we have chosen a minimum filter search radius of 25 cells. Each cell is 2.5 meters by 2.5 meters, so the resulting search radius is 62.5 meters. This distance was chosen because it is approximately the area of a city block. Larger and smaller distances were used in testing, and a search radius of 125 meters in diameter allowed for the extraction of most buildings, and in the absence of steep slopes, established good results. Rigorously establishing the ideal search radius given data resolution is an area for future research. A building must be longer than 125 meters in one direction before the top of the building is mistaken for ground elevation. If a location is mistaken for the ground, there is a good chance that it will be screened out by one of the other filtering criteria.

Starting from the cleaned and filtered DEM, a local minimum filter is applied to the data. A minimum filter creates a new grid layer with the same dimensions and cell size as the initial data set. Each cell in the new grid is populated with the minimum elevation value of the initial data set within a certain radius (25 cells in this case). This results in a new surface that represents the lowest elevation within the boundaries of the search radius. Figure 2-6 provides an example of how a minimum filter works on the eight adjacent cells.



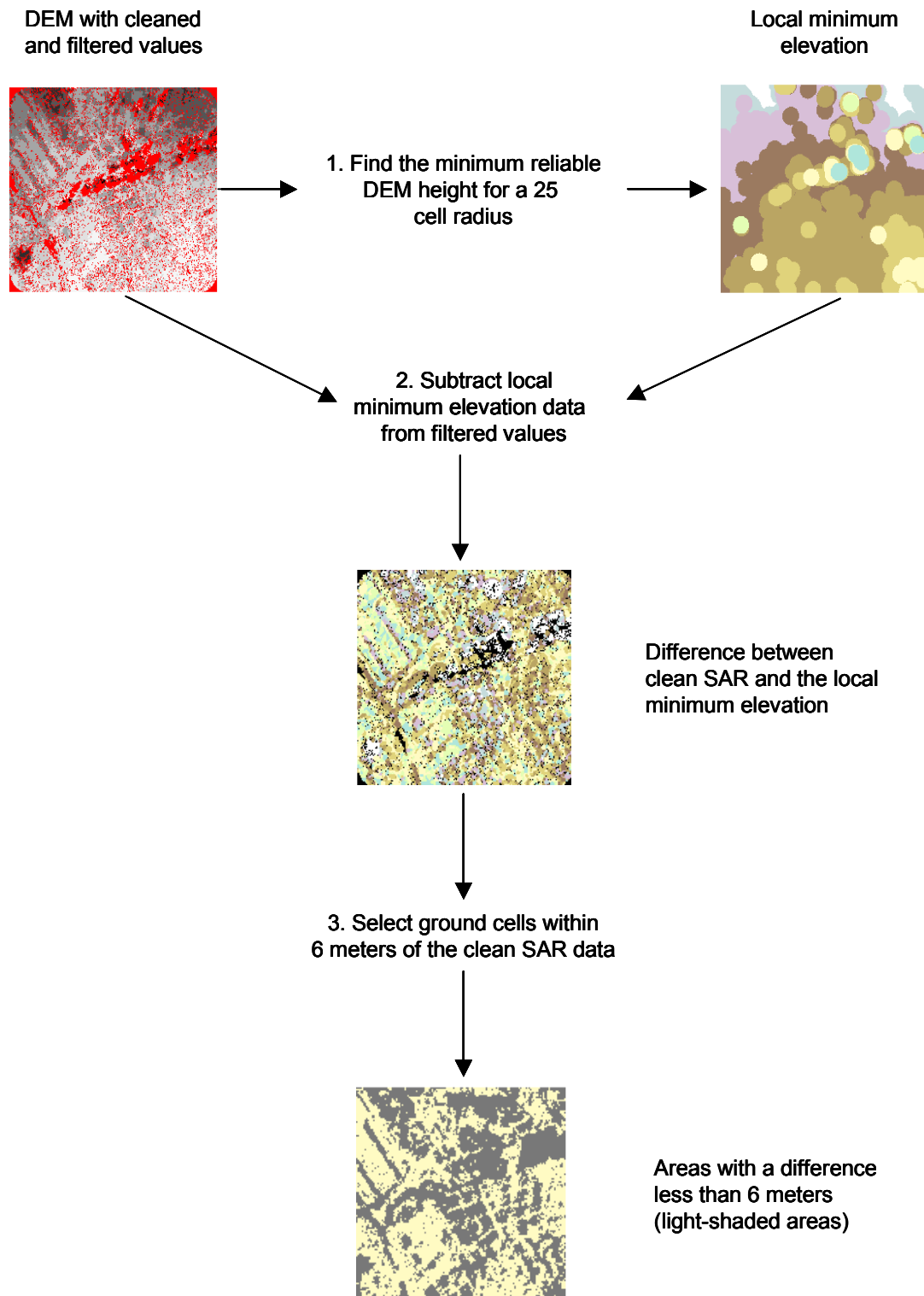
**FIGURE 2-6 Results of the Minimum Filter**

Figure 2-7 provides a flowchart of the Minimum Filter Process. To illustrate the concept, we use a part of the Wilshire Boulevard corridor as an example. The minimum elevation filter will strip out most buildings from the data, leaving a minimum height that corresponds to the bare-earth elevation or ground height in some areas, but not all areas. Spurious low data values, which

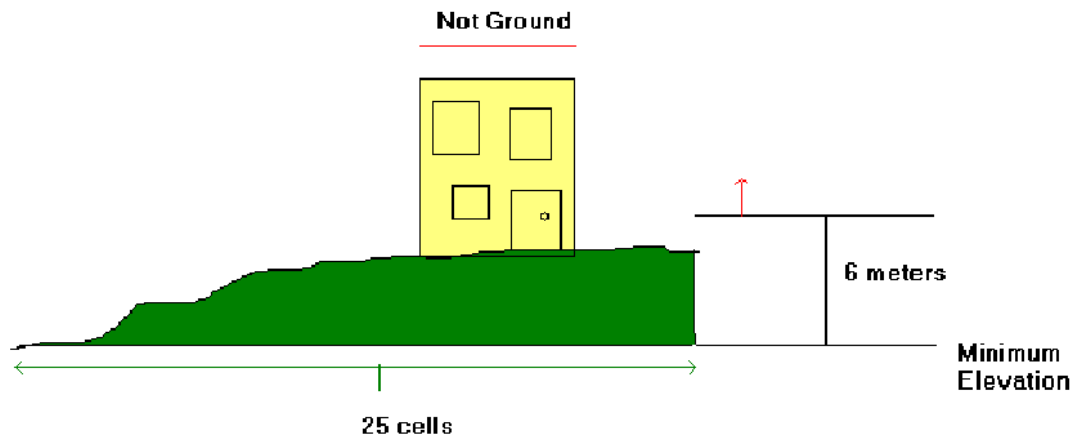
were not removed by the majority filter, will cause circles of low values in a minimum elevation data set. These values can correspond to shadowing as described earlier and can be seen in Figure 2-7 as circular patterns along Wilshire Boulevard (upper right-hand image).

A minimum elevation data set is very good for determining which cells are well above the lowest elevation and removing them. Subtracting the local minimum from the cleaned SAR data leaves the height above the minimum elevation. The minimum elevation can be envisioned as a substitute for the bare-earth elevation. Using this analogy, the difference between the SAR elevation and the minimum elevation represents an approximation of building and vegetation height. Because of errors in the minimum elevation data, it is not an accurate bare earth estimate, but it allows us to remove areas from further analysis that have a height significantly above the minimum elevation.

Removing cells greater than six meters above this minimum reliably extracts elevations associated with many buildings and trees from the data set without affecting the natural terrain. During testing, it was determined that 6 meters was high enough to accommodate a reasonable rise in terrain over 62.5 meters (search radius of 25 cells), but would still remove a significant portion of the built environment. The last image in Figure 2-7 shows the results for a small area around Wilshire Boulevard. The lighter areas represent land and the darker gray areas have been marked as unlikely candidates for a bare-earth elevation. This data set is combined with three other criteria in a Boolean operation where an area must pass all filters in order to be considered as ground. Elevations associated with houses that are less than six meters above the neighborhood minimum elevation have several additional filters with which they can be marked as part of the built environment. Figure 2-8 shows the rationale for using six meters to extract non-ground elevation areas.



**FIGURE 2-7 Minimum Filter Flowchart**



**FIGURE 2-8 Removing Cells more than Six Meters above the Local Minimum Elevation**

Both the six-meter criterion and the 25-cell criterion were determined through experimentation. As with the six-meter difference, the 25-cell search radius also represents a compromise. When the search radius increases, the minimum height assigned to each cell becomes less relevant to the site at the center of the radius. Natural topography will eventually be undercut by the minimum elevation. If the natural elevation is undercut by an amount larger than the height of extraction (in this case, 6 meters), then the height of the ground will be underestimated and the building stock will be overestimated. Choosing an appropriate search radius represents a trade-off between undercutting topography and including large buildings.

## 2.4.2 Local Median

It is more difficult to intuitively understand the rationale of the median filter than it is to understand the minimum filter. In searching for the ground, it is natural to look for the lowest point within a given area. However, as established in the previous section, this procedure can be problematic. Looking for the minimum elevation is very useful for screening off tall buildings but does little to screen off shorter structures. Optimizing the routines to address shorter structures introduces errors associated with undercutting topography. The median filter methodology works in a manner very similar to the minimum elevation algorithm, but there is little risk in undercutting topography, unless there is nothing on the ground.

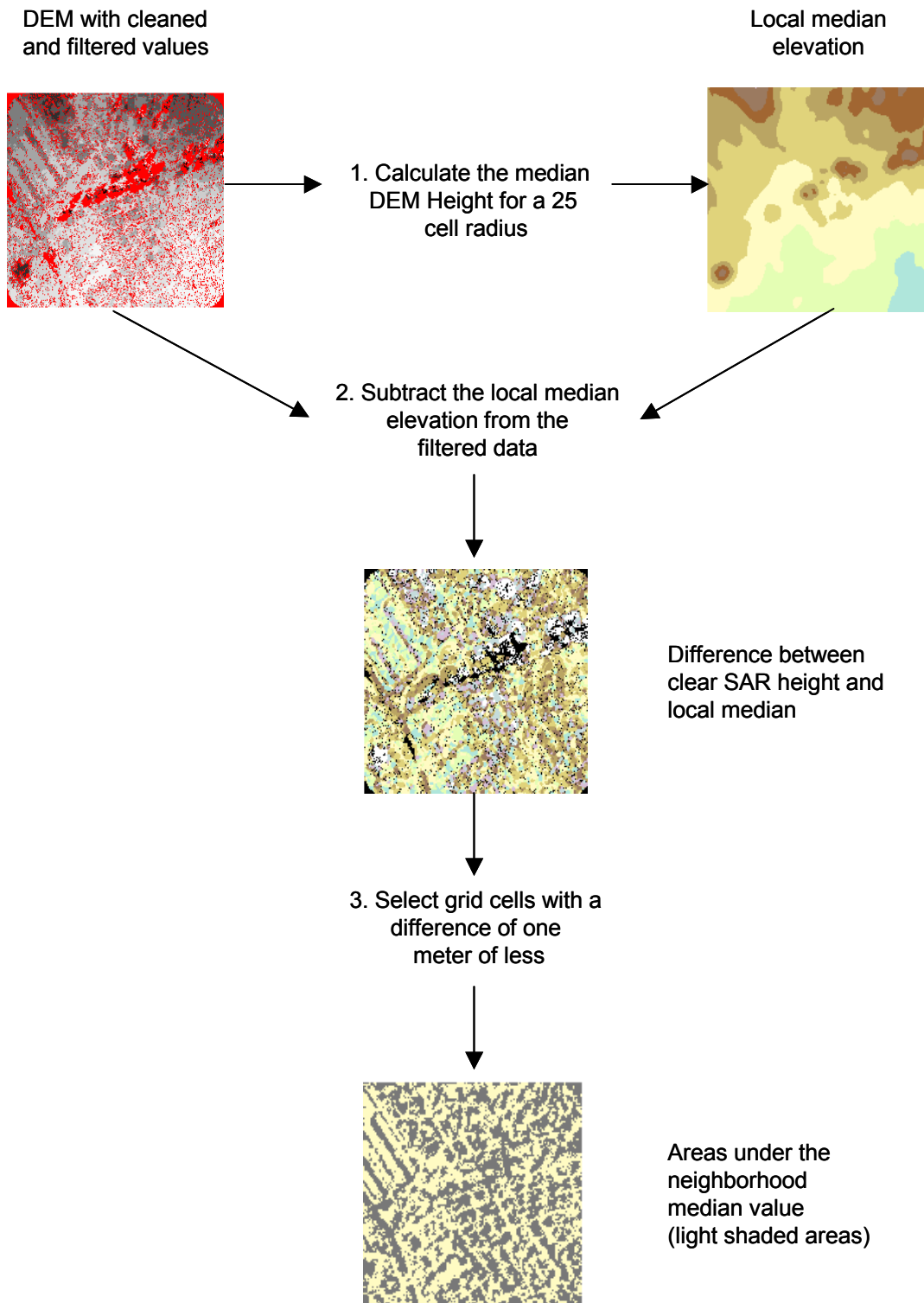


A good way to visualize the median elevation filter is to think about an urban landscape and imagine that one way to find the ground would be to throw out everything above the middle. It is a simple and effective solution that eliminates much of the built environment where the minimum elevation fails. There are many cases in which this criterion does not identify the ground, such as short buildings next to very tall buildings, but these elevations tend to be extracted by other procedures, which are discussed in the following sections. Very few grid cells associated with ground height appear to be extracted by this methodology.

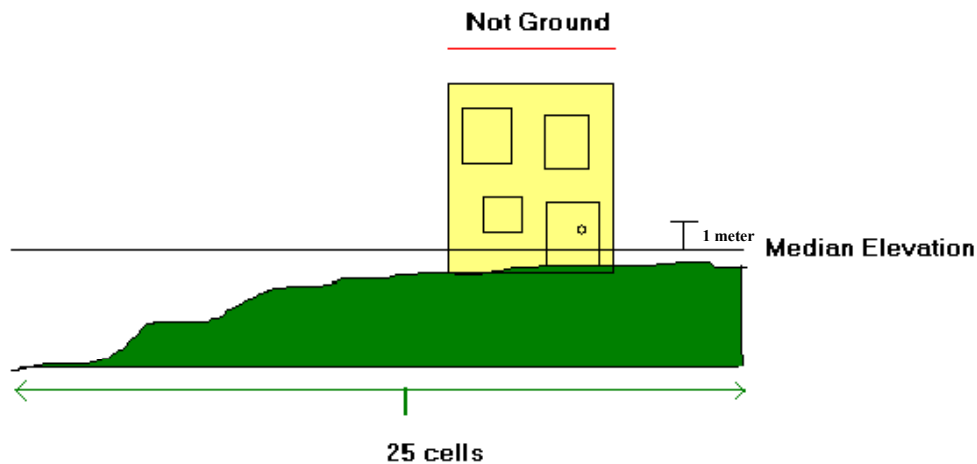
As with the local minimum filter, the median filter starts from the cleaned and filtered DEM. A local median filter is then applied to the data set. The median filter creates a new grid layer with the same dimensions and cell size as the initial data set. Each cell in the new grid is populated with the median elevation associated with a 25-cell radius, creating a new surface of the median elevations. Figure 2-9 presents a flowchart that describes how the median filter works.

The result of the median filter is an average ground height that is consistently above ground level, but below many features on the ground. This height is subtracted from the cleaned SAR data set. Everything with a difference of one meter or more is considered unlikely to be part of the ground. A difference of zero indicates that the ground height is the local median. These areas are not extracted, because for long and flat stretches of land, they are equal to the ground height.

Comparing the results of the minimum and median filters for the Wilshire Boulevard area (Figure 2-9, step 2 and Figure 2-7, step 2), it can be seen that the median filter is effective at extracting much of the built environment regardless of topography, whereas the minimum filter's effectiveness is limited by both topography and the height of the structure. Upon closer examination, it is also evident that the median algorithm is more effective at extracting smaller structures and clusters of vegetation. Figure 2-10 shows an illustration of how the median filter works in this study.

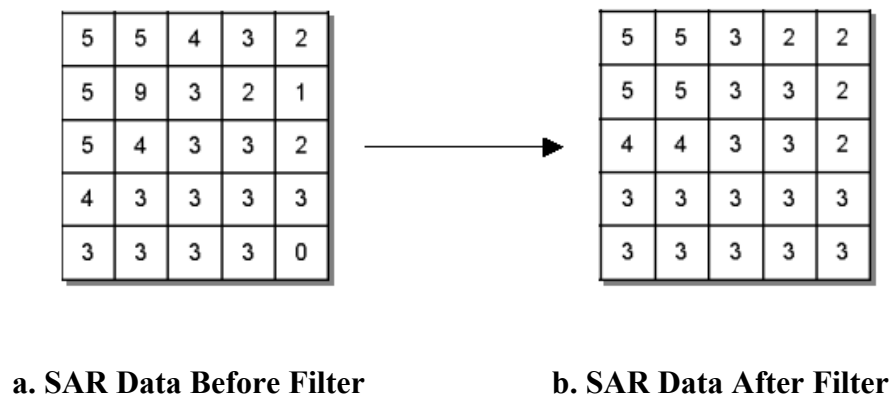


**FIGURE 2-9 Median Filter Flowchart**



**FIGURE 2-10 Removing Cells More Than One Meter Above the Median Elevation**

Finally, Figure 2-11 gives an example of how the median filter works when viewed as a grid system. Note once again that this operation is performed on the eight cells that surround a particular grid cell.

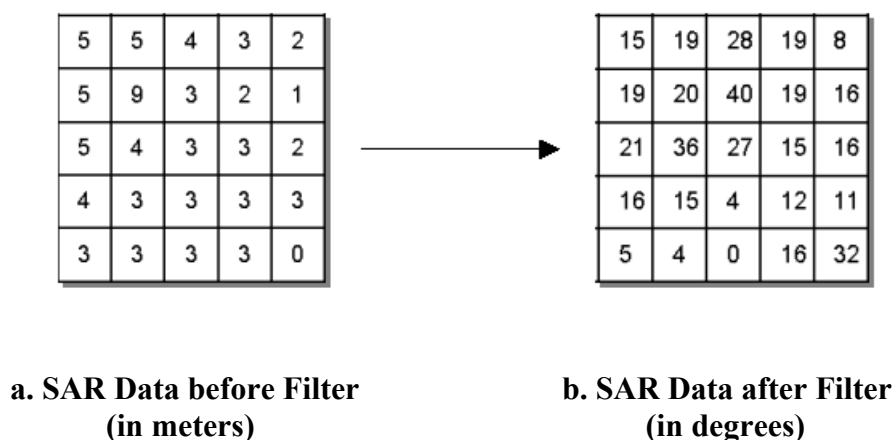


**FIGURE 2-11 Results of the Median Filter**

### 2.4.3 Slope between Neighboring cells

The third topographically-based screening method of removing buildings and trees from the elevation data is to extract areas with steep slopes. The steepest slopes in a DEM are usually

associated with objects projecting from the earth's surface. A new grid layer is created with the same dimensions as the original data set. Each cell is populated with the maximum slope determined from the raw SAR data set. The maximum slope is the maximum angle between a cell and the eight adjacent cells. The unfiltered, uncleaned SAR data are used instead of the filtered data set because the filtered data set removes anomalous data values that help detect the high slopes associated with buildings. Slopes above a twenty-degree angle are identified as areas associated with the built environment or vegetation. Topography with slopes above 20 degrees generally do not extend over long distances in urban environments. Figure 2-12 shows the grid scheme that is associated with this particular algorithm.



**FIGURE 2-12 Results of the Maximum Slope Filter (assumes 2.5 by 2.5 meter cell size)**

The effect of the computed slope can be observed for the Wilshire Boulevard area in Figure 2-13, image B. In this area, there are several steep hills that were not steep enough to be affected by the screening process. The Santa Monica Mountains just north of UCLA are extracted using this filter. The inability to extract building heights in mountainous regions is a limitation of this algorithm. The filter does a good job of extracting areas that might have been missed by the other algorithms, especially the areas surrounding corners of buildings and trees. The Veteran's Memorial Cemetery appears in the upper left-hand side of Figure 2-13 (image C) as two parallel lines of trees (trending southeast to northwest). The other filters do a good job in detecting the lines of trees in the cemetery, but the slope filter actually outlines the boundaries of trees. This filter effectively identifies the high slope elevations and assures that these elevations are not

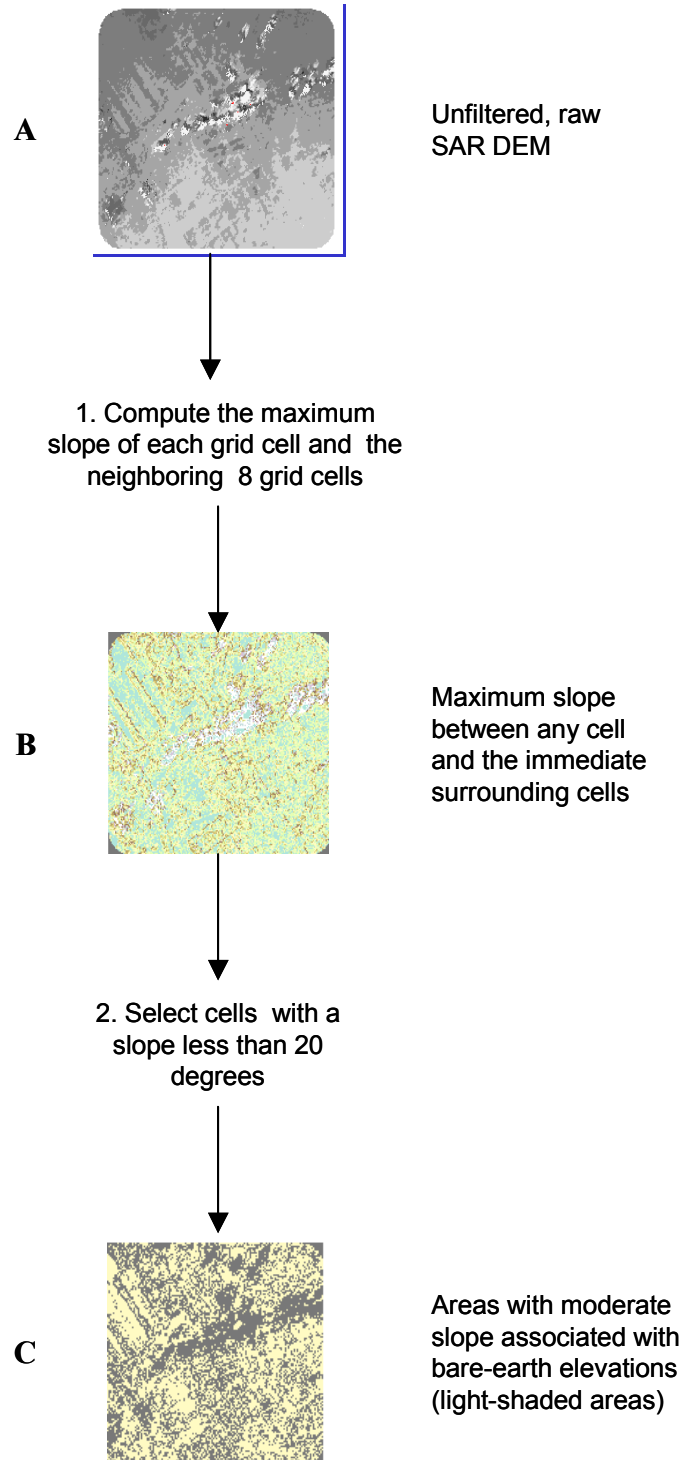
considered as ground height. The corridor of tall structures along Wilshire Boulevard is almost entirely removed, as represented by the dark areas in Figure 2-13, image C.

The reader may ask why twenty degrees? Twenty degrees is very low number, as most elevations associated with the built environment are much steeper and many naturally occurring hills in urban areas have slopes exceeding twenty degrees. Twenty degrees was chosen after reviewing slope maps for some of the pilot test areas (see Section 3.3). Although the slope of a specific urban area may be almost entirely angles, that are close to 90 or 0 degrees, the calculated slope from the SAR data will be a wide range of values. This anomaly must be considered when extracting the bare earth from the SAR data.

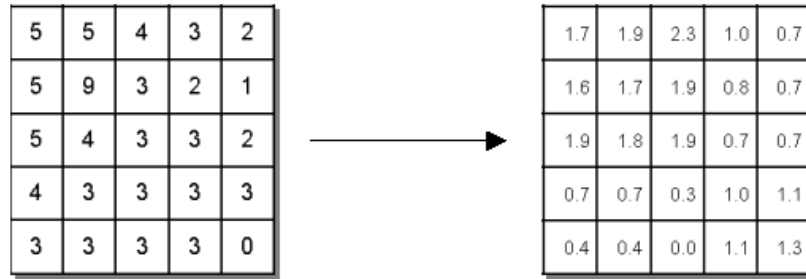
#### **2.4.4 Variance in Slope**

The final topographic screening algorithm begins with the slope calculated in the previous section. Using the slope values calculated above, an estimate of the variance of the slope of all cells within a 25-cell radius is computed. Areas where the standard deviation (square root of the variance) exceeds 20 degrees are extracted from the data set. As in the case of the previous filter, the theory is that the natural terrain will have a much more gradual change in slope. Unlike the previous filter, the variance in slope filter extracts entire areas surrounding sites with consistently variable slopes. These areas are typically associated with clusters of buildings. Figure 2-14 shows the grid scheme used to extract cells using this filter.

The effect of this filter can be seen in the last image in Figure 2-15. Much of the area removed had been removed in the previous steps. However, this procedure extracts large areas around tall buildings, ensuring that elevations affected by shadowing and lag effects are not left in the bare earth data set.



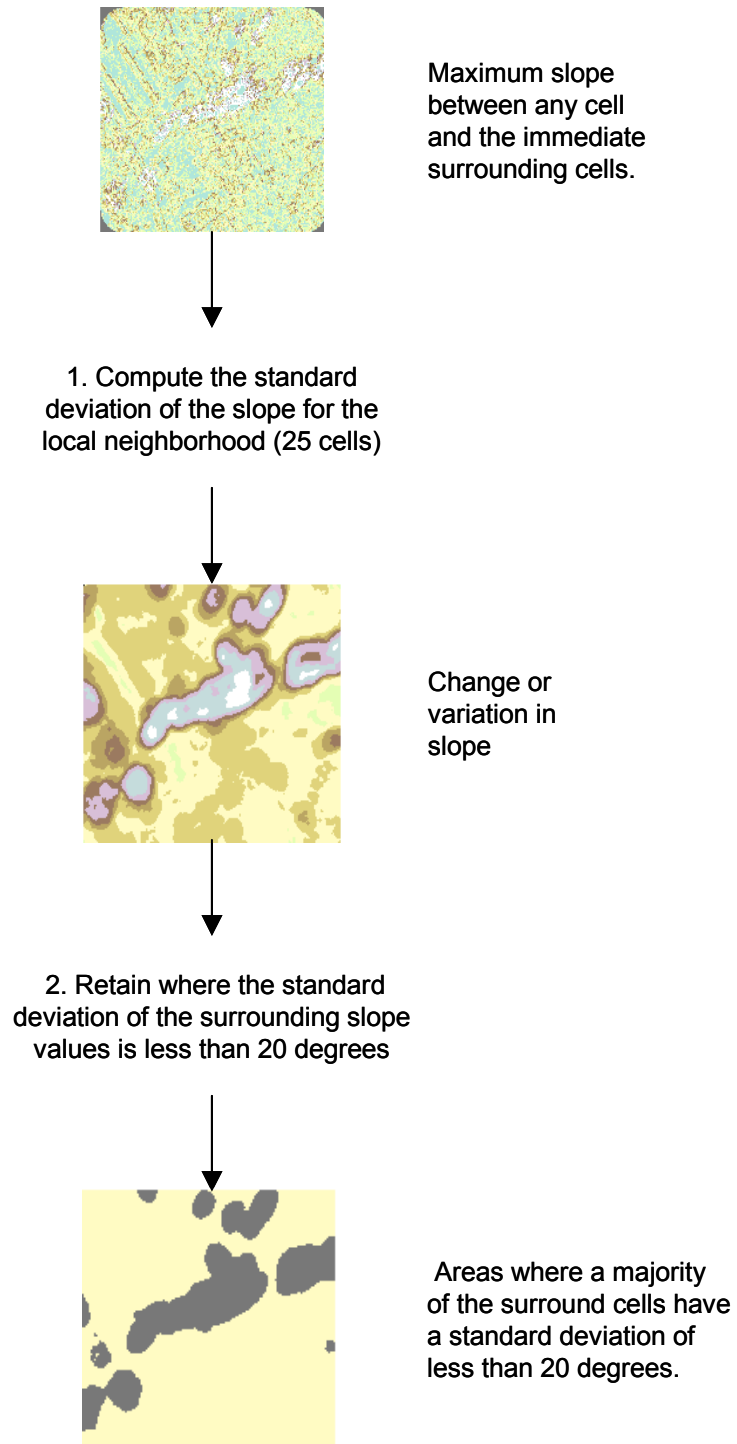
**FIGURE 2-13 Maximum Slope Filter**



**A. SAR data before Filter**

**B. SAR data after Filter**

**FIGURE 2-14 Results using the Variance in Slope Filter**

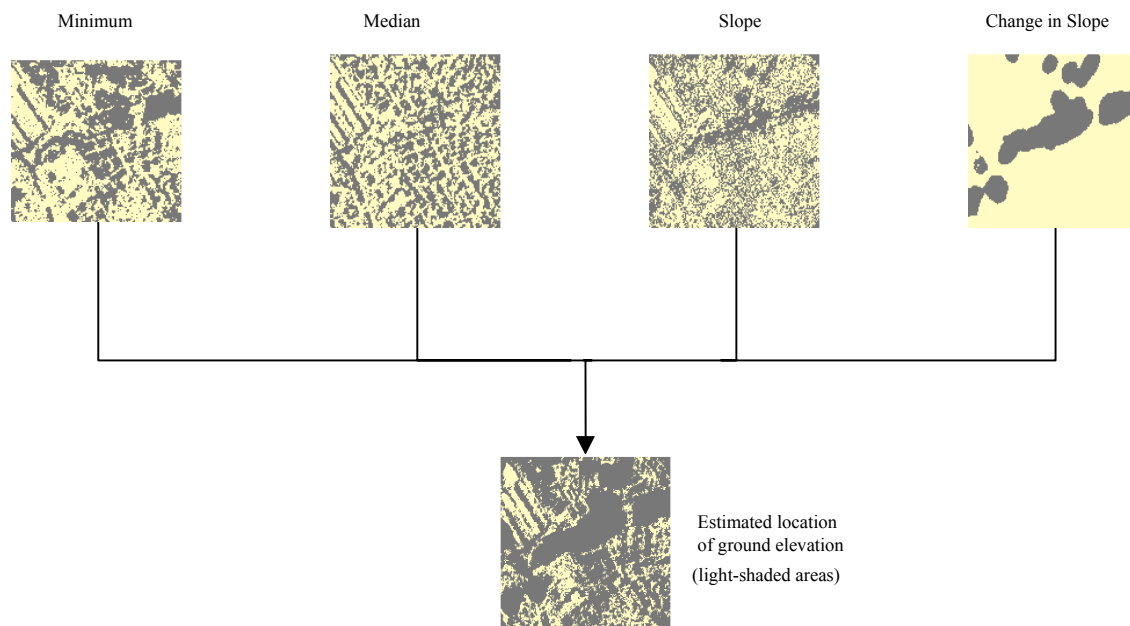


**FIGURE 2-15 Removing Cells where the Standard Deviation is greater than what would be expected from the Natural Terrain**



## 2.5 Combining the Filters

The results of the four topographically-based filters are combined with a Boolean "AND" operation (see Figure 2-16). If an area is found unlikely to be ground in any of the filters, it is extracted. Because a wayward elevation associated with the top of a building can raise the ground level significantly, it is safer to error on the side of extraction than inclusion. Notice in the Wilshire Boulevard example how the individual filters appear to fall short of extracting all of the cells associated with buildings and trees, but together, the filters appear to work to well in extracting a significant portion of the built environment.

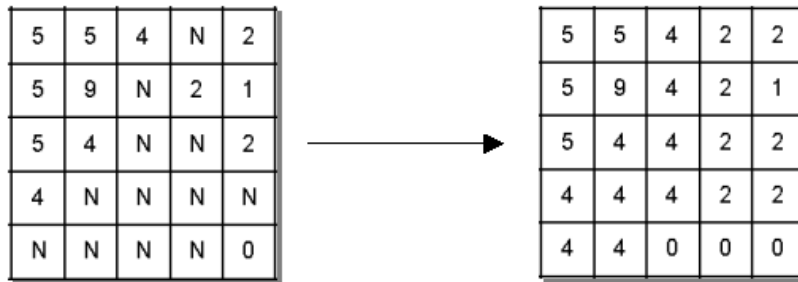


**FIGURE 2-16 Multiple Criteria Algorithm for Screening Out Cells likely to be associated with Trees and the Built Environment**

## 2.6 Allocation and Smoothing

The cells classified as the ground elevation form the basis of the Bare-earth algorithm. Once the bare earth regions are established, the digital elevations from the cleaned and smoothed DEM are placed into a separate grid cell layer. The ground elevations of the cells that were removed during the process of estimating ground height are now populated with the value of the nearest cell. This distance is measured as the distance from cell center to cell center in real world

coordinates, as opposed to cell coordinates. The height of the cell is not factored into the distance computation. If a cell is at an equal distance from two or more sources, it is assigned to the source that is first encountered in the algorithm. Figure 2-17 presents sample results from the Euclidean algorithm.



**a. SAR Data before Filter**

**b. SAR Data after Filter**

**FIGURE 2-17 Results of the Euclidean Allocation Filter (N=No Data)**

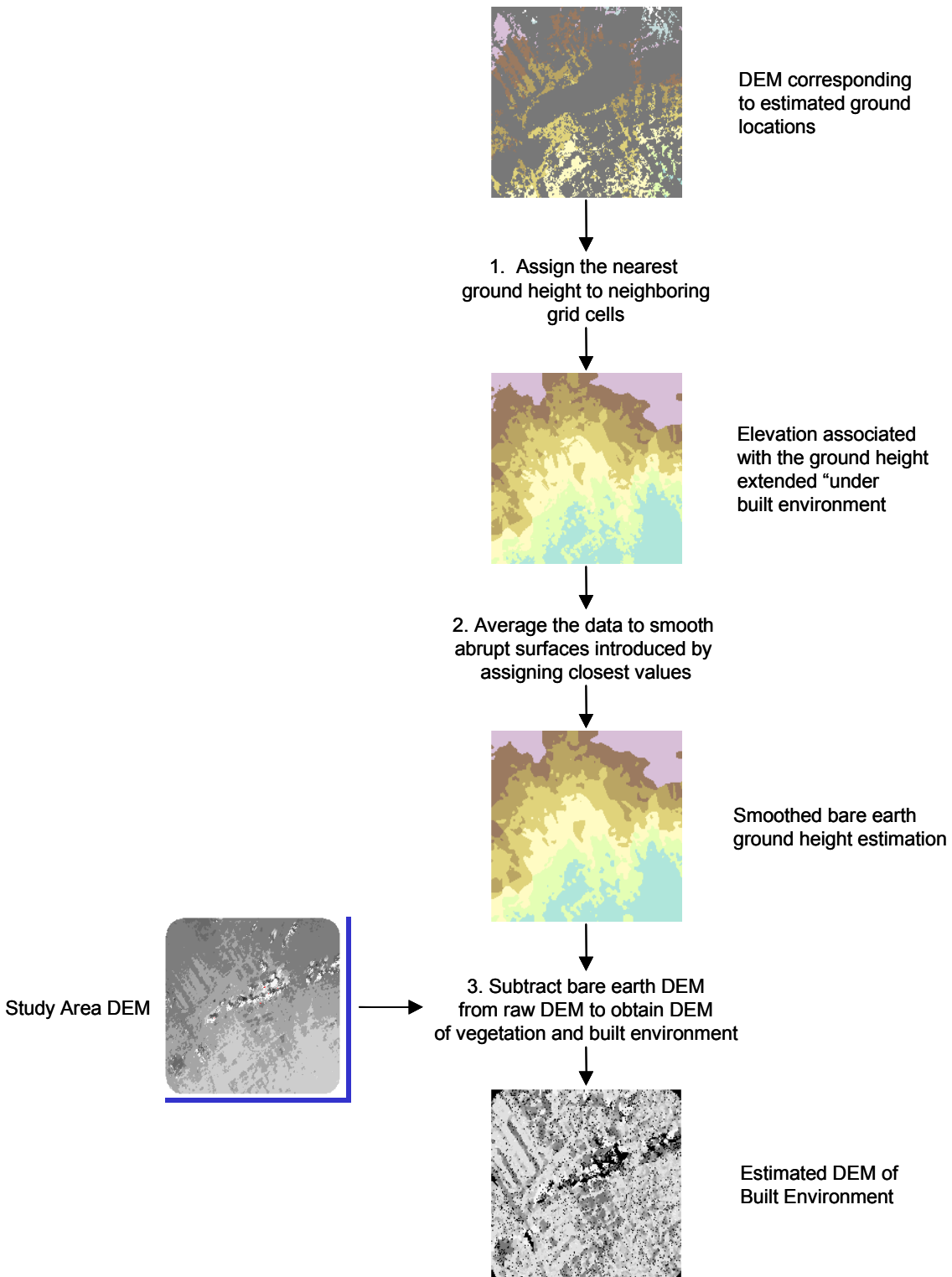
The Euclidean distance allocation serves to expand the calculated ground DEM values to those areas covered by vegetation and the built environment. Several interpolation algorithms were investigated in depth for an area surrounding the UCLA campus. This study area includes some of the sharp topography directly north of the campus. Algorithms that were investigated include spline, trend, inverse distance weighted, and several types of kriging (without the examination of semi-variograms). An *Avenue* program was written to vary the parameters of these interpolation options in ArcView and the results were exported to a spreadsheet. More than 136 images were generated for ten test regions.

Spatial interpolation is used in geostatistics to extrapolate a series of point samples into a surface, often over very long distances. It is useful in other applications that require the interpolation of sparse sample data for decision-making, such as business geographics. All of the interpolation algorithms attempt to predict the value at a given location based upon the trend of the surrounding data. The underlying principle used in these algorithms is that points close together in space are more likely to have similar values than points further apart (Tobler's Law of Geography). The equations vary in effect from honoring abrupt changes in the surface to

creating a very smooth, gradual elevation that might actually pass through very few of the sample points. Each equation has variables that must be optimized.

Ten test areas were each analyzed with a series of interpolation algorithms and the results were compared with the USGS ground elevation data. All of the algorithms depend in one way or another on a specified search radius or on a number of surrounding points. Assigning one number or one radius within which to search for a trend was not feasible, given the diverse topographical makeup and data density. An optimal value could possibly be achieved through a “neighborhood” analysis. We found that regardless of which values we chose, the interpolation algorithms typically amplified any errors in the data, rather than dampened them. Creating a customized linear interpolation algorithm that detected and minimized the effects of residuals might provide a more accurate Bare-earth algorithm. However, we found that an assignment to the closest cell was by far the most effective method of creating a surface from the ground elevation points.

The last step in creating the bare earth elevation is to average the data to smooth abrupt surfaces introduced by assigning the closest value. This function also serves to “soften” the effects of elevations associated with buildings or vegetation that may have been missed by the screening process. The completed bare-earth elevation is subtracted from the cleaned and filtered SAR data, resulting in an estimation of the elevation associated with vegetation and the built environment. This process of using Bare-earth algorithms to identify the heights of buildings is presented in Figure 2-18. The following section provides a detailed discussion on the procedures used to validate the Bare-earth algorithm.



**FIGURE 2-18 Methodology for using the Bare-Earth Algorithm to Estimate the Heights of Buildings**

## **SECTION 3**

### **VALIDATION OF THE BARE-EARTH ALGORITHM**

Validation of the Bare-earth algorithm was accomplished using GPS data, NGS (National Geodetic Survey) data, USGS DEM elevations, aerial photographs, raw SAR data, GIS databases, tax assessor databases, and observed data. As is typical with projects involving geospatial data, the validation process involved setting up various experiments to test the algorithms and then adjusting the variables based on the results of the tests. In these experiments, the control points were observed ground and building locations in aerial photographs. Agreement between the various sources was determined through both visual inspection and statistical analysis.

#### **3.1 Spot Checking Elevations with GPS Data**

By spot-checking our locations with a GPS unit at various sites around the University of Southern California (USC) campus, we were able to confirm that the USGS aerial photographs were registered with the TIGER street database (1990 census data) and the SAR data provided by Intermap Technologies. Although the USGS DEMs were too coarse to establish precise horizontal registration, the elevations were in agreement with the SAR data. The GPS readings were established using a Magellan ColorTRAK unit. Latitude and Longitude were recorded in the WGS 84 datum. Each location recorded involved at least a minute of averaging signals and at least four satellites. The locations chosen for calibration were landmarks that were not surrounded by features that could obstruct the SAR measurements. These landmarks included locations on the football field, the tennis courts, intersecting streets, and other identifiable objects in open areas.

The hand-held GPS unit provided very precise horizontal coordinates. However, the unit failed to provide the vertical accuracy necessary to establish a reasonable elevation. Some GPS data points were continually averaged in one location for a period of about fifteen minutes. Even with this averaging, vertical readings fluctuated by over twenty meters. The vertical accuracy of the unit was not listed in the documentation, but generally, the vertical accuracy of GPS units is much worse than the horizontal accuracy (Gilbert, 1997). Because there are often several

satellites broadcasting signals from several different horizontal directions from the user at any given point in time, GPS units are able to triangulate an accurate horizontal position. However, in the vertical direction, there are only satellite units above, and at approximately the same distance, so triangulation is much more problematic. We are investigating the feasibility of obtaining more accurate elevation readings using differential GPS.

### **3.2 Comparing Elevations with National Geodetic Survey Data**

The National Geodetic Survey (NGS), a division of the National Oceanic and Atmospheric Administration (NOAA), collects precise measurements of latitude, longitude, and elevation of sites above mean sea level. These data are made available in Digital Survey Data files. The vertical accuracy of these data is generally on the level of less than a foot. However, the data do not necessarily correspond to ground level elevations. All of the surveyed points are accompanied by text descriptions approximately a page long. A program written by ImageCat was used to extract the coordinates from the descriptive data, but the textual descriptions were not reviewed to determine which markers corresponded to the ground height. For example, one of the data points used contained the description "The bronze bench mark disc, in the top of the north abutment of the concrete bridge over the Arroyo Calabasas flood control channel". Another stated, "Set in the south end of the west concrete headwall for Bell Creek flood control". Since these points often do not represent ground level, fieldwork would be required to measure the height above ground level. The results of the following analysis, however, indicate that most of the points in this database are likely to represent a ground location.

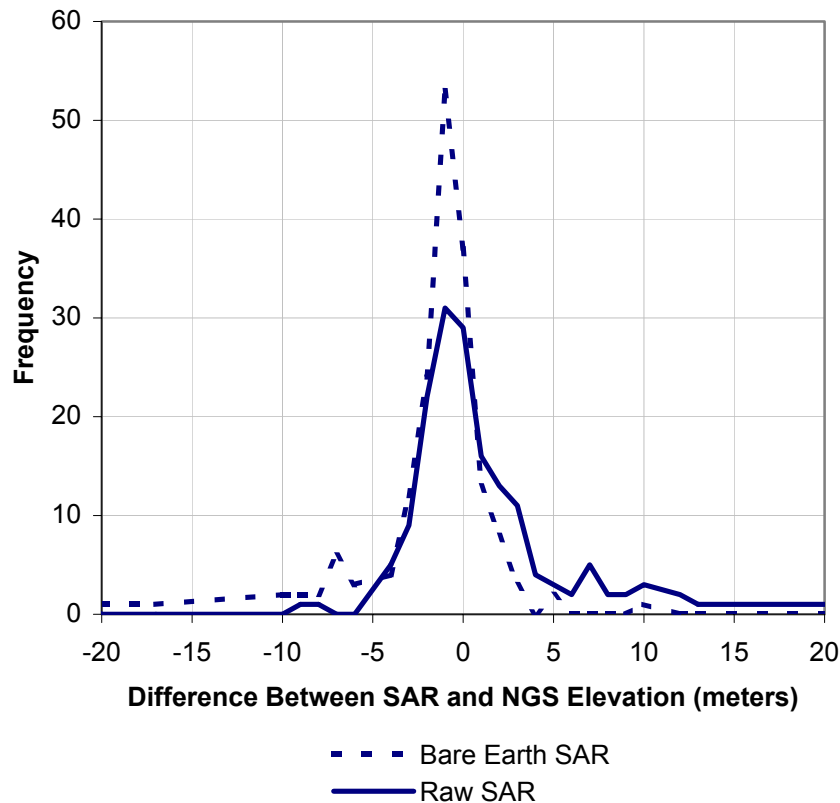
The survey data can be downloaded from the NGS website by USGS quadrangle ([http://www.ngs.noaa.gov/cgi-bin/ds\\_quads.prl](http://www.ngs.noaa.gov/cgi-bin/ds_quads.prl)). The survey data covering our study regions were downloaded and the points that fell within the bounds of the SAR data were cross-referenced with the raw SAR and bare earth elevation data.

179 points fell within the geographic region of our SAR data. Unfortunately, six surveyed points did not have an associated NGS height, and eight points did not have a raw SAR height associated with them because of problems in the data. Because of the large elevation difference between the San Fernando Valley and the Los Angeles basin, the remaining elevations were

separated into two sets of data. 129 of the remaining 165 points were located in the Los Angeles Basin, or the Downtown Los Angeles, Hollywood, and Santa Monica regions. The remaining 36 points were located in the San Fernando Valley.

The error associated with the raw SAR data, as reported by Intermap, is an absolute value of 1.5 to 5 meters (one standard deviation). That statistic was based on an analysis of a sample that included the highest elevations observed for single buildings, and not on a random collection of ground points. The accuracy of the bare-earth data, in comparison to the NGS data is very impressive given the noise level of the raw SAR data and that the NGS points do not always correspond to ground level elevations. A more accurate assessment of the NGS database could be performed by reading the text and extracting only those survey points that definitely qualify as ground level, such as those located on sidewalks. Many of the markings were on freeway overpasses and bridges over flood control channels. These could be extracted and the analysis redone. This would involve, however, sorting through hundreds of pages of descriptive text.

Figure 3-1 displays a histogram showing the difference between the SAR and the NGS survey data, for both the bare earth and the raw data. The majority of the data falls between three or four meters, which is consistent with the reported error of the SAR data. The Bare-earth algorithm decreases the absolute difference in most areas. Where the difference in elevation is very high, the NGS markers are probably not on the ground.



**FIGURE 3-1 Histogram Showing the Difference between SAR and NGS Elevations at Survey Data Points (165 locations)**

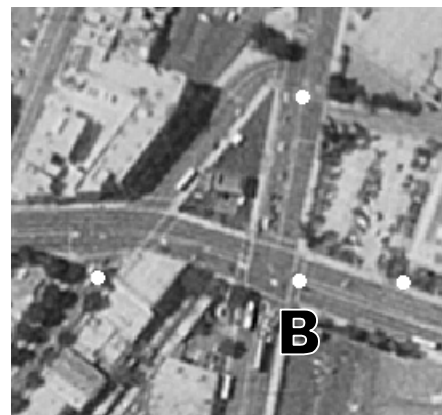
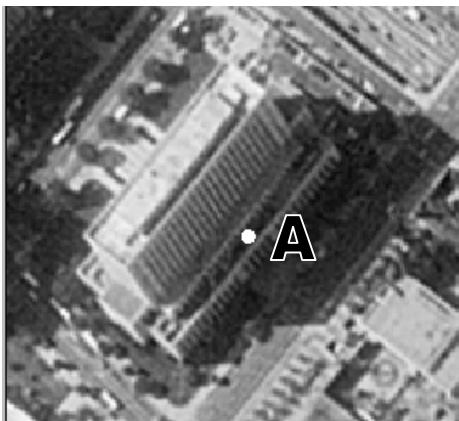
It is interesting to note the peaks around -7 meters in the bare-earth SAR data and 7 meters in the Raw SAR data (see Table 3-1). Seven meters is about the height of a bridge or a freeway overpass. To examine the possibility that a bridge or overpass may be the cause of the 7-meter spikes, the 11 sample points with an absolute difference of 7 meters were extracted from the database. Six of the 11 sampled points were identified as freeway areas. A review of the descriptions revealed that all of these locations were associated with onramps or freeway intersections. Of the remaining five, three were survey points associated with major street intersections. In these cases, the raw SAR elevation was 7 meters higher than the surveyed point, perhaps due to noise, stoplights or bridges. In two of the three major intersections, applying the Bare-earth algorithm brought the difference between the SAR elevation and the surveyed elevation to zero; in the other case the error was 2 meters.



**TABLE 3-1 The Difference between SAR and NGS Elevations (in meters)  
of Digital Survey Data Points (all locations)**

Difference	-7	-6	-4	-3	-2	-1	0	1	2	3	4	5	6	7
Bare Earth SAR	6	3	4	12	24	53	37	13	8	3		2		
Raw SAR			5	9	22	31	29	16	13	11	4	3	2	5

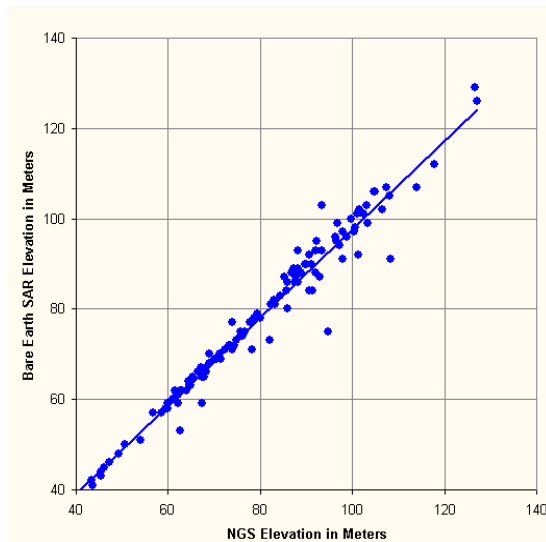
The remaining two points were areas in which the SAR elevations were 7 meters lower than the surveyed data. One of these data points fell directly on top of the first floor of the Los Angeles courthouse, as can be seen in Figure 3-2, photograph A. The accompanying descriptive text states that this point should actually be "1.4 feet south of a brass handrail" in front of the building. In the second case (point B), the surveyed point illustrated some of the difficulties discussed in previous sections. The point was located in an area of downtown Los Angeles where the ground transitions from a flat area to a steep terrain (Macy Street and Spring Street). The raw SAR height was 37 meters below the surveyed elevation, and the corresponding correlation was 0.74. The Bare-earth algorithm did a good job of bringing this error to within a tolerable level. This point is represented in Figure 3-2 as point B. The three survey points (shown as white solid circles) surrounding point B had an error of less than a meter, indicating that this error would have little or no impact on the measurement of building height.



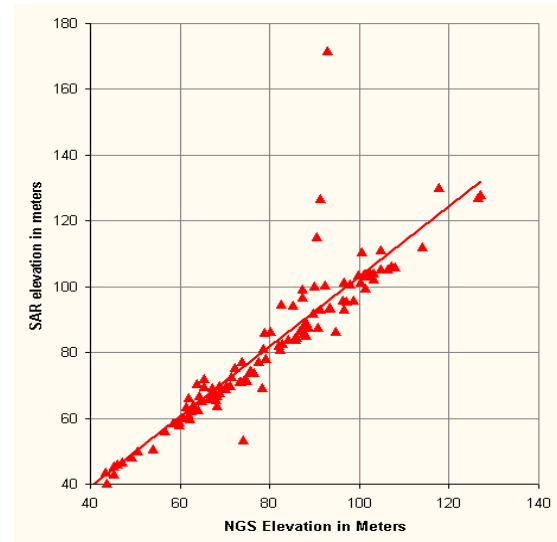
**FIGURE 3-2 NGS Survey Points where SAR Bare-Earth Elevations were 7 meters below  
the Surveyed Elevation**

A one-to-one comparison of the bare earth elevation to the NGS elevation in the Los Angeles area revealed a linear relationship between these data with a slope close to one and an intercept close to zero (see Figure 3-3). The equation for the best linear fit was  $y = 0.9821x - 0.3681$  with an  $R^2$  of 0.9807. If the y-intercept is constrained to zero, the equation becomes  $y = 0.9776x$  with an  $R^2 = 0.9807$  again. The y-intercept is close to zero here, indicating that there does not seem to be a systematic vertical shift in the two data sets. The average residual difference between the bare earth and the NGS survey data was -1.5769, with a standard deviation of 4.3543. Figure 3-4 shows a similar plot using the raw SAR elevation data.

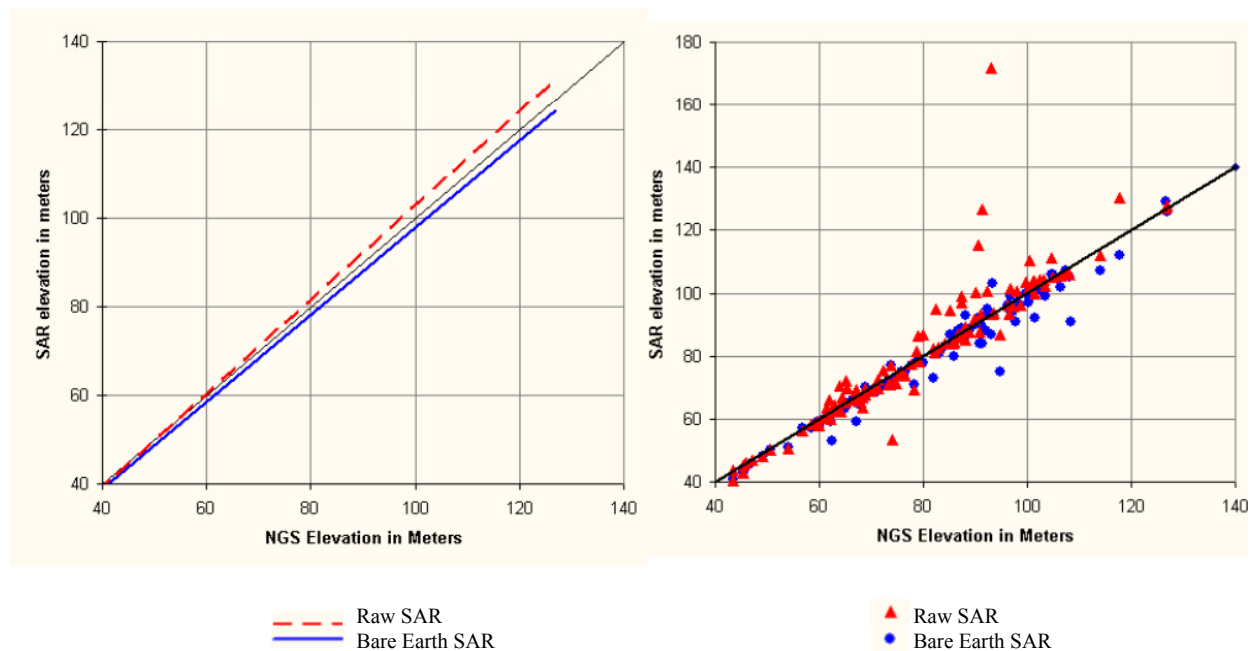
Figure 3-5 shows a comparison of the SAR versus NGS curves for both a raw SAR and bare-earth condition. We can see in the left-hand figure that the trend of the raw SAR data is slightly above the surveyed data and the trend of the bare earth data is slightly below the height of the surveyed data. The trends vary only slightly from an ideal match, which is shown as the 45-degree line. The scatter plot in the right-hand frame of Figure 3-5 shows a distribution of raw SAR and bare earth data points plotted as a function of the NGS data. As illustrated in the left-hand figure, the raw SAR data (triangles) are generally higher than the bare-earth (circles) elevations. Figure 3-6 illustrates the same trend for the San Fernando Valley.



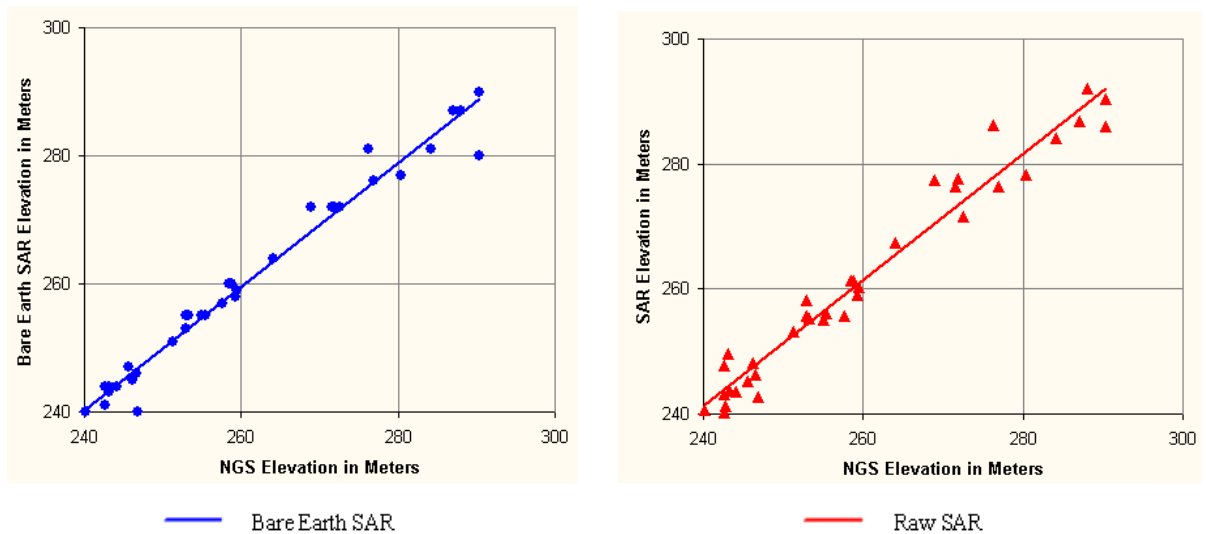
**FIGURE 3-3 NGS and Bare-Earth SAR Elevations at Survey Data Points in the Los Angeles Basin**



**FIGURE 3-4 NGS and Raw SAR Elevations at Survey Data Points in the Los Angeles Basin**



**FIGURE 3-5 NGS, Raw SAR and Bare-Earth SAR Elevations at Survey Data Points in the Los Angeles Basin**



**FIGURE 3-6 NGS, Raw SAR and Bare-Earth SAR Elevations at Survey Data Points in the San Fernando Valley**

This comparison with the NGS data demonstrates that the Bare-earth algorithm smoothes out the raw SAR data and brings the SAR data into agreement with the more precise surveyed data. Some discrepancies between elevations produced by the Bare-earth SAR algorithm and those recorded in the NGS surveyed data can be traced back to freeway overpasses and in one case, a hillside.

### 3.3 Comparisons with USGS 30-Meter DEM Data

The USGS 30-meter DEMs essentially cover most of the populated areas of the entire country. They can be downloaded at [http://edc.usgs.gov/doc/edchome/ndcddb/7\\_min\\_dem/states/CA.html](http://edc.usgs.gov/doc/edchome/ndcddb/7_min_dem/states/CA.html). These data have a vertical accuracy that varies from region to region and generally depends upon the slope of the terrain. The quoted RMS error for "level 1" accuracy is as high as 15 meters, although most of these areas have a RMS error of 7 meters. RMS error is assessed and reported by 7.5-minute quadrangles. These quadrangles correspond to the USGS grid for topographic maps. Elevations for comparison were gathered from a series of at least 28 control points. Elevations at the control points were taken from "...field control, aerotriangulated test points, spot elevations, or points on contours from existing source maps with appropriate contour interval" (USGS, 1995).

Through discussions with scientists at the USGS National Mapping Division, it was determined that these control points are generally not saved in any format; not even on paper. It was also determined that the RMS error quoted in the literature does not pertain to the error between the elevation reported and the true ground elevation. In fact, no such estimates are available (Bottlemy, 2000; Benson, 2000). The threshold value of 1/2 the contour interval quoted pertains to the error that exists between the DEM and the paper maps for Level 2 DEMs. Level 1 DEMs occasionally have errors estimated from ground truth data, and sometimes the given RMS error is associated with the error between the paper map and the DEM, depending on the methodology used to derive the DEMs, which depends on the year the DEM was created (Merrill, 2001). There is no given error associated with the contours of the paper maps. The error on these maps would depend on the contour interval and other factors, which change from quadrangle to quadrangle. Additionally, errors in horizontal accuracy or datum transformations will greatly impact the accuracy of USGS DEMs (Garbrecht, 1999)

The spatial resolution of the USGS DEM data is much coarser than the 2.5-meter posting that is associated with the SAR data. Thus, it cannot be used in place of the Bare-earth algorithm. However, the USGS DEM data provide another source of information to validate the Bare-earth algorithm, especially in flatter regions. The bare-earth elevation was validated using the USGS 30-meter DEMs by analyzing the height differences at street intersections, and through visual inspections. A description of these comparisons is given below.

In instances, where data sets were analyzed individually, it was possible to examine the applicability of the USGS elevations on a case-by-case basis. In terrain where the elevations change rather rapidly, a comparison with the USGS data is not appropriate. In flat terrain, especially in areas where there were many buildings, the USGS does provide an additional source of data for comparison. It was generally possible to visually assess the transects and determine the applicability of the USGS data. For street intersection elevations in the Santa Monica study region, this was not an issue. In mountainous areas, the differences became more apparent. The lower resolution of the USGS data is also fairly easy to assess visually. Changes in elevation might be represented in discrete steps when compared to the SAR data.

### 3.3.1 Visual Inspection of Selected Sites or Areas

A series of ten study areas were established to test the results of the Bare-earth algorithm. These ten study areas were also used to optimize the variables in the algorithm. The size of each study area varied from very small, such as the area surrounding the Los Angeles Convention Center, to very large regions in the San Fernando Valley. Study areas were chosen because of their significant natural and cultural features that can often influence SAR-derived elevation data. Table 3-2 lists the locations of these ten study areas along with brief descriptions as to why they were chosen.

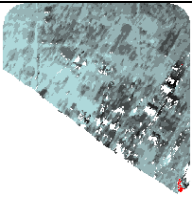
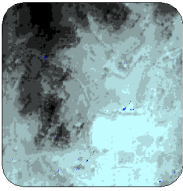
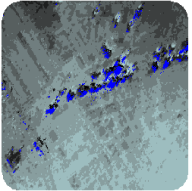
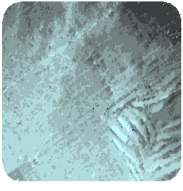
The ArcView programming language *Avenue* was used to export thumbnail images of the maps from each region. Visual Basic was used to arrange these images in a large spreadsheet that was printed for visual inspection. The *Avenue* code was also used to create images of every spatial variable in the final Bare-earth algorithm, as well as spatial variables that were discarded. Several topographic parameters were generated and investigated for their potential effectiveness in detecting ground elevations. A sample of the images cataloged in the spreadsheet is provided in Table 3-3. Thematic shading was done using an equal area range assignment. Although the ranges are not equally spaced (e.g. 25, 50, 75, 100) or rounded for quick interpretation (10, 30, 50, 100), this scheme allows for optimal visual interpretation. Table 3-3 presents the reader with a sample of various parameters computed while developing the Bare-earth algorithm. It was very useful to examine each aspect of the algorithm independently, and cross-reference each aspect with other parameters visually.

The larger spreadsheet used to create Table 3-3 was integral in developing the Bare-earth algorithm. As theories for extracting the bare earth were discussed, additional parameters were added to the spreadsheet, along with summary statistics. Transects were taken and graphed for each area (for a more in depth discussion of the transects, see Section 3.3.2). Scatter plots were then generated and correlation coefficients computed for each transect.

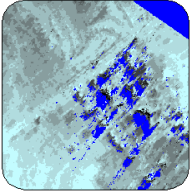
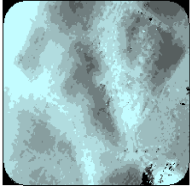
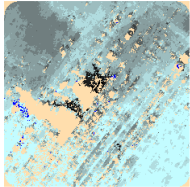
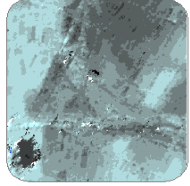
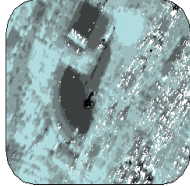
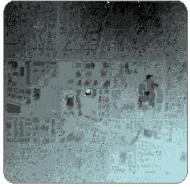
The spreadsheet was useful in optimizing the variables of the Bare-earth algorithm. For instance, an *Avenue* program was written to vary the search radius for the neighborhood median criteria. The corresponding bare-earth elevations were created for each of the study areas. The

difference between the USGS DEM and the bare-earth elevations was computed and areas classified as ground surface using each criterion were overlaid onto USGS aerial photographs. This analysis allowed the project team to detect when the neighborhood search radius was too small (i.e., leaving area on buildings) and when it was too large (the resulting ground data was too sparse).

**TABLE 3-2 Study Areas chosen for evaluating Bare-Earth Algorithm**

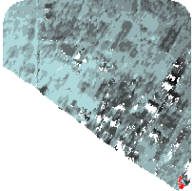

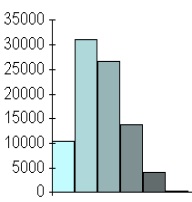
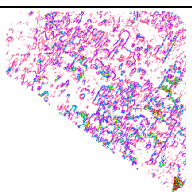
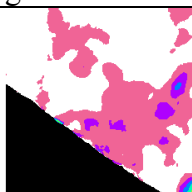
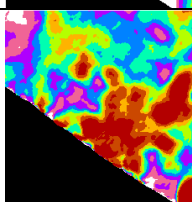
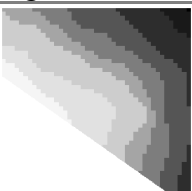

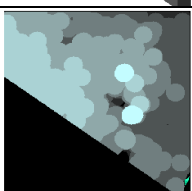
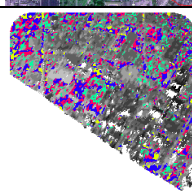
<b>Study Area</b>	<b>Description</b>	<b>SAR DEM</b>
<b>USC</b>	USC Campus. Slight slope with many buildings. Moderate shadowing problems. Near sensor. Low correlation.	
<b>UCLA</b>	Edge of the UCLA Campus. Some campus buildings and houses, leading up into very hilly terrain.	
<b>Wilshire Blvd.</b>	The "Miracle Mile" area. Several isolated high-rise commercial structures along the boulevard. Region varies topographically. There are many large apartments and houses as well.	
<b>W. Pico Blvd &amp; S. Beverly Glen Blvd</b>	Mostly residential with some big apartments and movie studios. Moderate terrain changes. There is also a big park in the area.	

**TABLE 3-2 Study Areas chosen for evaluating Bare-Earth Algorithm (continued)**

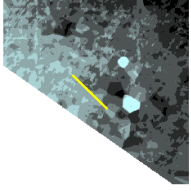
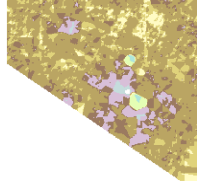
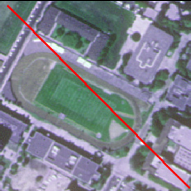
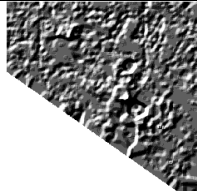
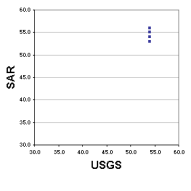
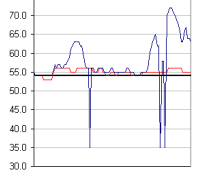
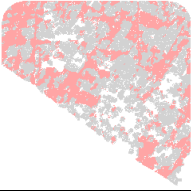
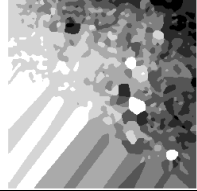
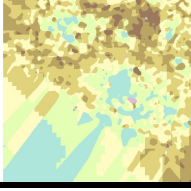
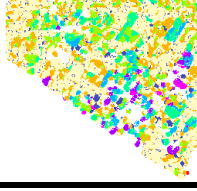
<b>Study Area</b>	<b>Description</b>	<b>SAR DEM</b>
<b>Century City</b>	Small cluster of high-rise buildings in moderately hilly terrain.	
<b>West of Dodger Stadium</b>	Very hilly area west of Dodger stadium.	
<b>Downtown</b>	Moderately hilly area with tall buildings. Bad shadowing.	
<b>Santa Ana / Santa Monica / Golden State freeway interchange.</b>	Freeway interchange in an industrial area.	
<b>Convention Center</b>	Large Building	
<b>San Fernando Valley</b>	Residential, commercial mix. Gently sloping.	



**TABLE 3-3 Sample of Image Catalog and Statistical Profile Generated for the USC Study Region**

A. Region Name	USC	B. Description	USC Campus. Slight slope with many buildings. Moderate shadowing problems. Near radar sensor. Low correlation.
C. Map of SAR DEM		D. Map of Average Height of SAR DEM	
E. Histogram of Elevation data		F. Statistical Summary of the Elevation Data	Rows = 529 Cols = 514 N = 249458 Mean = 24.208364 SD = 4.6451 Min = -39.5255 Max = 82.1399 Range= 121.6654
G. Map of Slope		H. Map of Mean Slope for a 25-Cell Radius	
I. Slope Statistics	RMean = 14.8579945 SD = 12.98890 Min = 0.00000 Max = 83.00000 Range= 83.00000	J. Map of Standard Deviation of Slope 25-Cells Radius	
K. USGS DEM		L. USGS aerial photo	
M. Map of Local Minimum 25-Cells Radius		N. Points Selected for Interpolation on Raw SAR Data	

**TABLE 3-3 Sample of Image Catalog and Statistical Profile Generated for the USC Study Region (continued)**

O. Interpolation Method  Inverse Distance Weighted Nearest Neighbor 12 Power 2		P. Interpolated Surface -USGS DEM	
Q. Profile with Photo		R. Hillshade of Interpolated Surface -USGS DEM	
S. Scatter Plot		T. Profile  — Bare Earth — USGS — SAR	
U. Cells Selected for Average Height		V. Average-based Ground Height (Slope 20, Area Slope 20, Height Within 3 of Minimum)	
W. Interpolated Ground Surface Estimate- USGS DEM		X. SAR Height - Interpolated Ground Height	

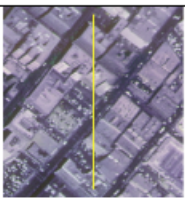
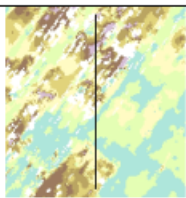
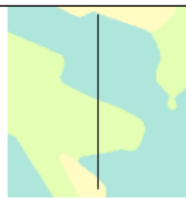

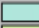
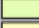


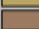
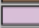



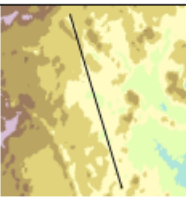

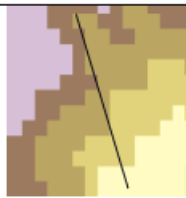

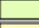

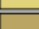
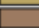



### 3.3.2 Visual Inspections of Transects

To further investigate the local effects of the Bare-earth algorithm, eight linear features were drawn on each of the study areas. These "transects" were drawn over significant features in the data that warranted further investigation. In some cases, they were large buildings, clusters of large buildings, or flat streets. Elevation values from each dataset (i.e., USGS DEM, the raw SAR data, and the results of our bare-earth DEM) were extracted at equal intervals along each

transect line and graphed for comparisons. Thematic maps and images of these data sets were extracted using ArcView and imported into a large spreadsheet with aerial photos. This allowed for an analysis of discrepancies between the visible objects in the photos and bare-earth elevation data.

Table 3-4 contains a sample of images from the larger spreadsheet. Starting with the column on the left, we have USGS aerial photos from two different regions. The region in the first row is a relatively flat area with tall buildings; the second area is the UCLA campus showing a steep hill. Looking at the photographs, you can recognize the features that will affect digital elevation estimates, such as major roads, buildings, trees, and so forth. In the second column, we show the raw, unfiltered SAR elevation data. The heights corresponding to these colors are outlined in the last column. These ranges apply to all of the raster thematic maps. By reviewing the SAR data in relation to the aerial data, it is easy to understand how certain objects affect the elevation data. In the upper row, for instance, the effects of lag and shadowing become clear. Streets are visible as areas of lower elevation. Differences in building heights can be detected both through the shading of the SAR data and through the shadows cast in the aerial data. In the UCLA series (second row), ridges of trees can clearly be delineated in both data sets. The flatter areas can be seen as tennis courts or parking lots.

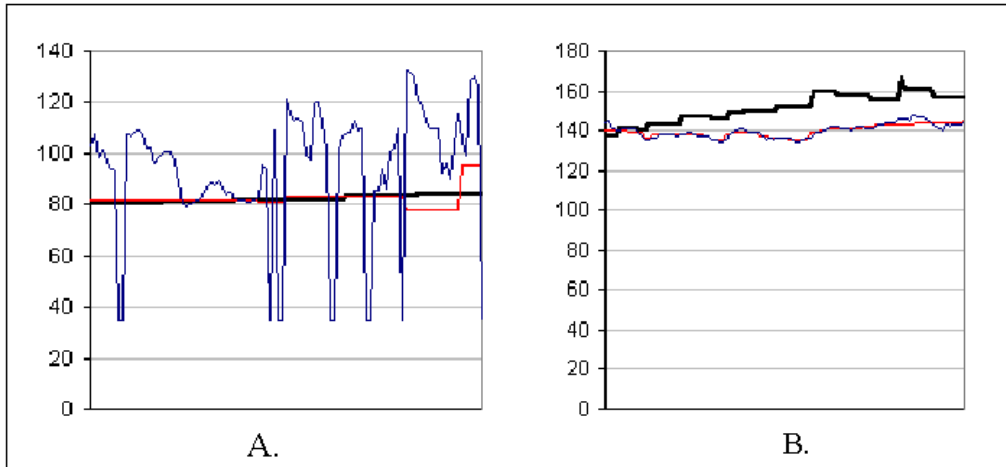
**TABLE 3-4 Elevation Data from a Linear Sample (Transect)**

	USGS Air Photo	SAR	Bare earth	USGS DEM	Legend
A.					<ul style="list-style-type: none"> <li> -92 - 81</li> <li> 82 - 89</li> <li> 90 - 100</li> <li> 101 - 108</li> <li> 109 - 117</li> <li> 118 - 126</li> <li> 127 - 343</li> <li> No Data</li> </ul>
B.					<ul style="list-style-type: none"> <li> 34 - 125</li> <li> 126 - 134</li> <li> 135 - 141</li> <li> 142 - 148</li> <li> 149 - 159</li> <li> 160 - 171</li> <li> 172 - 225</li> <li> No Data</li> </ul>

The results of the Bare-earth algorithm are displayed in the third column. For transect A, the patterns created by the bare-earth DEM are not consistent with what we would expect from ground elevation data because the Bare-earth algorithm has screened out much of the area. The remaining digital elevations are allocated to the surrounding cells creating a map of the bare earth. Still, we can tell that the elevations derived from the Bare-earth algorithm are somewhat consistent with the USGS data shown in the fourth column.

Figure 3-7A shows an elevation profile (in meters) for the transect shown in Table 3-4, line A. The line is broken up into 100 equal segments. The elevation of each point is posted from left to right on the graph. The lightest line corresponds to the SAR data, the medium weight line corresponds to the bare earth data, and the darkest line corresponds to the USGS data. We can see that although there are discrepancies between the USGS and the bare-earth data, the USGS data provides a good source of comparison. Though looking at this graph, it would be very difficult to predict the elevation of the ground using SAR data alone.

In Figure 3-7B, which corresponds to Table 3-4 line B, there is a much wider discrepancy between the USGS data and the bare-earth data. By comparing the bare-earth data to the SAR data, we can see that there is little variance in these two data sets. By examining the aerial data for this same area, we see that most of the elevations along the transect are associated with the ground. Although we cannot determine from the available information whether the SAR or the USGS data is more accurate, we can assume that this discrepancy is the reason for the variations seen in Figure 3-7B. These two examples illustrate that although the USGS DEM provides an important source of comparison, it is not an appropriate source of data for estimating bare-earth elevations.



**FIGURE 3-7 Graph of Elevation Values Along a Transect**

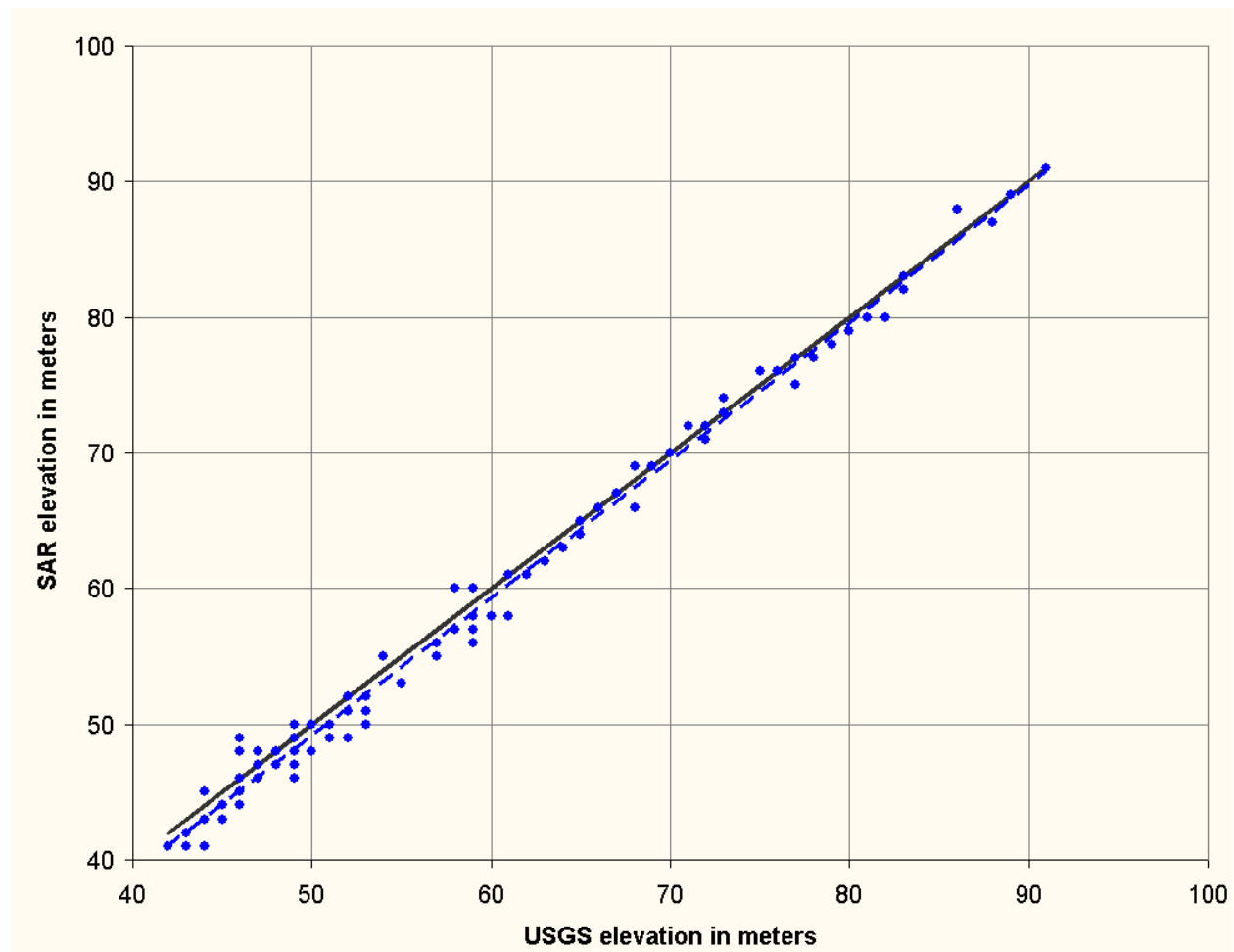
### **3.3.3 Comparison of Elevations at Street Intersections**

The SAR elevations were also compared to the USGS DEM data by examining elevations at street intersections. We felt that intersections would be good points of comparisons because of the high likelihood of actually locating and comparing ground elevation points. The spatial extent covered by this limited analysis was a one-mile square area that included a residential section of Santa Monica. We chose this area because we had canvassed the heights of buildings in this area in another phase of this study. Thus, we were familiar with the terrain and buildings in this neighborhood.

A street database (extracted from the 1990 TIGER census files) was first overlaid onto USGS aerial photographs. Because TIGER data is sometimes lacking in accuracy, the streets were adjusted so that the street centerlines corresponded with the center of the streets in the USGS aerial photograph. The nodes that intersected two or more line segments were extracted and written to a separate point file. This point file was used to compare elevation data from the Bare-earth algorithm and the USGS DEM database. In addition, we eliminated any intersections that included heavy vegetation (such as trees). Aerial photos were used to perform this extraction. In the end, we were left with a little over 100 points (or intersections) to perform these comparisons.

We also used this exercise to examine the relative difference in elevation between the ground and what we perceived to be the heights (or roofs) of single-family dwellings. To some extent, this was also a check on the relative error of the raw SAR measurements. That is, if no difference was seen between ground-based SAR elevations and the elevations associated with structures, then it would be difficult to characterize the heights of short structures or buildings.

The first scatter plot is displayed in Figure 3-8. SAR-derived bare-earth elevations are plotted along with the corresponding USGS DEM elevations. There are two lines on the graph, the solid one indicates the line of perfect agreement, i.e., there is exactly a one-to-one correspondence between the two datasets. The dashed line indicates the best linear fit of the data using least squares approach. The two lines are essentially indistinguishable from each other at the higher elevations. For the lower elevations, these lines are still very close. The equation for the best-fit line is  $y = 1.017x - 1.7071$ , where  $r^2 = 0.9925$ . The negative intercept indicates that for the best fit, the USGS registers a higher elevation than the SAR data. This may be due to a different interpretation of "sea level" elevation of 1.7 meters, or it may be due to an error in either of the data sets. This difference is inconsequential for the bare-earth algorithm, as it will not affect the calculated height of the building. In this limited analysis of the Santa Monica area, the correlation coefficient was very high. This implies that although there may have been a small vertical shift between the two data sets, there is very high correlation between data sets. Given the small scaling, the data sets were in strong agreement on the location of the ground elevation. This underscores both the success of the algorithm and the need to compute the bare earth, rather than use a different data set, such as the USGS DEM.

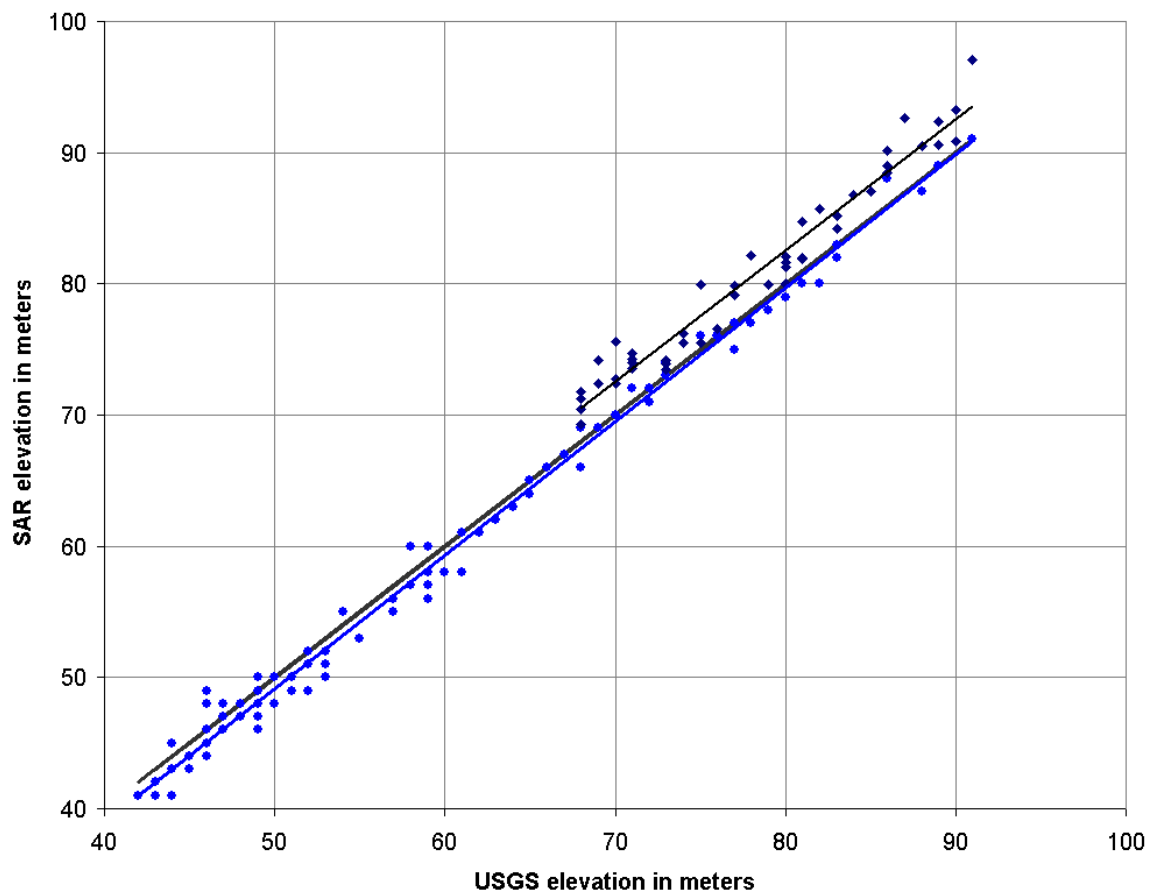


**FIGURE 3-8 USGS DEM and Bare-Earth SAR Elevations at Street Intersections (Santa Monica Area)**

In Figure 3-9, a small sample of rooftop elevations has been added to the previous data set. The elevation each rooftop was estimated by taking the maximum or highest observed SAR elevation within the building footprint. These values are represented in the figure by the dark diamonds. The reason why the new data points only show up at the higher elevations is because the selected study area was located in the more hilly part of Santa Monica. Approximately 40 structures were included in this limited analysis.

This simple analysis shows that all of the elevations associated with rooftops are higher than the mean line representing the bare earth. The equation of the least squares fit of the rooftop data is  $y = 1.0011x + 2.4129$ . The y-intercept in this last equation is roughly 4 meters higher than the

previous intercept. This corresponds to about 12 feet, or roughly the height of a one-story building, given the slightly reduced height of single story buildings in SAR data (due to mixed pixel effects and error). The conclusion from this comparison is that the SAR-derived bare-earth estimates of ground elevation compare very favorably with the USGS DEM data and that there is enough difference between the bare earth results and the raw SAR elevations of rooftops to conclude that building heights can be detected using SAR technology.



**FIGURE 3-9 Comparison of SAR-derived Bare-Earth Elevations with the Heights of Single-Family Dwellings, as determined through use of Raw SAR Data**



## SECTION 4

### GENERATING THE BARE EARTH TERRAIN USING SAR TECHNOLOGY

To test the application of the Bare-earth algorithm to larger regions, we applied our methodology to three areas of Los Angeles: a portion of the San Fernando Valley, Downtown Los Angeles, and the Wilshire Blvd./Santa Monica area. The extent of our study areas is displayed in Figure 4-1. There are over 212 square kilometers of data within the three regions. Quantifying the bare- earth terrain for an extended area allowed us to investigate how the algorithm would perform in a variety of situations. Intermap data was purchased for three noncontiguous areas. These areas were selected because of their diversity in terms of development types and density. The data surrounding downtown Los Angeles, for example, contain a dense core of very tall buildings as high as 1,000 feet.



**FIGURE 4-1 Study Areas**

The Downtown area of Los Angeles is very typical of many large U.S. cities. You have a mix of very tall commercial office buildings and smaller, shorter retail establishments. You also have large pockets of industrial buildings. Just a few miles away from the center of downtown, you have single- and multi-family residential areas. These areas are essentially the older areas of Los Angeles, with many blocks developed prior to the 1920's.

The San Fernando Valley is considered a suburb of Los Angeles, although it is within the city of Los Angeles and constitutes a substantial portion of the population of the city. The area was developed primarily after World War II; there is also a lot of recent construction, i.e., post-1970. Like much of the development in America during this time period, the San Fernando Valley is characterized by expansive areas of single-family, residential dwellings crossed by main thoroughfares lined with malls and large commercial or industrial buildings. This area was chosen as an example of this type of development.

The Wilshire Blvd./ Santa Monica study region is a very diverse area, in terms of building stock and topography. This area includes clusters of very tall buildings (over 10 to 15 stories), industrial areas, high-density residential and extended single-family dwellings. In addition, this area borders the Santa Monica Hills, thus making the topography of this region very diverse.

Our goal in studying these three areas was to 1) test the Bare-earth algorithm in its effectiveness to extract non-ground elevations for large regions, and 2) re-calibrate the parameters of the algorithm to optimize the separation of the bare earth and the built environment.

#### **4.1 San Fernando Valley**

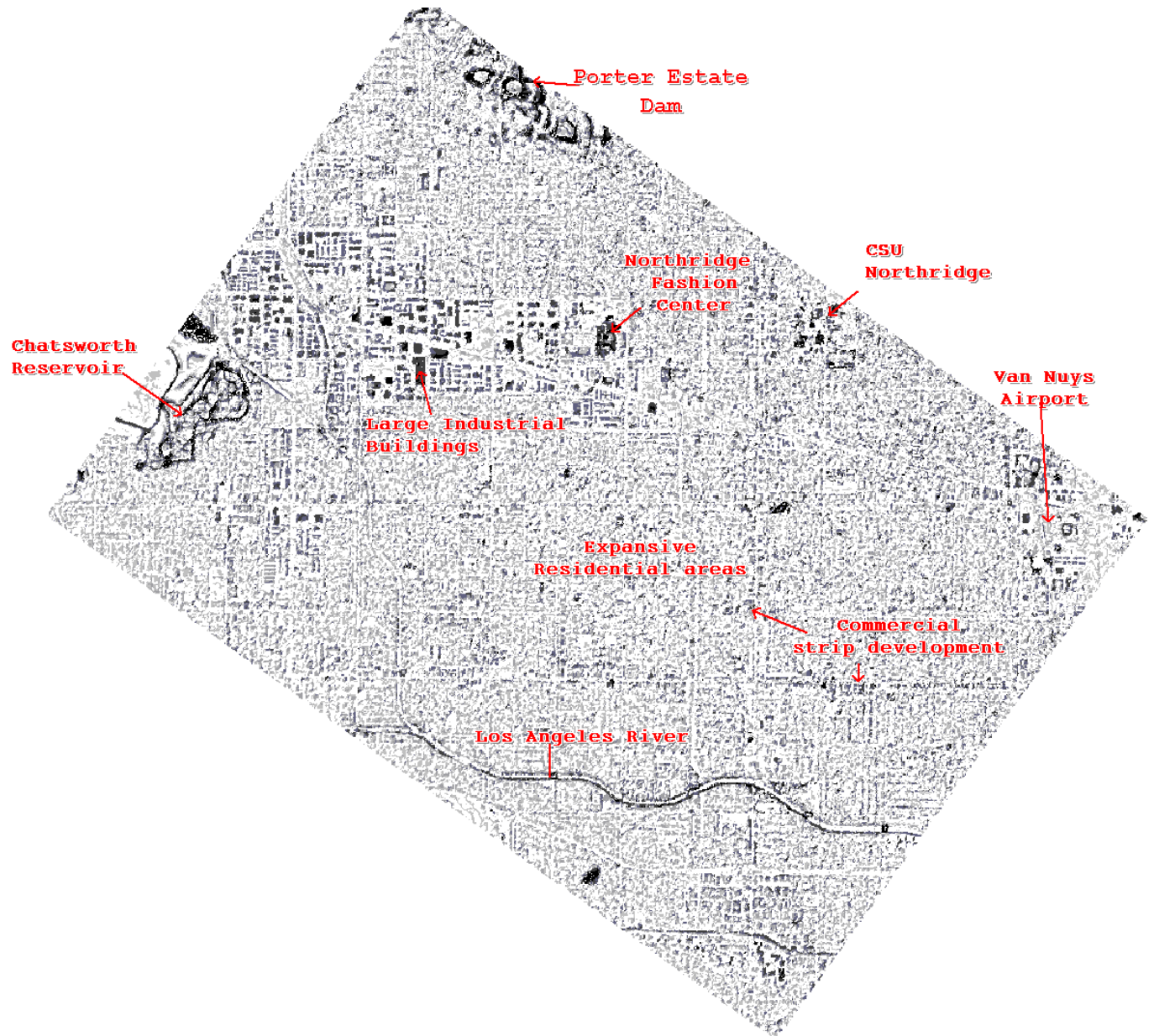
The application of the Bare-earth algorithm to the San Fernando Valley produced a very crisp separation of the built environment and bare earth, Figure 4-2. This separation is particularly evident where there are large building footprints, e.g., northwest portion of the study area. In this figure, the white, or no shade areas represent ground elevations. The shaded areas represent buildings or trees, with darker shades indicating higher elevations.



**FIGURE 4-2 Ground Elevations and Building Footprints for San Fernando Valley**

Figure 4-3 provides annotation to the footprints in Figure 4-2. The region is transected every ten blocks or so by major streets lined with large buildings. In some areas, this can be seen very clearly. For example, this is very evident in the area just west of the Northridge Fashion Center. There are also several clusters of large buildings that can be identified as specific buildings or facilities, such as the Van Nuys Airport, CSU Northridge, several large malls, and the large

industrial buildings that surround the railroad tracks. These areas are delineated extremely well. Therefore, most large manmade structures have been effectively identified or stripped out of the image by the Bare-earth algorithm.



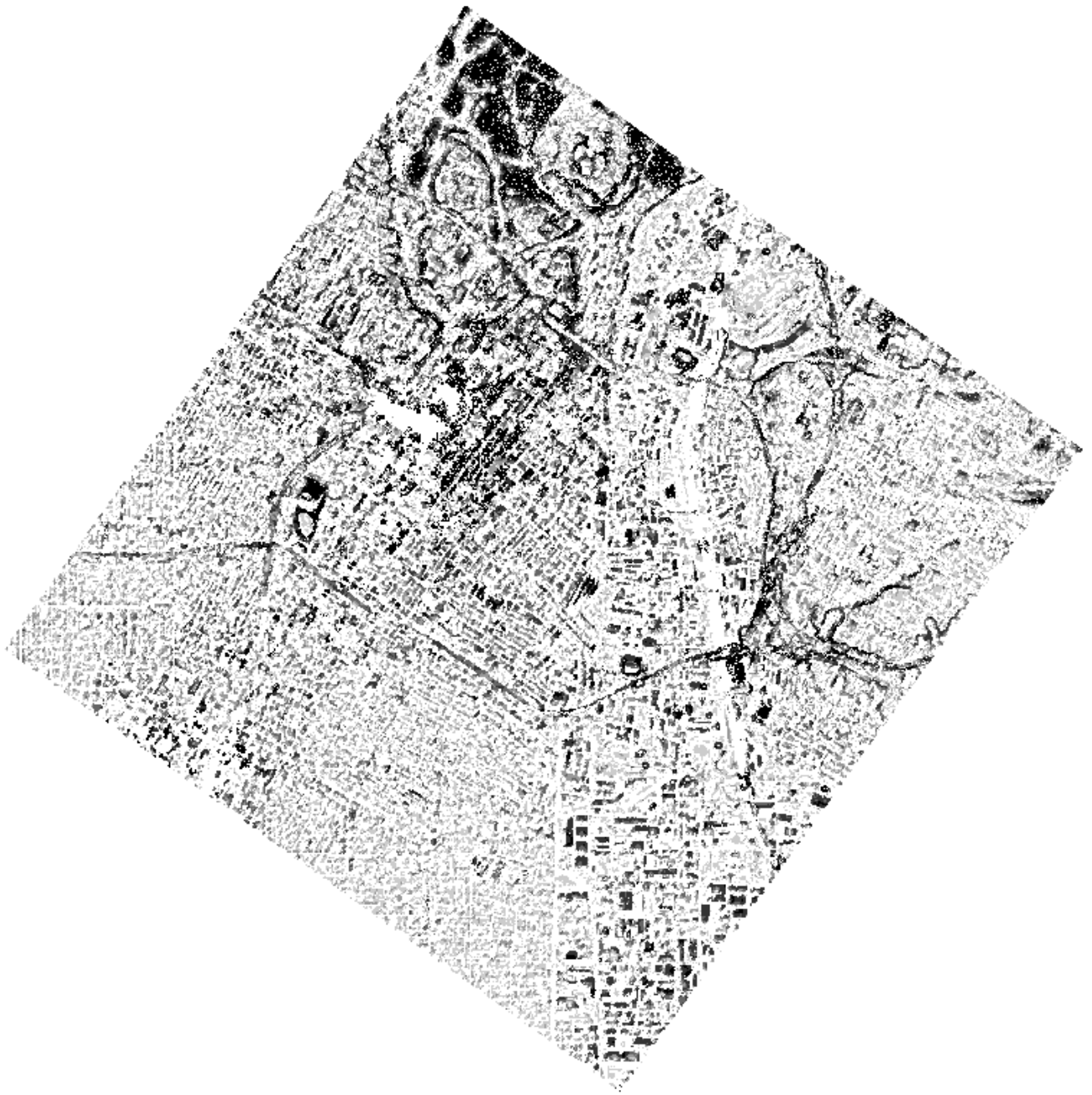
**FIGURE 4-3 Ground Elevations and Building Footprints for San Fernando Valley (with Annotation)**

There were three significant features in the San Fernando area that were not large buildings but were interpreted as not being bare earth. Two of the areas were associated with large manmade dams: the Porter Estate Dam and the Chatsworth Reservoir. These areas are generally characterized by steep slopes and the presence of large manmade structures. The third feature is the channelled Los Angeles River that runs through the San Fernando Valley. As in the case of the two reservoirs, the algorithm detected the sharp changes in elevation and assumed that this area was either a building or a row of tall trees. The algorithm interpreted the bottom of the stream channel as ground elevation and the walls of the channel as some manmade structure. For a distance of 62.5 meters surrounding the channelled streambed, the elevation of the ground is interpreted falsely as being above the ground level. Essentially, this is the same problem that we have with freeways when they are below grade thoroughfares.

Future research should focus on recognizing these longer structures as non-buildings and devising tests or criteria that include these areas as ground surface.

## **4.2 Downtown Los Angeles**

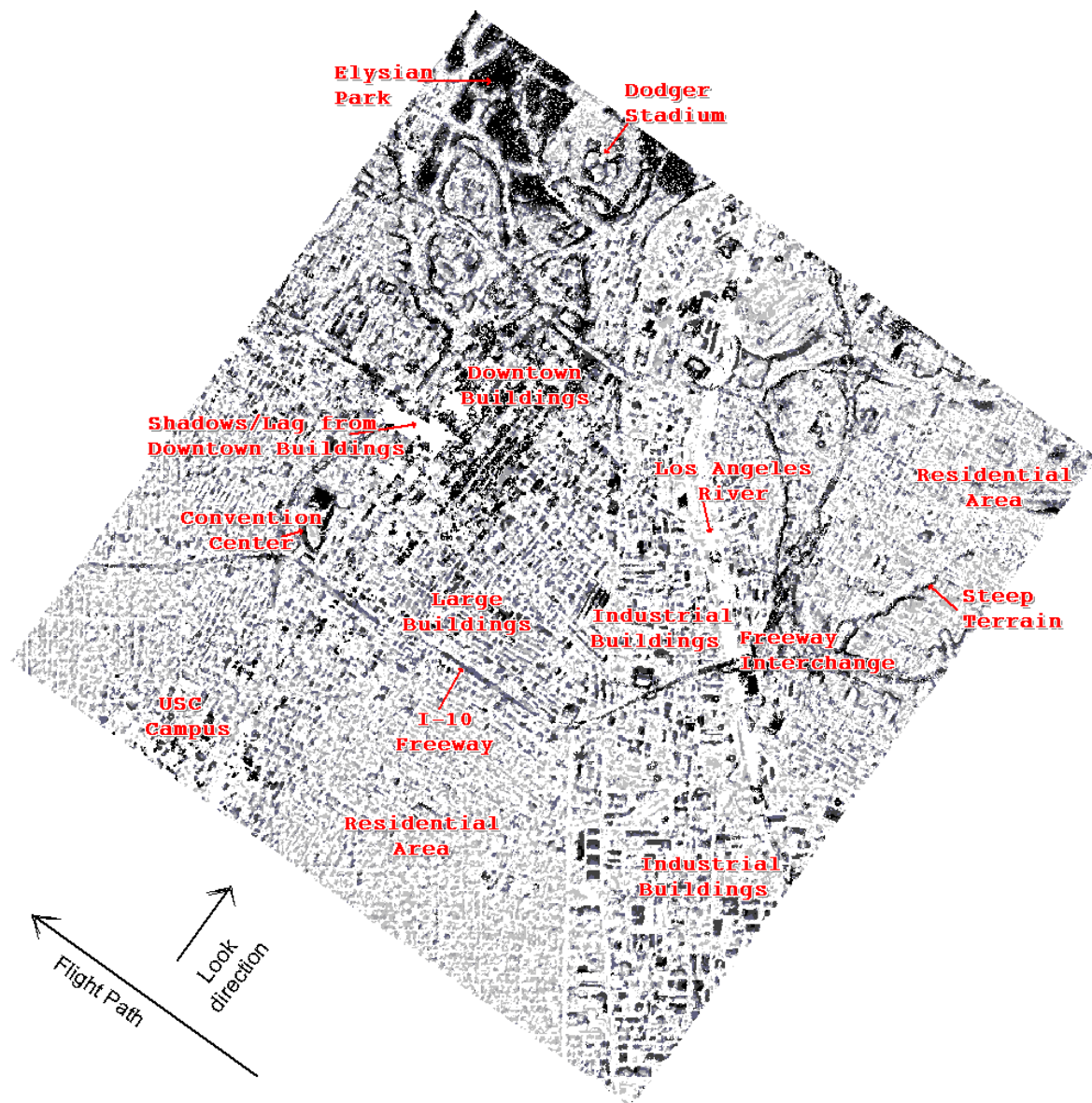
Figure 4-4 displays ground elevations and extracted building footprints for the downtown region. As in the previous figures, the white or non-shaded areas represent ground surface and the shaded areas indicate buildings or other structures; the darker the shade, the higher the elevation. In contrast to the San Fernando Valley, this area is characterized by many topographic changes in elevation. In the top part of the figure, you see large, dark areas that are associated with the Elysian Park area. The area generally slopes downward from north to south.



**FIGURE 4-4 Ground Elevations and Building Footprints for Downtown Los Angeles**



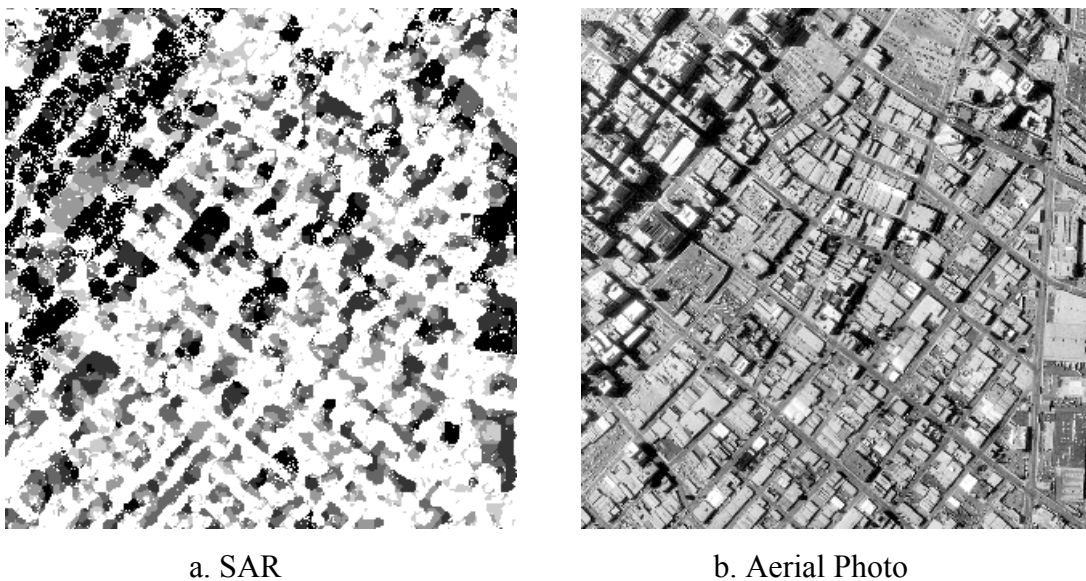
Figure 4-5 provides annotation to the previous image. Detecting the footprints of very tall buildings, particularly during a single pass of the area, is considered very difficult, if not impossible. Because of shadowing and lag problems, some buildings disappear completely and others have very narrow swaths of data associated with them. Because the data are obtained through side-looking radar, there will always be structures that are missed because they are in the shadows of other taller buildings.



**FIGURE 4-5 Ground Elevations and Building Footprints for Downtown Los Angeles (with Annotation)**

Some of the problems associated with extracting the bare earth in this area include 1) not detecting the ground in steep terrain (Elysian Park Hills), 2) interpreting some of the areas around the Los Angeles River as long buildings, and 3) showing or interpreting very little of the Downtown area as ground surface. This last problem can be attributed in large measure to the steep terrain in this area. There were a number of observations, however, that provided positive reinforcement for the existing algorithm. These included 1) the algorithm worked almost perfectly in separating the bare earth from the built environment in the industrial area, 2) the results in the residential areas followed a close delineation of the major streets and roadways, 3) some major streets in the central part of the city were, in fact, identified, 4) the algorithm correctly identified above-grade freeway structures as manmade, and 5) the algorithm worked correctly to identify many large building structures as buildings and not as large fields.

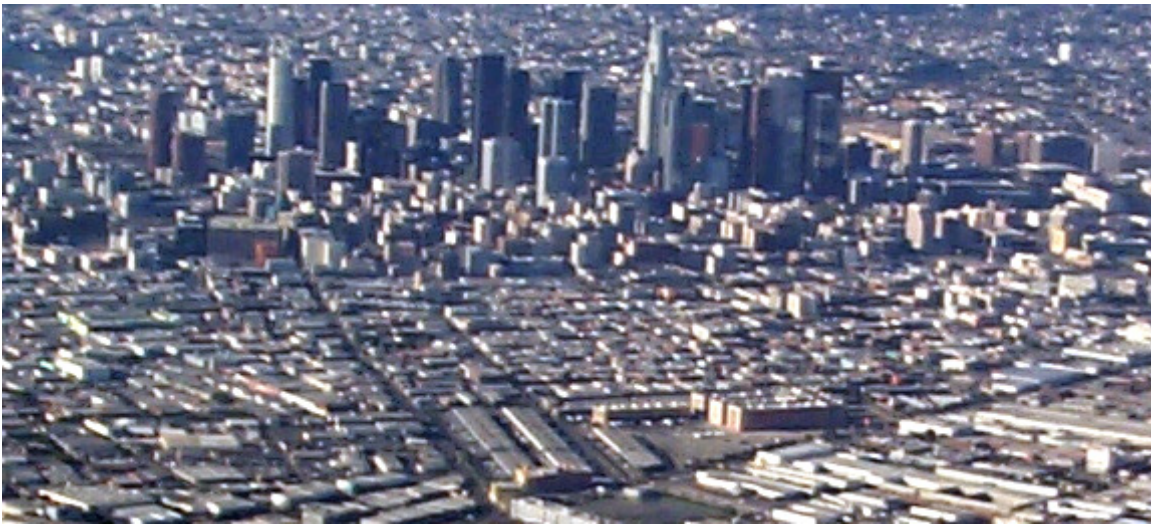
Outside the main downtown core, “shadowing” and “lag” did not appear to be a major problem. Figure 4-6, displays two images of the area just east of downtown. Figure 4-6a displays the ground elevations and building footprints resulting from the algorithm, while Figure 4-6b shows the same area as seen in a USGS aerial photograph. Again, in Figure 4-6a, the white areas represent the ground surface and the darker areas indicate buildings.



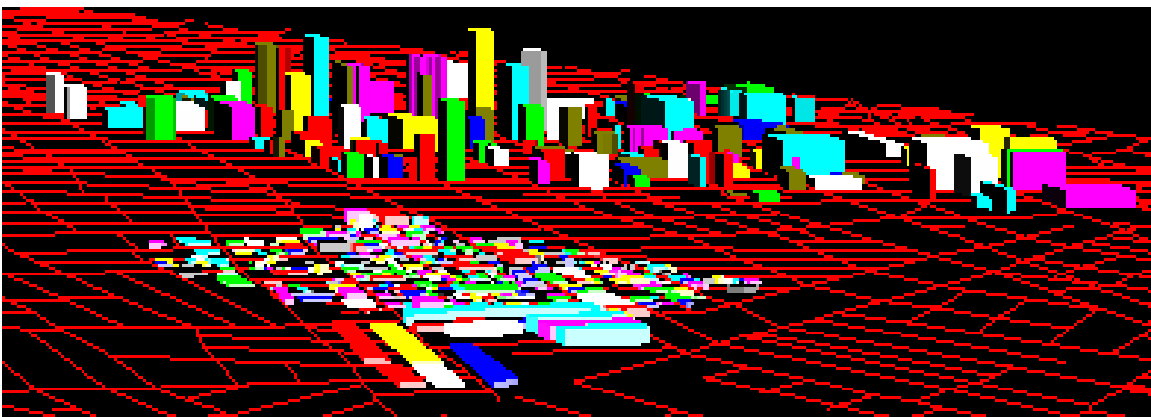
**FIGURE 4-6 Comparison of SAR-derived Bare-Earth Elevations and with Aerial Photograph (Industrial Area of Los Angeles)**



Figures 4-7 and 4-8 display similar views of the Downtown Los Angeles area using two different sources of data. Figure 4-7 is a photo taken from a commercial airplane. Figure 4-8 was created using the Bare-earth algorithm and SAR elevation data for this area. Figure 4-8 is the result of 1) identifying the footprints of major buildings in downtown using USGS aerial photos, 2) determining the maximum elevation associated with each footprint using the SAR data, and 3) subtracting from that elevation, the ground surface as determined by the Bare-earth algorithm.



**FIGURE 4-7 Aerial Photo of Downtown Los Angeles**



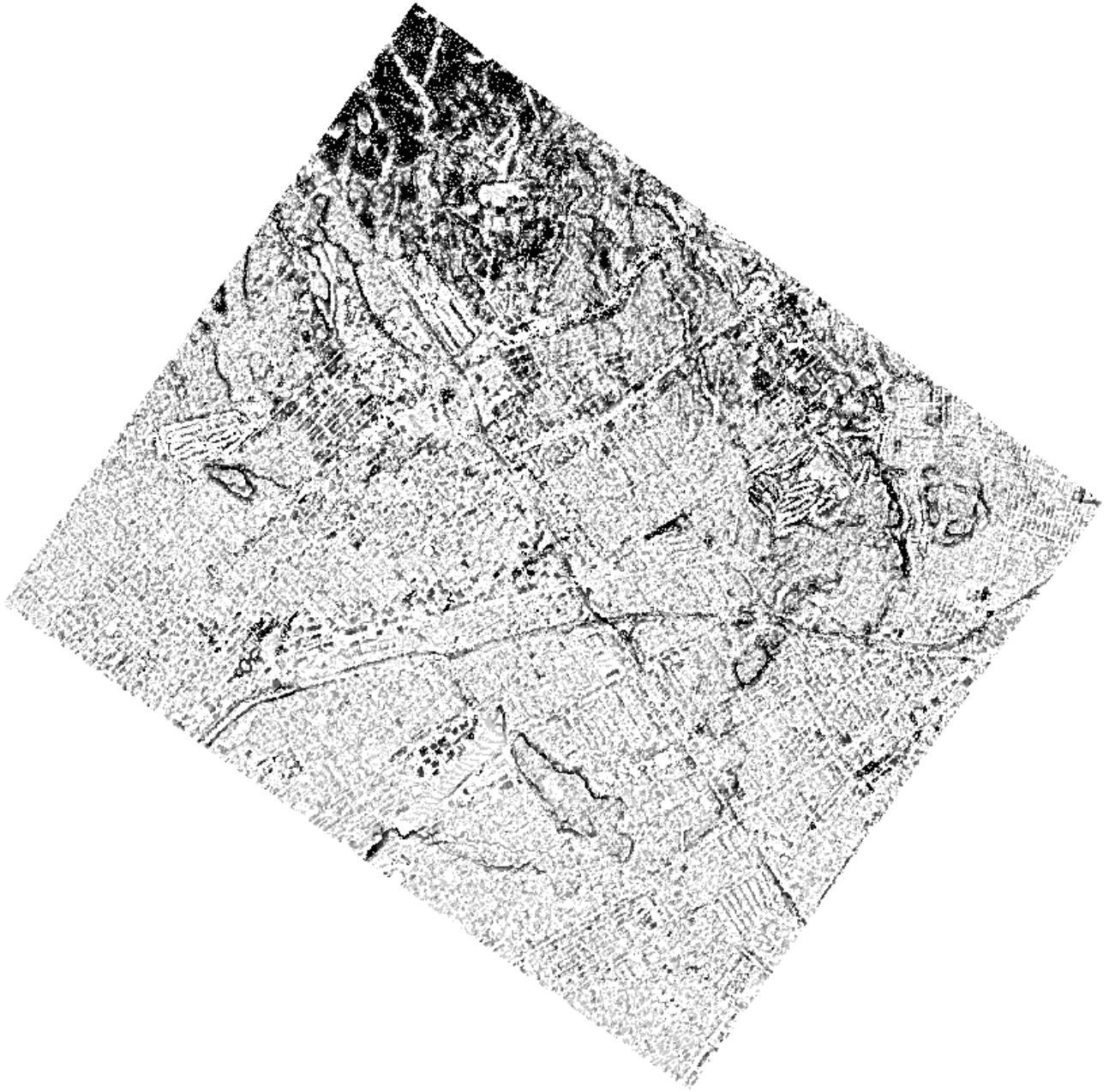
**FIGURE 4-8 Three-Dimensional View of Downtown Los Angeles created using Bare-Earth Algorithm and SAR Data**

The calculated heights of buildings in Figure 4-8 were then fused with street data and transferred to VRML using *Avenue* programming. The colors are random and for visualization only. The buildings in the foreground of the VRML image (Figure 4-8) are the industrial buildings in Figure 4-6b. Not all of the buildings are in the right height proportion to each other, but the two main peaks of tall buildings are clearly captured, with shorter buildings in between and surrounding these crests. This is significant, given the shadow and lag in the raw SAR data.

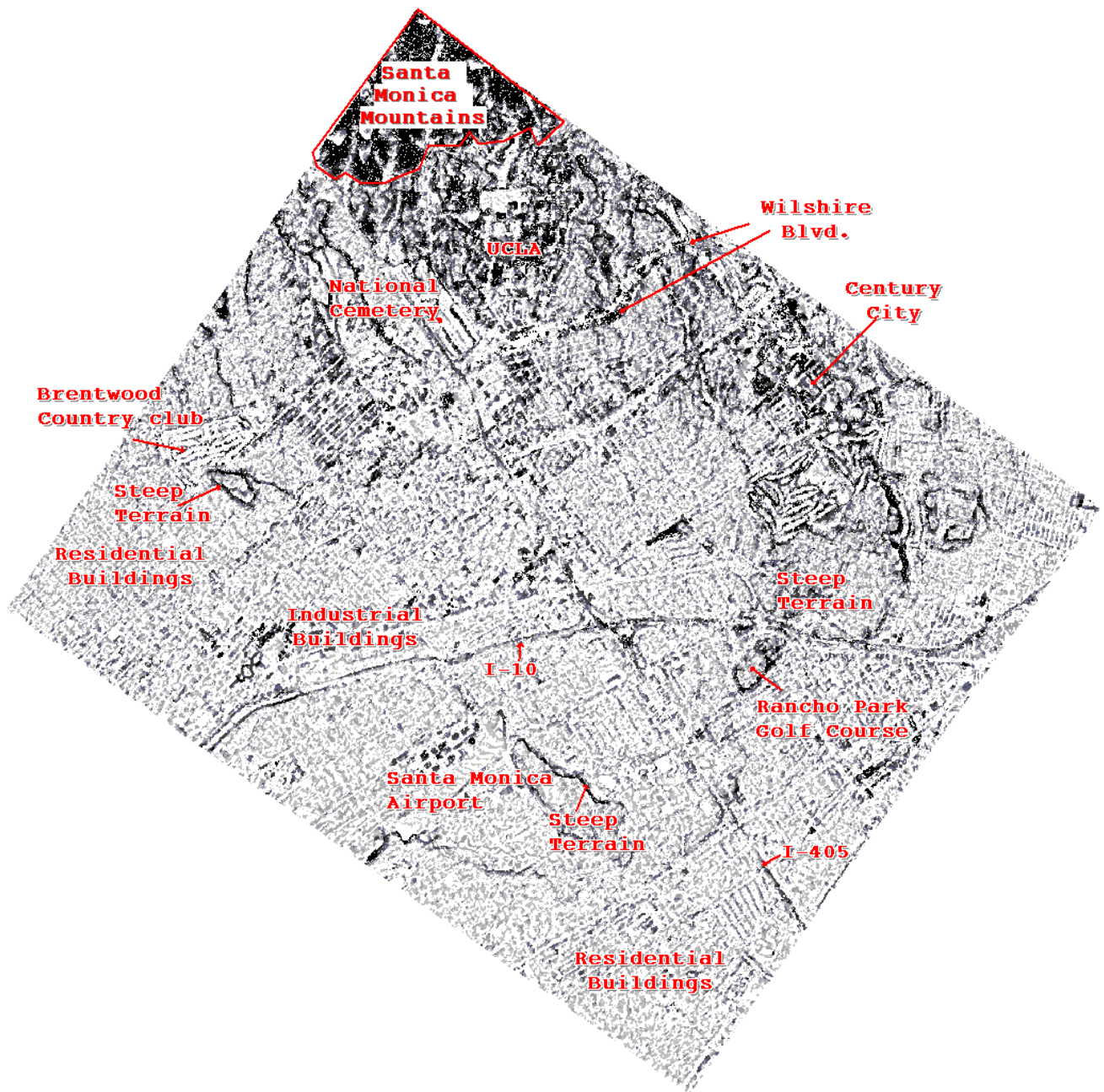
### **4.3 Wilshire Blvd./Santa Monica Area**

The Wilshire Blvd./Santa Monica area is a very diverse area that includes high-rise buildings, single-family and multi-family residences, commercial construction and large open areas, such as parks. This area was studied extensively during the testing phase of our Bare-earth algorithm development. As had been demonstrated in the other study areas, the results in the hilly areas, such as the Santa Monica Mountains produced unreliable results. Areas where there was clear separation of the bare earth and tall buildings included along Wilshire Blvd, the UCLA campus, Century City, and the Santa Monica airport.

Figures 4-9 and 4-10 present the results of our Bare-earth algorithm for the Wilshire Blvd./Santa Monica area. Large areas of high-density residential development can be easily discerned from lower density residential areas, both by the heights of structures and the densities of the footprints. This area represents a very diverse array of building use, much of which can be inferred from the pattern of the extracted footprints. This area is topographically challenging as well. Although the algorithm worked very well in the steep regions directly around Wilshire Boulevard, there were several areas where the steep terrain caused problems for the algorithm. In general, these problem areas corresponded closely to where the slope of the earth changed suddenly. To test this hypothesis, we used the USGS DEM data to map where these sudden changes were occurring. The slope was calculated using the USGS DEM data and mapped. The resulting slope map (Figure 4-11) revealed that the areas that undercut the natural terrain in the Figures 4-9 and 4-10 corresponded to areas with steep slopes. These inaccuracies appear in Figure 4-10 as areas labeled "Steep Terrain".

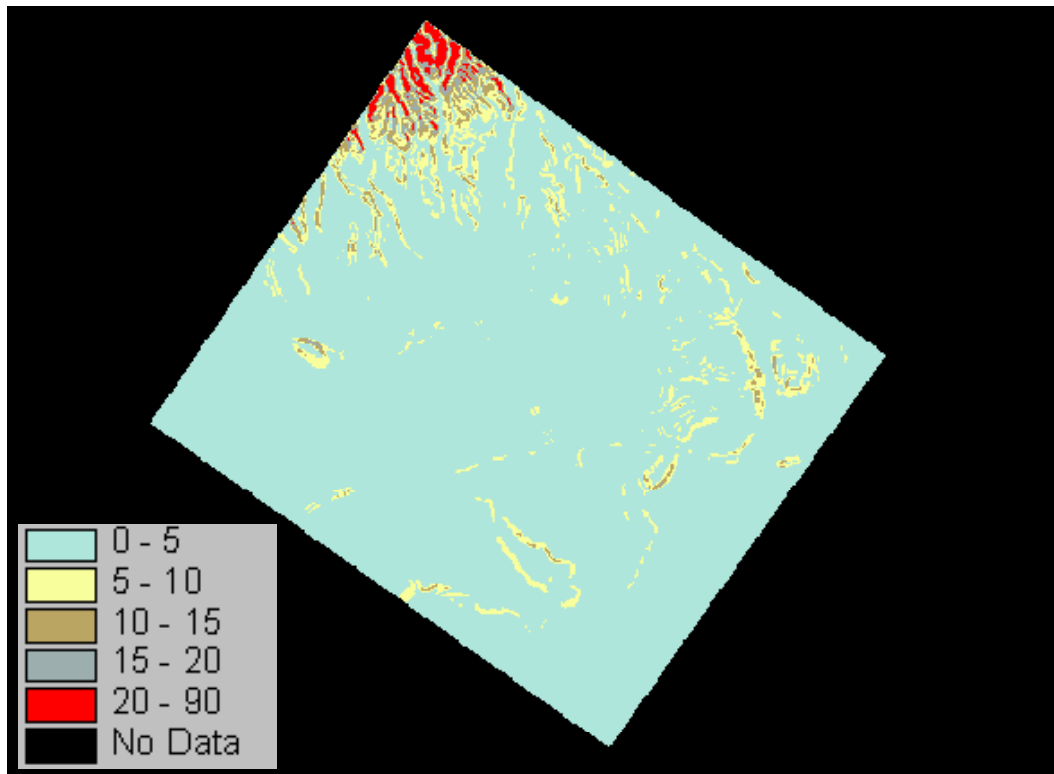


**FIGURE 4-9 Ground Elevations and Building Footprints for the Wilshire Blvd.  
and Santa Monica Area**



**FIGURE 4-10 Ground Elevations and Building Footprints for the Wilshire Blvd. and Santa Monica Area (with Annotation)**





**FIGURE 4-11 Slope of the Wilshire Blvd./Santa Monica Region as Computed from USGS 30-Meter DEMs (in Degrees)**

#### **4.4 Assessment of Bare-Earth Algorithm**

The lessons learned from applying the Bare-earth algorithm on large sets of data were very similar to those learned in the previous section, i.e., Validation of the Bare-earth algorithm. These lessons were:

- Areas that are densely populated with buildings (particularly tall buildings) are problematic. The algorithm, however, does a good job at stripping out everything that is not part of the ground. As we saw in Century City, the elevations from the surrounding areas are extended to underfill areas populated by tall buildings. The algorithm does a poor job of detecting small or moderately tall buildings in clusters of high-rise buildings from SAR data. This problem, unfortunately, is not addressable with the SAR data, since the SAR signal does not penetrate to ground level in these areas.

- Areas with steep hills were problematic, but for very short distances. The ground surface will not be detected in these areas until the ground levels out. These situations will result in mild errors that resemble a single contour line around the base of the hill.
- Mountainous areas, such as the Santa Monica Mountains, yield inaccurate results. Fortunately, the number or density of buildings in these areas will be small.
- Many large manmade structures such as highways, channeled streambeds, and dams are interpreted as being above ground, and must be distinguished from the heights of buildings.

We also learned that it was difficult to optimize the criteria defined in Section 2 for all areas. What worked best for some areas was not always the best solution in other areas. As we will see in the next section, a large part of the solution in this regard is better and more accurate data.

There needs to be more work done to understand the influence of natural terrain on our bare-earth calculations. For example, it should be possible to detect changes in the natural terrain by analyzing the relationship between slope and the variance of the slope. Modifying the thresholds to allow more terrain to be interpreted as ground on natural hills should allow the algorithm to identify more of the building stock. In the next section, we examine a new technology that could offer high-resolution elevation data that might overcome many of the problems uncovered above.

## SECTION 5

### TESTING THE BARE-EARTH ALGORITHM WITH LIDAR DATA

The Bare-earth algorithm in this study was created using SAR as the elevation data source. Artifacts such as lag and shadowing which caused the algorithm to become ineffective in dense urban settings may actually be non-existent using LIDAR technology, i.e., light detection and ranging (Bolter, 2000). These artifacts, as we have seen, have caused buildings to be lost, and have directly influenced our ability to accurately detect the bare earth in certain situations. However, the advantage of using LIDAR data comes at a cost. Because the technology requires a very narrow swath, it may take many days or weeks to complete a comprehensive survey of a large city. On the other hand, using SAR, imaging a large area may be accomplished in one flyover. As with all new technologies, pricing will change with availability and competition. Today, there are over 100 companies that offer LIDAR capabilities<sup>2</sup>. Also, there may be a hybrid solution involving using SAR data for the majority of a city and LIDAR data for the dense urban cores.

After completing the testing of the Bare-earth algorithm using SAR data, we conducted a limited validation study using LIDAR data that was received from the National Oceanic Atmospheric Administration (NOAA). In October 1997, NOAA collected LIDAR data for much of the Southern California coastline. The intended use of these data was to monitor coastal erosion. Most of the areas covered by this acquisition did not include buildings. However, there were several stretches of coastline that did capture residential development, i.e., from Manhattan Beach to Redondo Beach, and part of Long Beach, California. Unfortunately, these areas did not overlap with any of the SAR data.

LIDAR data is collected as a series of elevations at specific points. These points do not represent a grid, as with SAR data. The data are made available as an ASCII file of a series of latitude, longitude, and elevations for specific locations, or "x,y,z" data. The data were downloaded in the raw xyz format and translated into 2.5-meter postings, so that the same search radii could be applied using these new data. The data was converted to 2.5-meter grid cells by averaging all the elevations that fell within each of the 2.5-meter grid cells. LIDAR data is

generally collected with a density of point locations that far exceed SAR data resolution. LIDAR data is much more accurate than SAR data, and this accuracy led to a more accurate registration of ground elevation.

## **5.1 Manhattan Beach and Redondo Beach**

To test the application of the Bare-earth algorithm using LIDAR data, we started with the same set of parameters used in the SAR tests. That is, the same search radii and the same height thresholds. Manhattan Beach and Redondo Beach were chosen for the initial tests. Our goal was to assess whether the Bare-earth algorithm could be universally applied regardless of the type of elevation data used. Specifically, we were interested in whether the resolution or accuracy of the results (i.e., bare earth extractions) would improve if better elevation data were used.

While the initial results here were promising, we did not feel that the improved accuracy was commensurate with the level of improvement in the data, i.e., only marginal improvement was seen. Therefore, we re-visited the basic procedures used to filter the data to see if the parameters or models needed to be adjusted to optimize the performance of the algorithm. The first discovery that we made was that because of the improved accuracy of the data, the majority and median filters were not necessary. The majority filter was not needed because the presence of anomalous or spurious points was essentially eliminated. Because the data were so much more accurate than the SAR data for residential building heights, the threshold for the minimum elevation filter had to be changed. The software code was modified and the bare earth was then recalculated. This time, the results appeared to perfectly outline much of the housing stock, thus allowing an accurate representation of the bare earth.

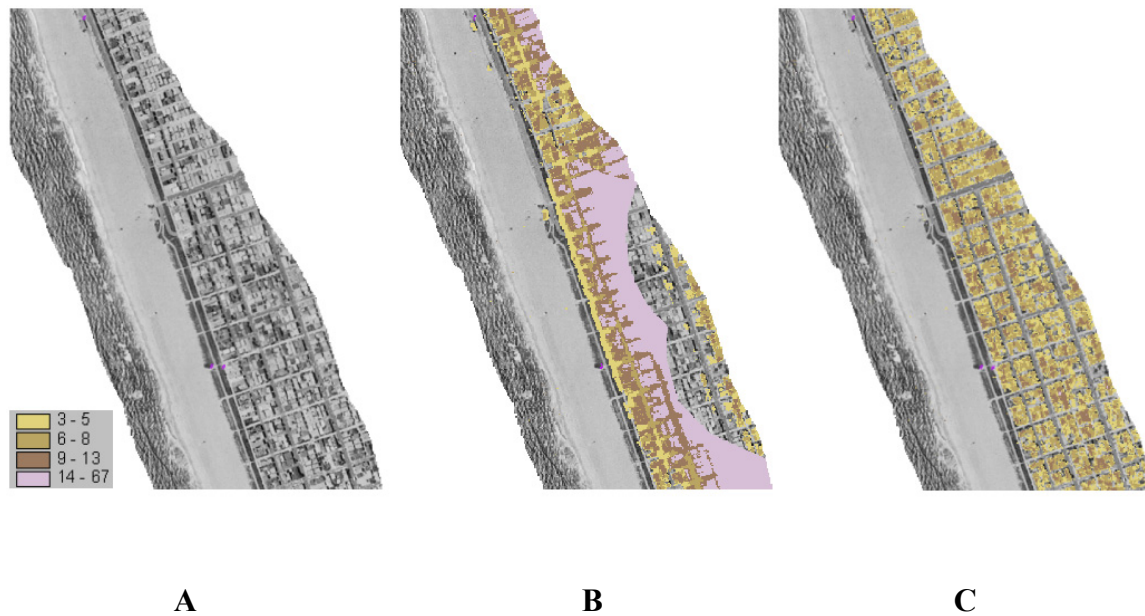
To focus on this problem, the algorithm was modified to produce map layers of all intermediate data layers. During this process, it was discovered that the difference between the LIDAR data and the derived bare earth was greater than 6 meters for a large portion of the area. The difference between the neighborhood minimum elevation and the raw elevation was examined for areas with higher than expected values. Investigation of street elevations in this area

---

<sup>2</sup> See <http://www.airbornelasermapping.com/>



revealed that heights below 9 meters might actually catch these steep slopes. Adjusting the parameters of the Local Minimum filter (see Section 2.4.1) to identify differences of 9 meters instead of 6 meters led to more crisp elevation surface for Manhattan Beach. To validate these results, USGS aerial data were obtained for these sites and the extracted heights were overlaid on top of this imagery. These results are presented in Figure 5-1. Figure 5-1, map B presents the initial results of the algorithm using the 6-meter criteria for the local minimum filter. Map C displays the results after changing the threshold from 6 meters to 9 meters. For the vast majority of the area, this change led to significantly better results. In Map C, it is very easy to see the ground elevations via the streets. Similar results were achieved in Redondo Beach with the improved algorithm.

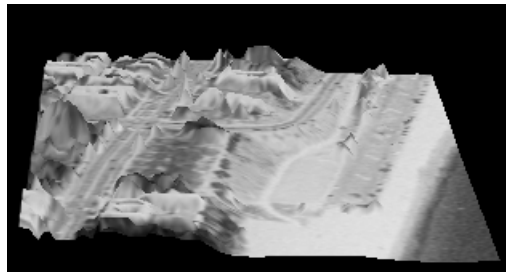


**FIGURE 5-1 Bare Earth Results using LIDAR Data in Manhattan Beach  
(elevations in meters)**

- A) USGS aerial photography of Manhattan Beach**
- B) Ground Elevations and heights of buildings using initial algorithm**
- C) Ground Elevations and heights of buildings using modified algorithm.**

## 5.2 Long Beach

The Bare-earth algorithm – both initial and modified for use with LIDAR data - was applied in the Long Beach area. In this area of Long Beach, there are many tall condominiums on the oceanfront. The area has a steep cliff that is roughly fifteen to twenty meters above sea level. The condominiums that have been built here often are built into the cliff, i.e., split- or multi-level. The entrances of these buildings face north, and thus are located several stories above sea level. The south sides of these buildings face the ocean and thus have floors that are very close to sea level, see Figure 5-2.



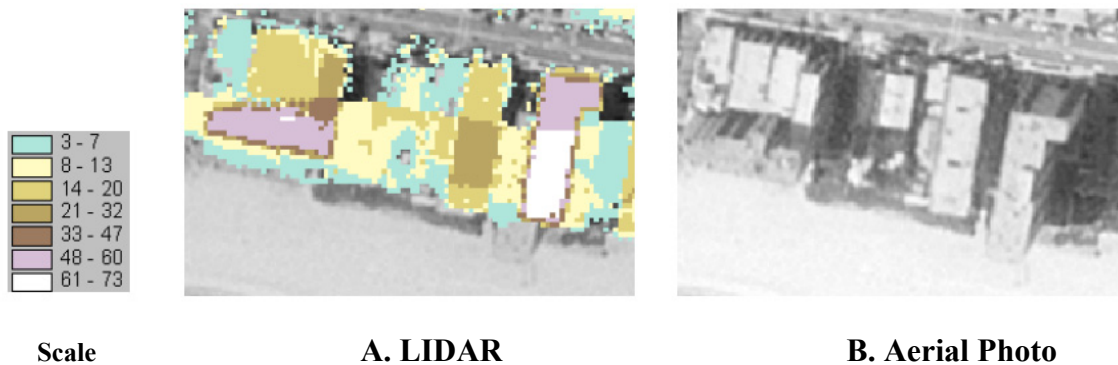
**FIGURE 5-2 Three-Dimensional View of Cliff leading up from the Beach.  
Image created from USGS Aerial Data Draped Over LIDAR Data  
(no vertical exaggeration)**

Beyond the cliff and oceanfront condominiums is a high-density residential area with many large houses and apartments.

In this series of tests, it was found that the initial (or 6-meter threshold) filter did a better job at matching the actual bare-earth elevations. We believe that in this case, the 9-meter threshold was too high to effectively extract two-story apartment buildings. The 9-meter difference between the minimum and the raw LIDAR height was well above the threshold necessary to exclude these buildings from being considered as ground elevation candidates. Thus, the modified algorithm overestimated the amount of bare earth in this area.

This particular area of Long Beach is characterized by natural terrain with slope gradients higher than 20 degrees from horizontal. Despite the steep terrain, the Bare-earth algorithm did a reasonably good job of extracting the elevation of the tall buildings that are built into the cliff.

The difference in height between the front and back of these buildings varied depending on the height of the cliff. Figure 5-3, image A, displays the estimated elevation (based on the use of LIDAR) for several tall structures along the beach. The structures can be identified in the corresponding aerial photograph, which is provided in image B of the same figure. Obtaining this level of accuracy in building heights was a very pleasant surprise.



**FIGURE 5-3 Large Buildings on a Cliff in Long Beach**

Even though these were limited tests, we feel that they demonstrate the importance and value of obtaining high-resolution digital elevation data. These applications using LIDAR technology helped to demonstrate how the problems encountered in the SAR tests (miscalculating bare-earth elevations in areas of steep slope) could be overcome with higher quality information. Future tests might focus on re-investigating some of the problem areas in the San Fernando Valley and Downtown Los Angeles to see if using LIDAR data eliminates these problems. In any event, we are extremely encouraged by the success of the Bare-earth algorithm using advanced LIDAR technology.



## **SECTION 6**

### **CONCLUSIONS AND RECOMMENDATIONS**

This report is Volume 1 of a two-part series that focuses on the application of remote sensing technologies – synthetic aperture radar (SAR) and LIDAR – for bare-earth detection and building inventory development. This particular report discusses our findings in bare-earth detection. Once the bare-earth elevation is separated from the remotely sensed elevation, this elevation can be analyzed in terms of its effectiveness in detecting the heights of buildings. If the ability to detect the height of buildings is established, the classification of the landscape into residential, commercial, and industrial land uses can be addressed. This is the subject of the second report in this series.

The methodology used to detect the bare earth is based on a series of filters and mathematical operations on the data. The most essential of these are: 1) a Majority filter that helps to screen out anomalous or spurious data; 2) a Local Minimum filter that is effective at screening out tall and moderate-sized buildings; 3) a Median filter that is particularly effective at screening out short to medium height buildings; 4) a Slope filter that is designed to eliminate topographic changes associated with objects such as buildings and trees protruding from the ground; 5) a Variance filter that focuses on eliminating large clusters of buildings; and 6) an Euclidean Allocation operation that creates a surface from the areas identified as most likely to be associated with ground height.

Based on an analysis of three large study areas and numerous site-specific studies, we have developed an algorithm utilizing a mild, multifaceted approach that distinguishes the spatial characteristics of the built environment from the ground. These filters are mild in the sense that the search radii and thresholds are devised such that they conservatively estimate the location of the ground, and multifaceted in the sense that they identify the location of the ground through several different filters that address different aspects of the problem. Although there are several principles that would seem to be likely candidates for finding the bare-earth elevation simply and quickly (i.e. interpolating the street height, minimum elevation, or the most frequent elevation) these methodologies did not work well when put to the test for large areas. The most effective solution involved approaching the problem gently from several different spatial perspectives.

In general, the results of the Bare-earth algorithm were very successful given the quality of the SAR data in urban areas. The results of the algorithm were even more encouraging when used with LIDAR data. Areas where the Bare-earth algorithm did particularly well in detecting the height of the ground were areas of moderate height and terrain. Examples include industrial areas, commercial corridors, and residential neighborhoods (e.g., the San Fernando Valley). Other successes include the industrial buildings located just east of downtown Los Angeles and the commercial and residential neighborhoods of Santa Monica, which are often very hilly. Throughout much of the region, a comparison of detailed city maps, aerial photographs, and the building footprints that resulted from the application of the Bare-earth algorithm was encouraging.

The optimal thresholds and variables associated with some of the filters were different for the two data types studied (SAR and LIDAR). The LIDAR data did not require as many data filtering operations. Some of the thresholds used in the Bare-earth algorithm were initially optimized for the SAR elevations, which because of noise in the data, generally resulted in diminished building heights in residential areas. A thorough investigation of the optimal values for LIDAR should be performed in the future.

There are several variables and thresholds within the algorithm that would be more effective at accurately identifying the height of the ground if modified in conjunction with the natural slope of the terrain. The natural slope can be separated from the slope associated with manmade terrain by examining the relationship between neighborhood slope and variance in slope. That is, areas where there is a steep slope over a long distance but a low variation in the slope index are more likely to be associated with the natural terrain. Because of this, we believe that additional research is required to examine the relationship between slope, search radius, and threshold parameters.

The algorithm did not work in mountainous terrain, a known limitation. However, the algorithm also did not work for steep hillsides in moderate terrain. In these areas, long contour-like areas of land would be left by the algorithm, incorrectly perceived as being above the ground. These long irregularities are not unlike the results of some large manmade features that caused problems for the algorithm. Both the Los Angeles River, a manmade drainage basin, and several

freeways were left behind. An area of further research is to determine the possibility of detecting and extracting these sinuous features from the results.

The algorithm was especially problematic in clusters of large buildings. This is a limitation of the data, as the radar does not penetrate to the ground in these areas. For example, there is a large hill in the middle of downtown Los Angeles known as "Bunker Hill" that was largely undetected. Even so, the general character of the downtown area seemed to be captured. Certainly enough to identify the area as an urban core, and perhaps estimate the building stock with a high margin of error.

LIDAR stands out as a possible technology for detecting building height in even the densest urban cores. Although expensive, the prospect of using LIDAR in these cores and supplementing this data with SAR seems reasonable. Our limited studies with LIDAR data indicate that with slight adjustment due to the accuracy of the data, LIDAR can be used to capture the height of buildings almost perfectly. Further research is needed to optimize all variables and thresholds with respect to the natural terrain. The subject of the next report in this series focuses on using the results of the Bare-earth algorithm to estimate the building stock.





## SECTION 7

### REFERENCES

- Baltsavias, E.P., "A Comparison Between Photogrammetry and Laser," in *ISPRS J. Photogramm. Remote Sensing*, Vol. 54, pp 83 – 94, July 1999.
- Benson, Dale. USGS. Personal interview. 24 October 2000.
- Berry, J.K, *Beyond Mapping: Concepts, Algorithms, and Issues in GIS*, GIS World, Inc., Fort Collins, CO, 1995.
- Black, J., "Business Is Blooming-Imagery Vendors Expand into New Markets," in *GeoWORLD*, Vol. 13, No.9, pp. 34 – 38, September 2000.
- Bolter, R. and Leberl, F., "Shape-from-Shadow Building Recognition from Multiple View SAR Images," in *Proceedings of In 24th Workshop of the Austrian Association for Pattern Recognition, (ÖAGM/AAPR)*, Villach, Carinthia, Austria, pp. 199 – 206, 2000.
- Bottlemy, Becky. USGS. Personal interview. 25 October 2000.
- Brunn, A., Gulch, E., Lang, F., and Forstner, W., "A Hybrid Concept for 3D Building Acquisition," in *ISPRS J. Photogramm. Remote Sensing*, Vol. 53, pp. 119 – 128, February 1998.
- Chang, K. and Verbyla, D.L., *Processing Digital Images in GIS*, OnWord Press, Sante Fe, NM, 1997.
- Davis, B.A. and Easson, G.L., "High-Resolution Remote Sensing for Risk Assessment and Hazard Mitigation."
- Dobson, J.E., Bright, E.A., Coleman, P.R., Durfee, R.C., and Worley, B.A., "LandScan: A Global Population Database for Estimating Populations at Risk," in *PE&RS*, Vol. 66, No. 7, pp. 849 - 857, July 2000.
- Eguchi, R.T., J.D. Goltz, H.A. Seligson, P.J. Flores, T.H. Heaton, and E. Bortugno (1997), Real-time loss estimation as an emergency response decision support system: The Early Post-Earthquake Damage Assessment Tool (EPEDAT), *Earthquake Spectra*, 13, 815-832.
- Eguchi, R.T., Huyck, C.K., Houshmand, B., Tralli, D.M., and Shinozuka, M., "A New Application for Remotely Sensed Data: Construction of Building Inventories using Synthetic Aperture Radar Technology," in *Proc. of the 2nd Multi-Lateral Workshop on Development of Earthquake and Tsunami Disasters Mitigation Technologies and Their Integration for the Asia-Pacific Region*, Kobe, Japan, March 1 – March 2, 2000.

EQE International, Inc. and The Geographic Information Systems Group of the Governor's Office of Emergency Services, *The Northridge Earthquake of January 17, 1994: Report of Data Collection and Analysis: Part B: Analysis and Trends*, April 1997.

Foody, G.M., "Image Classification with a Neural Network: From Completely-Crisp to Fully-Fuzzy Situations," in *Advances in Remote Sensing and GIS Analysis*, John Wiley & Sons, England, pp. 17 – 38, 1999.

Freeman, T., "What is Imaging Radar?" from the *NASA/JPL Imaging Radar Home Page*, October 2, 2000, <<http://southport.jpl.nasa.gov/desc/imagingradarv3.html>>

Gamba, P. and Houshmand, B., "Digital Surface Models and Building Extraction: A Comparison of IFSAR and LIDAR Data," in *IEEE Transactions on Geoscience and Remote Sensing*, Vol. 38, No. 4, pp. 1959 - 1968, July 2000.

Garbrecht, J. and Martz L.W., "Digital Elevation Model Issues In Water Resources Modeling," in *Proc. of the 19<sup>th</sup> ESRI International User Conference*, Environmental Systems Research Institute, San Diego, California, July 26 - July 30, 1999.

Gens, R., "SAR Interferometry: Software, Data Format, and Data Quality," in *PE&RS*, Vol. 65, No. 12, pp.1375 – 1378, December 1999.

Gilbert, C., "GPS Consumer Series: The Vertical Component of GPS," in *EOM*, Vol. 6, No. 5, May 1997.

Goodenough, D.G., Charlebois, D., Matwin, S., MacDonald, D., and Thomson, A.J., "Queries and Their Application to Reasoning with Remote Sensing and GIS," in *Proc. of IGARSS'94, the IEEE 1994 IGARSS Annual Conference*, California Institute of Technology, Pasadena, California, pp. 1199 – 1206, August 8 – August 12, 1994.

Hagg, W., Segl, K., and Sties, M., "Classification of Urban Areas in multi-date ERS-1 images using Structural Features and a Neural Network," in *Proc. of IGARSS'95, the IEEE 1995 IGARSS Annual Conference*, Duomo, Firenze, Florence, Italy, July 10 – July 14, 1995.

Hinton, J.C., "Image Classification and Analysis using Integrated GIS," in *Advances in Remote Sensing and GIS Analysis*, John Wiley & Sons, England, pp.207 – 218, 1999.

Isaaks, E.H. and Srivastava, R.H., *An Introduction to Applied Geostatistics*, Oxford University Press, New York, NY, 1989.

Jiang, X. and Bunke, H., "Fast Segmentation of Range Images into Planar Regions by Scan Line Grouping," in *Mach. Vis. Applicat.*, No. 7, pp. 115 – 122, 1994.

Kirscht, M. and Rinke, C., "3D Reconstruction of Buildings and Vegetation from Synthetic Aperture Radar (SAR) Images," in *Proc. of the IAPR Workshop on Machine Vision Applications (MVA '98)*, Makuhari, Chiba, Japan, pp. 228 - 231, November 17 – November 19, 1998.

Landgrebe, D.A., "Machine Processing of Remotely Acquired Data," in *Remote Sensing of the Environment*, Addison Wesley, Reading, Massachusetts, pp. 349 – 373, 1976.

Longley, P.A. and Mesev, V., "The Role of Classified Imagery in Urban Spatial Analysis," in *Advances in Remote Sensing and GIS Analysis*, John Wiley & Sons, England, pp. 185 – 206, 1999.

Massonnet, D., et al., "Image of an Earthquake," in *Nature*, Vol. 364, No. 8, July 1993.

Mather, P.M., "Land Cover Classification Revisited," in *Advances in Remote Sensing and GIS Analysis*, John Wiley & Sons, England, pp. 7 – 16, 1999.

Merrill, Gary. Personal interview. 9 January 2001.

Monmonier, Mark, *Cartographies of Danger*, The University of Chicago Press, Chicago, IL, 1997.

Multidisciplinary Center for Earthquake Engineering Research, *Research Progress and Accomplishments*, 1997-1999, July 1999.

National Institute of Building Sciences, *Hazus Technical Manual Volume I-III*, Federal Emergency Management Agency, 1997.

Oliver, C. and Quegan, S., *Understanding Synthetic Aperture Radar Images*, Artech House, Norwood, MA, 1998.

Perry, D.M., Peterson, R.W., and Robinson, G.M., "Optical Interferometry of Surfaces," in *Science's Vision: The Mechanics of Sight*, Scientific American, Inc., pp. 56 – 61, 1998.

Piau, P., "Performances of the 3D-SAR Imagery," in *Proc. of IGARSS'94, the IEEE 1994 IGARSS Annual Conference*, California Institute of Technology, Pasadena, California, pp. 2267 – 2271, August 8 – August 12, 1994.

Quint, F. and Bähr, H.P., "Feature Extraction for Map Based Image Interpretation," in *Proc. of the 3<sup>rd</sup> International Colloquium of LIESMARS*, Wuhan, China, pp. 1 – 8, 1994.

Quint, F. and Sties, M., "Map-based semantic modeling for the extraction of objects from aerial images," in, Basel, Schweiz, Birkhäuser Verlag, pp. 307 – 316, 1995.

Sapeta, K., "Have You Seen the Light? LIDAR Technology is Creating Believers," in *GEOWorld*, Vol. 13, No. 10, pp. 32 – 36, October 2000.

Schilling, K.J., Vögtle, T., and MüBig, P., "Knowledge Based Analysis of Satellite Images," in *Proc. of the ISPRS Commission III Symposium: Spatial Information from Digital Photogrammetry and Computer Vision*, München, pp. 732 – 736, 1994.

Shinozuka, M. and Rejaie, S.A., "Disaster Management and Restoration by Using Remotely Sensed Images," in *Proc. of the 2<sup>nd</sup> International Conference on Decision Making in Urban and Civil Engineering*, Lyon, France, November 20 – November 22, 2000.

Slatton, K.C., Crawford, M.M., Gibeaut, J.C., and Gutierrez, R., "Removal of Residual Errors From SAR-Derived Digital Elevation Models For Improved Topographic Mapping of Low-Relief Areas," in *Proc. of the 1997 IGARSS Conference*, Singapore, August 1997.

Strozzi, T., Wegmiller, U., and Werner, C., "GAMMA Differential Interferometry and Geocoding Software," from the *Gamma Remote Sensing Home Page*, October 2, 2000, <<http://www.gamma-rs.ch/diff.htm>>.

Tobler, W. 1970. "A Computer Movie Simulating Urban Growth in the Detroit Region." *Economic Geography* 46(2):234-240.

United States Geological Survey, *Standards for Digital Geospatial Metadata*, United States Geological Survey, Reston, VA, 1995.

Weidner, U. and Forstner, W., "Towards Automatic Building Extraction from High Resolution Digital Elevation Models," in *ISPRS J. Photogramm. Remote Sensing*, Vol. 50, pp. 38 – 49, August 1995.

Zebker, H. A., P. A. Rosen, R. M. Goldstein, A. Gabriel, and C. Werner, 1994, On the derivation of coseismic displacement fields using differential radar interferometry: The Landers earthquake, *Journal of Geophysical Research - Solid Earth*, vol. 99, no. B10, pp. 19617-19634.

"7.5 minute Digital Elevation Models for California," from the *USGS EROS Data Center, Sioux Falls, SD Home Page*, October, 2000, <[http://edc.usgs.gov/doc/edchome/ndcdb/7\\_min\\_dem/states/CA.html](http://edc.usgs.gov/doc/edchome/ndcdb/7_min_dem/states/CA.html)>.

"Airborne Laser Mapping," from the *Airborne Laser Mapping Home Page*, October 2000, <<http://www.airbornelasermapping.com/>>.

"Coastal Sediment Transport Assessment Using SAR Imagery (C-STAR)," from the *Institute for Applied Remote Sensing Home Page*, October 2000, <<http://www.ifars.de/cstar/cstar.htm>>.

"LIDAR Data Retrieval Tool," from the *NOAA Coastal Services Center Home Page*, October 2000, <[http://www.csc.noaa.gov/crs/tcm/ATM\\_download.html](http://www.csc.noaa.gov/crs/tcm/ATM_download.html)>.

"NGS Data Sheet By USGS Quad Map Name," from the *National Geodetic Survey Home Page*, October 2000, <[http://www.ngs.noaa.gov/cgi-bin/ds\\_quads.prl](http://www.ngs.noaa.gov/cgi-bin/ds_quads.prl)>.

"Products Available from the USGS EROS Data Center," from the *USGS EROS Data Center, Sioux Falls, SD Home Page*, October, 2000, <<http://edc.usgs.gov/dsprod/prod.html>>.

"SRTM Mission Statistics," from the *NASA Jet Propulsion Laboratory Home Page*, October 2000, <<http://www.jpl.nasa.gov/srtm/statistics.html>>.

“Star-3i,” from the *Intermap Technologies Home Page*, October 2000, <[http://www.intermaptechnologies.com/HTML/mapp\\_star3i.htm](http://www.intermaptechnologies.com/HTML/mapp_star3i.htm)>.

“Theory of Synthetic Aperture Radar Electromagnetic Theory,” from the *Atlantis Scientific Inc. Home Page*, October 2000, <[http://www.atlsci.com/library/sar\\_theory.html](http://www.atlsci.com/library/sar_theory.html)>.



## **APPENDIX A**

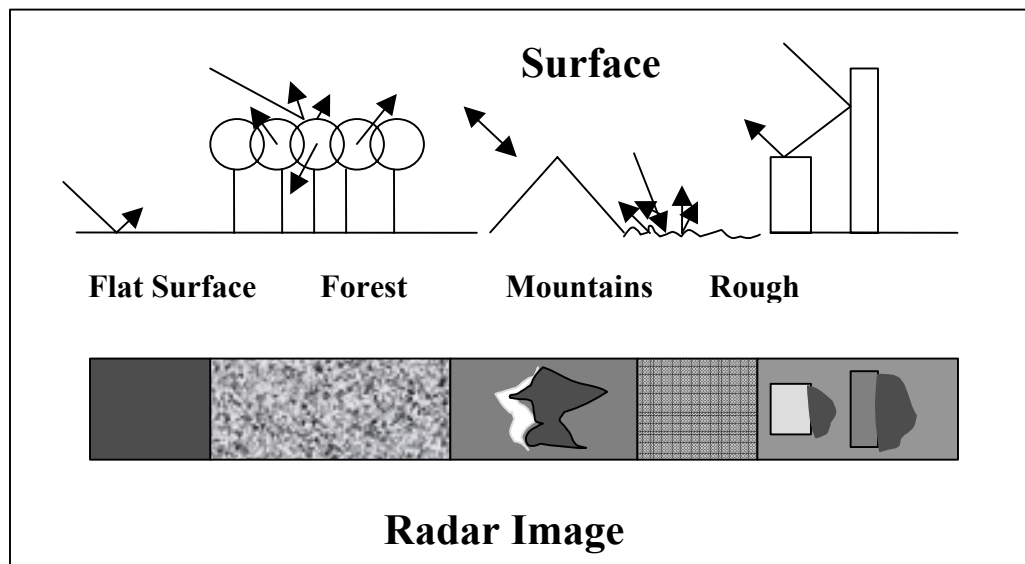
### **BASIC PRINCIPLES ON SAR IMAGING**

Radar imaging works by sending microwave pulses toward a target and measuring the return time and intensity that is reflected back to the sensor or antenna. Normally, wavelengths are on the order of 1 cm to 1 m, which corresponds to a frequency range of about 30 GHz to 300 MHz. For an imaging radar system, about 1500 high-power pulses per second are transmitted toward the target, with each pulse having a duration of about 10-50 microseconds. Typical bandwidths fall in the range of 10 to 200 MHz. Higher bandwidths correspond to finer resolutions of the image.

The term synthetic aperture radar, or SAR, refers to the technique used to simulate a long antenna by combining signals (echoes) received by the sensor as it moves along a particular flight track. In the case of SAR, both phase and amplitude information are used, in contrast to conventional radar that uses only amplitude. This allows a larger aperture to be synthesized, thus allowing for higher resolution images. SAR imaging is possible using both airborne (airplane) and space borne (satellite) platforms. For example, in the U.S., airborne systems are operated by the National Aeronautics and Space Administration (NASA) with its Air-SAR system, and by Intermap Technologies, through its Star-3*i* system. Satellite-based systems that offer SAR capabilities include Radarsat, ERS-1 and ERS-2, and J-ERS. These systems should be distinguished from those that primarily offer optical imaging, e.g., SPOT, IKONOS and Landsat.

The products from SAR imaging fall into three basic categories: elevation data, reflectance or intensity data, and correlation information. Elevation information is possible when IFSAR data are collected. IFSAR refers to interferometric synthetic aperture radar and is usually performed using an airborne or space borne platform with several antennae. A SAR image is formed for each receiving antenna with each image having an associated magnitude and phase. The difference in return times from the two antennae appear as a difference in phase for each pixel imaged. These differences will vary from pixel to pixel and this information eventually characterizes the height differences on the ground. See <http://southport.jpl.nasa.gov> or <http://erim.org> for more details on SAR and IFSAR.

When a radar image is viewed, what is seen is a mosaic of dots of varying shades and intensities. Each pixel represents a radar backscatter for that area on the ground. Depending upon the roughness of the surface, the moisture level of that area, or the “look” angle from the sensor, the processed image may be light or dark. Light or bright areas represent high backscatter, or areas, which return a large fraction of the radar energy back to the sensor; dark areas represent low backscatter, or areas, which tend to reflect much of the energy away from the sensor. Flat areas typically result in low backscatter, while areas containing extensive vegetation tend to be high backscatterers. Depending upon the orientation of buildings and streets relative to the sensor, backscattering may be high or low. Figure A-1 provides an illustration of radar images based on different surface conditions. These surface textures caused by SAR imaging can be very useful in determining landuse. Unfortunately, they are highly dependent on the orientation of the SAR data with respect to the sensor.



**Figure A-1 Radar Image versus Ground**

Figure A-2 shows an aerial view of the Federal Building located on Wilshire Blvd. near the 405 Freeway. The building is essentially a rectangular-shaped building with a large tower located on the southern boundary. The tower is roughly 10 meters higher than the rest of the building. The overall height of the building (excluding the tower) is over 70 meters. Although the outline in Figure A-2 suggests an “H” shape footprint for the building, only the top portion of outline



where the tower is located is the actual building. The lower part of the “H” footprint surrounds possibly a parking structure.

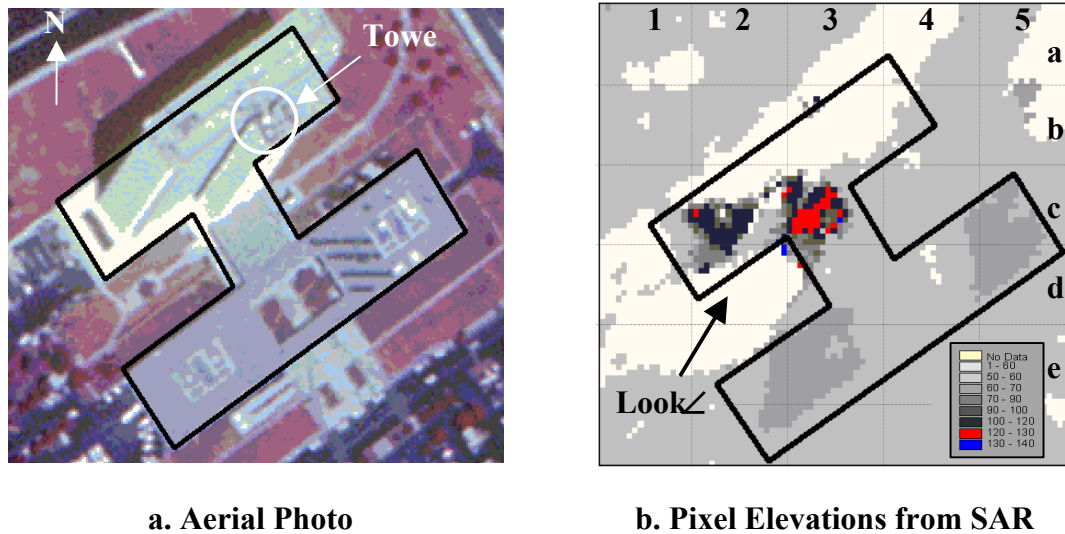
In Figure A-2b, we observe for the same outline the pixel elevations as determined through analysis of airborne SAR data. The airborne SAR data for this study was provided by Intermap Technologies Ltd. located in Alberta, Canada and Englewood, Colorado. These data were collected during a flight in late May of 1998 and the general “look” or observation angle is seen in Figure A-2b. The posting of SAR data was 2.5 m. The measurable heights in Figure A-2b are seen in quadrants 2c and 3c. In 2c, we are picking up the elevation of the top of the building. In 3c, we are measuring the elevation of the tower. In 3e, and 5c and 5d, we are picking up equipment located on top of the parking structure, which are observable from the aerial photograph in Figure A-2a. Note that the elevations shown in the legend have not been normalized to the actual ground height.

What is also evident from this figure is that we are picking up elevation data for only part of the building, i.e., quadrants 2c and 3c. The white areas of the figure indicate parts of the image where no data have been collected. These “no data” areas include quadrants 3a, 3b and 4a. Because of the observation or look angle of the sensor, the tower in quadrant 3c is obstructing our view of these areas. These areas are referred to as “shadow” zones. In addition, there are “no data” zones in quadrants 1d, 1e, 2d and 2e. The reason for this problem is due to a phenomenon called “lag” or “layover” effects.

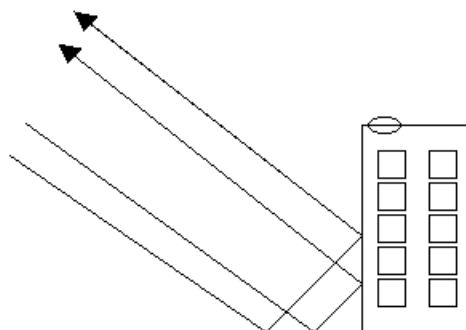
Shadow zones, seen in quadrants 3b and 4a, are simply zones that are behind the buildings. Since the data are collected from the airplane in a side looking direction, rather than being collected straight down, as with LIDAR data, there are areas which the radar does not penetrate because a structure is literally in the way.

Layover refers to a situation where imaging is often complicated by multiple signals overlaying onto the same pixel. The right angles, which are formed between a building and the ground, form an area where the radar waves will ricochet from the ground, to the building, back to the antennae. The extra distance caused by the ricochet will place the perceived distance from the antennae farther than it actually is. Figure (A-3) illustrates how this can happen for a large area

next to a building, facing the antennae. Multiple signals are detected creating a blank space (1d, 1e, 2d and 2e) where the true distance should be recorded. Because of the right angles, these signals in Figure A-2 end up overlaying on top of each other, causing not only a gap in elevation, but a stronger intensity reading from a location on top of the building (indicated by the oval circle in Figure A-3 (lag). This phenomenon is more of a problem with tall structures.



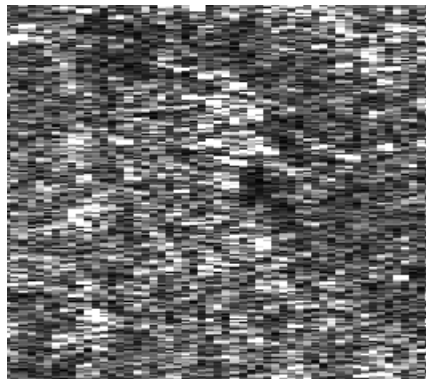
**Figure A-2 Aerial Photo and SAR Elevation Data for Federal in West Los Angeles. Note that Tower in Fig. 5a. is meters higher than the rest of the**



**Figure A-3 Lag or Layover Effects with tall buildings.**

The effects of lag and shadowing are tempered by utilizing the building footprint. However, in downtown areas, the lag and shadowing effects will obscure the heights of buildings. Utilizing optical data to aid in the extraction of the height can help detect these buildings, but not detect their height.

SAR vertical accuracy is also affected by noise. Noise can be caused by radiation from other sources. Radar waves will also ricochet from surface to surface, causing a speckling affect. These waves will also interfere with each other, effectively canceling themselves out or resonating with each other to form higher amplitudes. When looking at a SAR image, this causes a salt and pepper effect (See Figure A-4). In order to create an interferogram in an area with low correlation, the phase data must be averaged for several pixels. The averaging essentially dampens the elevation recordings that are within the noise level, such as in the case of small houses.



**Figure A-4 Salt and Pepper Effect Caused by Noise in SAR Intensity Image**





*A National Center of Excellence in Advanced Technology Applications*

University at Buffalo, State University of New York  
Red Jacket Quadrangle ■ Buffalo, New York 14261-0025  
Phone: 716/645-3391 ■ Fax: 716/645-3399  
E-mail: [mceer@acsu.buffalo.edu](mailto:mceer@acsu.buffalo.edu) ■ WWW Site: <http://mceer.buffalo.edu>



University at Buffalo The State University of New York

ISSN 1520-295X